FABRICATION AND CHARACTERIZATION OF URANIUM-MOLYBDENUM-ZIRCONIUM ALLOYS

A Thesis

by

CONNOR TODD WOOLUM

Submitted to the Office of Graduate and Professional Studies of
Texas A&M University
in partial fulfillment of the requirements for the degree of

MASTER OF SCIENCE

Chair of Committee,	Sean McDeavitt
Co-Chair of Committee,	Delia Perez-Nunez
Committee Member,	Raymundo Arroyave
Head of Department,	Yassin Hassan

December 2014

Major Subject: Nuclear Engineering

ABSTRACT

As part of a global effort to convert reactors that require highly enriched uranium to instead operate with low enriched uranium, monolithic fuel plates consisting of a U-Mo fuel meat with a zirconium foil barrier layer and clad in aluminum are being investigated. Interactions have been noted to occur between the fuel meat and the zirconium foil during fuel plate fabrication. These phases must be characterized as part of the fuel qualification process in order to determine potential behavior in a reactor environment; the observed phases are often too small to fully characterize so this study was initiated to characterize the equilibrium phases present in the U-Mo-Zr ternary alloy system.

Alloys containing molybdenum (7 wt% and 10 wt%) and zirconium (2 wt%, 5 wt%, and 10 wt%) were fabricated and homogenized at 950°C. They were then subjected to annealing at 650°C for periods of 1, 2, and 5 hours in order to study phase characteristics. Characterization was performed using various techniques including electron-probe micro-analyzer, X-Ray diffraction, and differential scanning calorimetry analysis.

Generally, the alloys appeared somewhat similar in terms of microstructure, with the exception of a couple unusual features. A solid solution matrix phase containing intermetallics was typically observed. The density of these intermetallic regions varied with each alloy, but not significantly across varying heat treatments. These intermetallic phases were often observed to have compositions consistent with Mo_2Zr, except in U-7Mo-10Zr. In this alloy the precipitates were often consistent with zirconium rich impurity phases; that particular sample could have had an anomalous high impurity composition.

One unusual result of the annealing was observed for the U-7Mo-2Zr alloy in back scattered electron imaging. An area that appeared to be a solid solution was visible along grain boundaries for the homogenized sample. This area appeared to be composed of a very dense region of precipitates for the annealed samples. The phase composition was unable to be analyzed due to the very small size of the precipitates.

The U-10Mo-5Zr and U-10Mo-10Zr alloys exhibited significant depletion of molybdenum from the matrix phase, while the other alloys exhibited a slight increase in molybdenum. This increase in molybdenum content should contribute to the stability of the γ-phase.

The work presented here addresses a knowledge gap in the behavior of the ternary U-Mo-Zr system. Phase evolution and stability of various U-Mo-Zr alloys are examined through casting and heat treating these alloys. Subsequent analyses provide details relevant to the advancement of fuel systems capable of converting many reactors.

DEDICATION

I dedicate this thesis to my family for their constant support and sacrifices that have enabled me to grow into the person I am today.

ACKNOWLEDGEMENTS

I would first and foremost like to thank my advisor Dr. McDeavitt. This work would not have been possible without his guidance and assistance throughout my undergraduate and graduate studies. I appreciate his relaxed teaching and mentoring style and have learned a great deal from him.

I would also like to thank the FCML manager, Dr. Perez-Nunez. Her dedication to the lab is obvious and her assistance throughout this project ensured things went smoothly.

I owe a great deal of gratitude to Dr. Guillemette of the Texas A&M Geology Department for his assistance with EPMA work. His unparalleled expertise in acquiring and interpreting data was crucial to the outcome of this project.

Thanks also to Dr. Anup with the Materials Science & Engineering Department at Texas A&M for his assistance with performing XRD on my samples and obtaining reference XRD data.

I am thankful for my FCML colleagues, all of whom have helped me in some fashion throughout this research endeavor. The countless discussions about life in general or research specific topics made this work both productive and enjoyable. Sandeep Irukuvarghula and Sangjoon Ahn taught me a great deal about U-Mo and U-Zr alloys, along with equipment. Grant Helmreich taught me the art of polishing. I appreciate the help of Jeff Clemens to encapsulate samples in quartz tubing. Jessica Taylor assisted with the tedious task of sample preparation.

Finally, I would like to extend my deepest gratitude to my family for their constant support throughout my academic career.

NOMENCLATURE

at%	Atom Percent
BCC	Body Centered Cubic
BSE	Back Scattered Electron
DSC	Differential Scanning Calorimetry
DU	Depleted Uranium
EDS	Electron Dispersive Spectroscopy
EPMA	Electron-Probe Micro-Analyzer
FCC	Face Centered Cubic
FCML	Fuel Cycle and Materials Laboratory
GTRI	Global Threat Reduction Initiative
HEU	Highly Enriched Uranium
INL	Idaho National Laboratory
LEU	Low Enriched Uranium
RERTR	Reduced Enrichment for Research and Test Reactors
U-xMo-yZr	Alloy composition (x=wt% Mo, y=wt% Zr, balance U)
WDS	Wavelength Dispersive Spectroscopy
wt%	Weight Percent
XRD	X-Ray Diffraction

TABLE OF CONTENTS

LIST OF FIGURES

Page

LIST OF TABLES

Page

1. INTRODUCTION

The Reduced Enrichment for Research and Test Reactors (RERTR) program is an effort to remove highly enriched uranium (HEU) from civilian circulation. It began in 1978 and continues to this day, although some efforts were suspended from 1989 to 1995 [1]. It is part of a larger effort under the Global Threat Reduction Initiative (GTRI) program [2].

The RERTR program converts reactors that are fueled with HEU to reactors capable of operating on low enriched uranium (LEU), thus removing HEU from circulation. HEU poses a proliferation concern due to its potential use for nefarious purposes. To date, over 60 reactors have been converted since the inception of the program [3]. A uranium silicide fuel was one of the first new fuels developed under the auspices of RERTR and that fuel form enabled the conversion of many nuclear reactors. However, this silicide fuel is only approved for uranium loadings up to 4.8 g/cm^3 [1]. There are more advanced reactors that require a higher uranium density than uranium silicide dispersion fuel can provide. It was determined by the RERTR program that a uranium-molybdenum fuel alloy was a strong candidate to fill this gap [4].

This uranium-molybdenum fuel is being investigated in two forms: a dispersion fuel and a monolithic fuel. A dispersion fuel is an atomized fuel alloy combined with a matrix material (often aluminum), and compacted while a monolithic fuel is a solid fuel alloy. An alloy containing 10 wt% molybdenum was selected as the candidate most likely to have the best performance characteristics. These performance features include minimal fuel swelling and fuel-cladding interactions, as well as phase stability [5, 6]. The

monolithic fuel with 10 wt% molybdenum allows for a uranium loading of up to 15.6g/cm^3, an increase from 8g/cm^3 for the dispersion fuel [7]. This fuel is typically clad in aluminum, which has unfavorable interactions with the U-Mo fuel meat (Figure 1-1) during fabrication that may cause excessive swelling during operation [8]. In order to address these interactions, a foil barrier layer has been proposed and tested. Zirconium was chosen as a prime candidate due to its neutron transparency, high thermal conductivity, and slow interdiffusion zone growth rate, among other reasons [9].

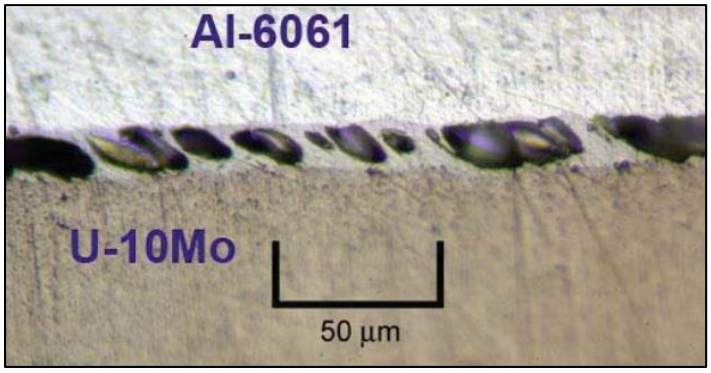

Figure 1-1. Interaction layer between aluminum cladding and fuel [5].

Placing the zirconium foil between the U-Mo fuel and aluminum cladding mitigates some negative interactions, but the zirconium and fuel metals do interact during fuel plate fabrication [5]. Fabrication involves co-rolling the fuel alloy (U-10Mo) and zirconium foil after they have been heated to approximately 650°C. Several passes are made, then the plate is reheated to increase ductility. This process continues until the foil reaches the desired final thickness of roughly 0.33 mm [7]. It is important to know characteristics of the interaction zones in order to ensure the fuel will remain safe and behave in a predictable manner in a reactor. However, these interaction zones are too small

to analyze when sectioned from the fuel plates themselves. The research presented in this document attempts to recreate bulk samples of similar composition to what may be found in these interaction zones.

Alloys containing molybdenum (7 wt% and 10 wt%) and zirconium (2 wt%, 5 wt%, and 10 wt%) were fabricated and homogenized at 950°C. They were then subjected to annealing at 650°C for periods of 1, 2, and 5 hours in order to study phase characteristics. Characterization was performed using various techniques including electron-probe micro-analyzer, X-Ray diffraction, and differential scanning calorimetry analysis.

2. BACKGROUND

This section outlines the scientific background to support the work presented throughout this document. It also includes information relevant to standard fuel plate processing that was used as guidance when determining various experimental variables.

2.1. Alloy Characteristics

2.1.1. Uranium Metallurgy

Uranium metal exists in the α-phase at temperatures below 663°C. Alpha-phase uranium is an orthorhombic structure and has unfavorable properties for nuclear reactor applications [10]. While it has a high fissile atom density and high thermal conductivity as a pure metal, it has numerous issues that make it unsuitable as reactor fuel. Alpha phase uranium exhibits poor corrosion resistance, low hardness, low yield strength, and anisotropic swelling under irradiation [11]. The swelling presents a significant challenge when fuel is expected to be in a reactor for years and maintain its integrity.

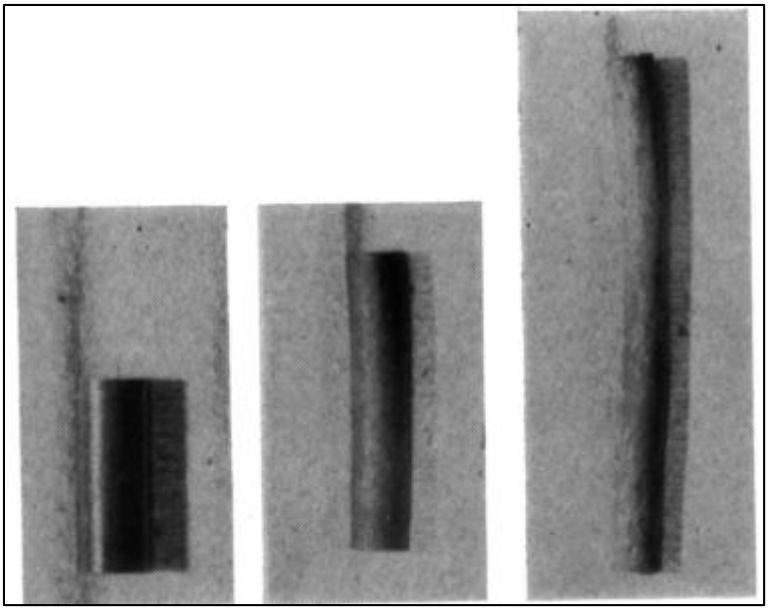

Figure 2-1. Example of uranium after irradiation. Burnup (L to R): 0 at%, 0.053 at%, 0.11 at%. [12].

Beta phase uranium (β-U) exists in a complex tetragonal lattice structure between 663°C and 764°C [10]. Irradiation behavior of β-U is also unsatisfactory for use as reactor fuel in its pure metal form. It exhibits swelling similar to α-U [12].

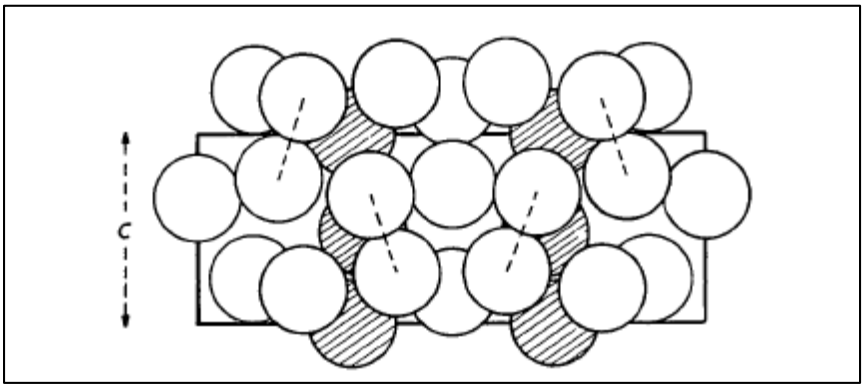

Figure 2-2. Section through the (110) plane of the β-U structure. Open circles: atoms in main layer; shaded circles: atoms in subsidiary layer. [13].

The γ-phase of uranium is a body centered cubic (BCC) phase that is isotropic. This phase exists between 764°C and 1133°C in pure uranium metal [10]. The isotropic nature of this phase suggests it would have more favorable swelling properties. Unfortunately, uranium metal cannot readily be stabilized in the γ-phase by quenching [11]. However, alloying with various metals can allow for a metastable γ-U to exist at low temperatures. Molybdenum is soluble in uranium to ~35 at% and allows for the stabilization of the desired γ-phase [4].

2.1.2. The Uranium-Molybdenum System

Uranium with 10 wt% molybdenum was chosen for the monolithic fuel form for US reactors. This fuel appears to offer a balance of γ-phase stability and uranium density. This alloy also has good swelling and thermal conductivity properties [5]. The addition of molybdenum to uranium allows for the stabilization of the γ-phase at room temperature by quenching. This metastable phase has been observed to decompose as a function of time and temperature. Figure 2-3 shows some of these relationships, which clearly indicate that an increase in molybdenum content increases the onset time of γ-U decomposition. Even a slight decrease of a couple of weight percent of molybdenum can have a dramatic effect on the onset time of phase decomposition, which is extremely relevant when considering the stability of U-Mo fuel alloys.

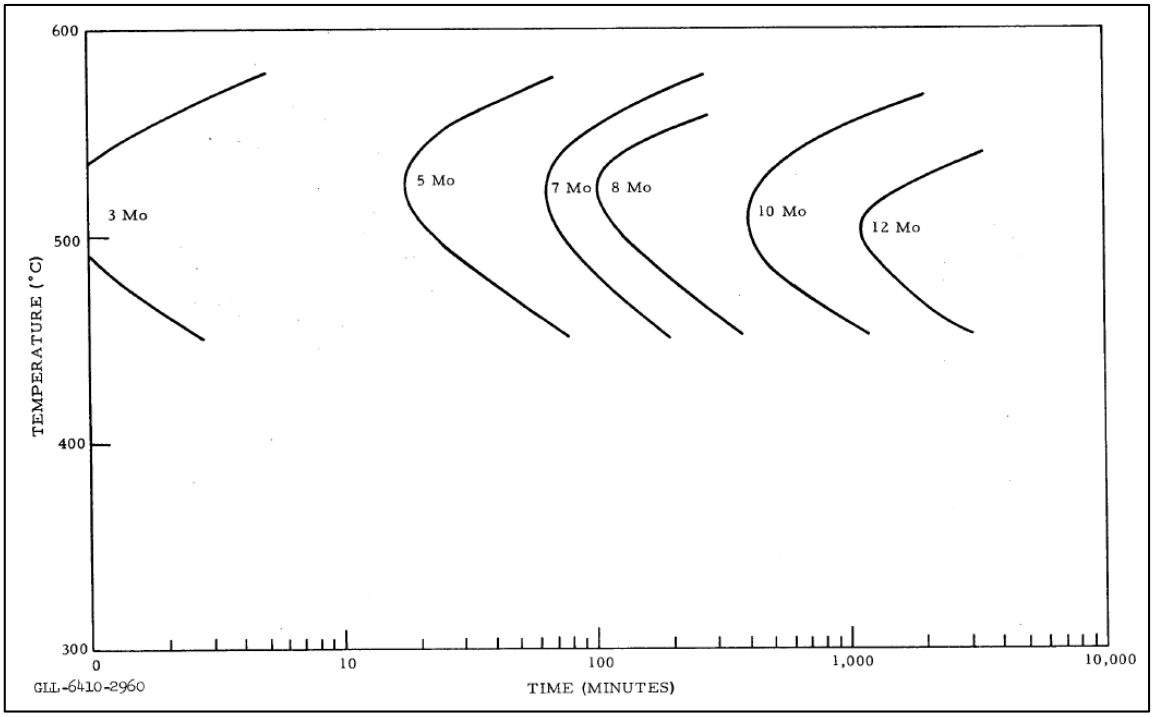

Figure 2-3. TTT diagram of uranium-molybdenum alloys showing the decomposition of γ-phase into α-phase (compositions given in wt%) [14].

Upon decomposition of the γ-U phase, α-U and U_2Mo (γ') are formed as shown in the phase diagram presented in Figure 2-4. This eutectoid reaction is observed to occur at 565°C [15]. The γ'-phase is an ordered tetragonal body centered phase with a=3.427Å and c=9.834Å. The structure of the γ'-phase is a molybdenum atom surrounded by eight uranium atoms. These uranium atoms are surrounded by another four molybdenum atoms each [16]. It was expected that all three of the above listed phases would be observed throughout the course of this research.

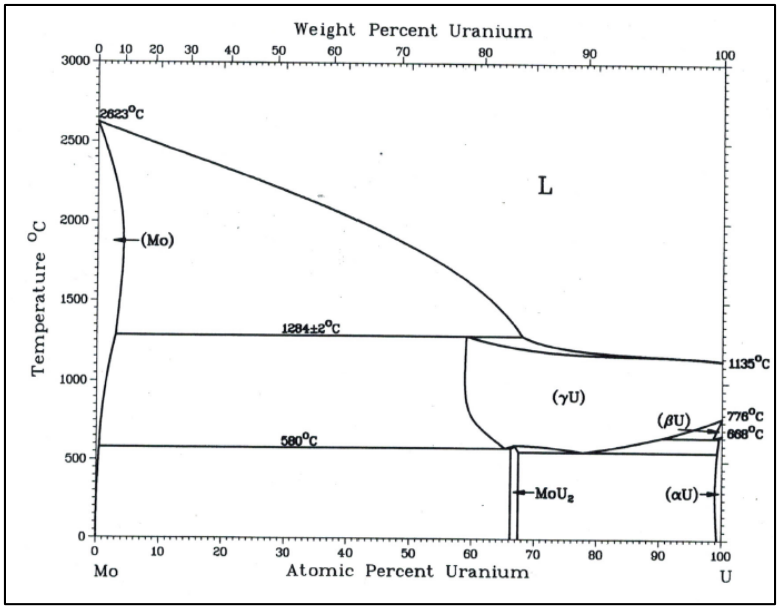

Figure 2-4. Binary phase diagram of the uranium-molybdenum system. [17].

2.1.3. The Uranium-Zirconium System

The U-Zr system is also well studied, although arguably more complicated than the uranium-molybdenum system. Many of the phase transformations that may occur in the U-Zr system are presented in Table 2-1 which was compiled by Sheldon and Peterson [18].

Table 2-1. Various points of interest for the U-Zr system [18].

Reaction	Composition of the respective phases, at.% Zr			Temperature, °C	Reaction type
$L \leftrightarrow U$		0.0		1135	Freezing point
$\gamma U \leftrightarrow \beta U$		0.0		776	Allotropic transformation
$\beta U \leftrightarrow \alpha U$		0.0		669	Allotropic transformation
$\gamma_1 \leftrightarrow \gamma_2 + \beta U$	10.9	42.4	1.1	693	Monotectoid
$\beta U \leftrightarrow \alpha U + \gamma_2$	0.8	0.5	60	662	Eutectoid
$\alpha U + \gamma_2 \leftrightarrow \gamma$	~0.5	~66	63	617	Peritectoid
$\gamma_2 \leftrightarrow \gamma + \alpha Zr$	~81	~78	99.6	606	Eutectoid
$L \leftrightarrow \beta Zr$		100		1855	Freezing point
$\beta Zr \leftrightarrow \alpha Zr$		100		862	Allotropic transformation

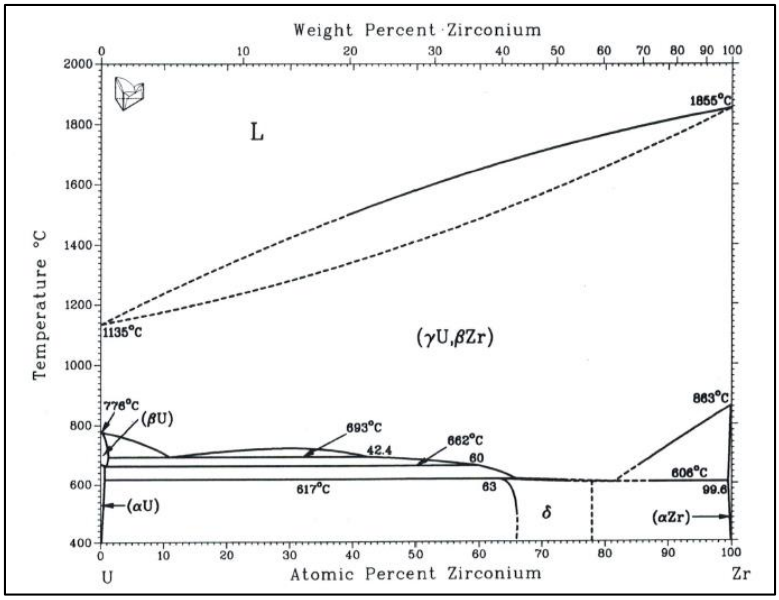

Figure 2-5. Binary phase diagram of the uranium-zirconium system. [17].

Based on the binary phase diagram in Figure 2-5, it was determined that γ-U, β-Zr, α-U, and δ-phase (UZr_2) may be observed in the alloys generated for this research. The δ-phase is the only intermetallic phase in the U-Zr system [19]. Its formation methods are extremely complicated and still debated [19, 20]. It is a complex phase characterized by a modified C32 ($A1B_2$-type) structure [21]. The δ-phase formation has been observed to be significantly inhibited by the presence of nitrogen and oxygen impurities that stabilize α-U and α-Zr [18].

2.1.4. The Molybdenum-Zirconium System

The binary phase diagram for the Mo-Zr system is presented in Figure 2-6 and shows that the Mo_2Zr intermetallic phase exists at ranges from roughly 33 at% to 40 at% zirconium depending on the temperature. This intermetallic phase is characterized by a

Laves cubic $MgCu_2$ (C15) phase [22]. Research on the swelling and phase stability of the Mo-Zr system was conducted in the 1970's using Cu ion irradiation. It was observed that radiation induced the precipitation of Mo_2Zr intermetallics along grain boundaries, which increased with temperature and dose [23].

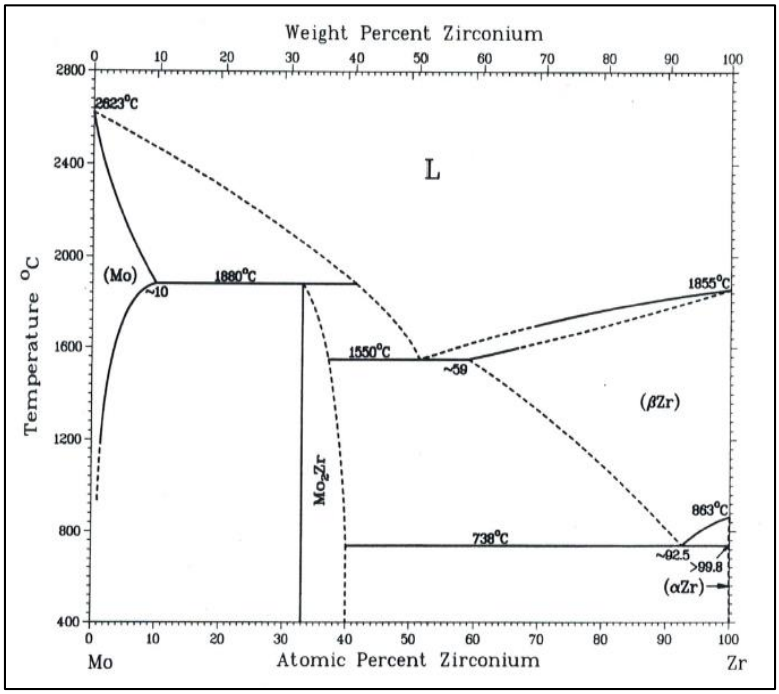

Figure 2-6. Binary phase diagram of the molybdenum-zirconium system. [17].

2.1.5. The Uranium-Molybdenum-Zirconium System

The ternary U-Mo-Zr system has not been extensively studied. Some phase diagrams exist (Figure 2-7 and Figure 2-8), along with TTT diagrams (Figure 2-9) from studies performed in the 1960's [24, 25]. The ternary phase diagram in Figure 2-7 shows the approximate location of the six alloys that were fabricated and studied as part of this

research. More recently, this ternary system has become of interest in order to understand possible behaviors of U-Mo fuel plates with a zirconium foil barrier layer [9].

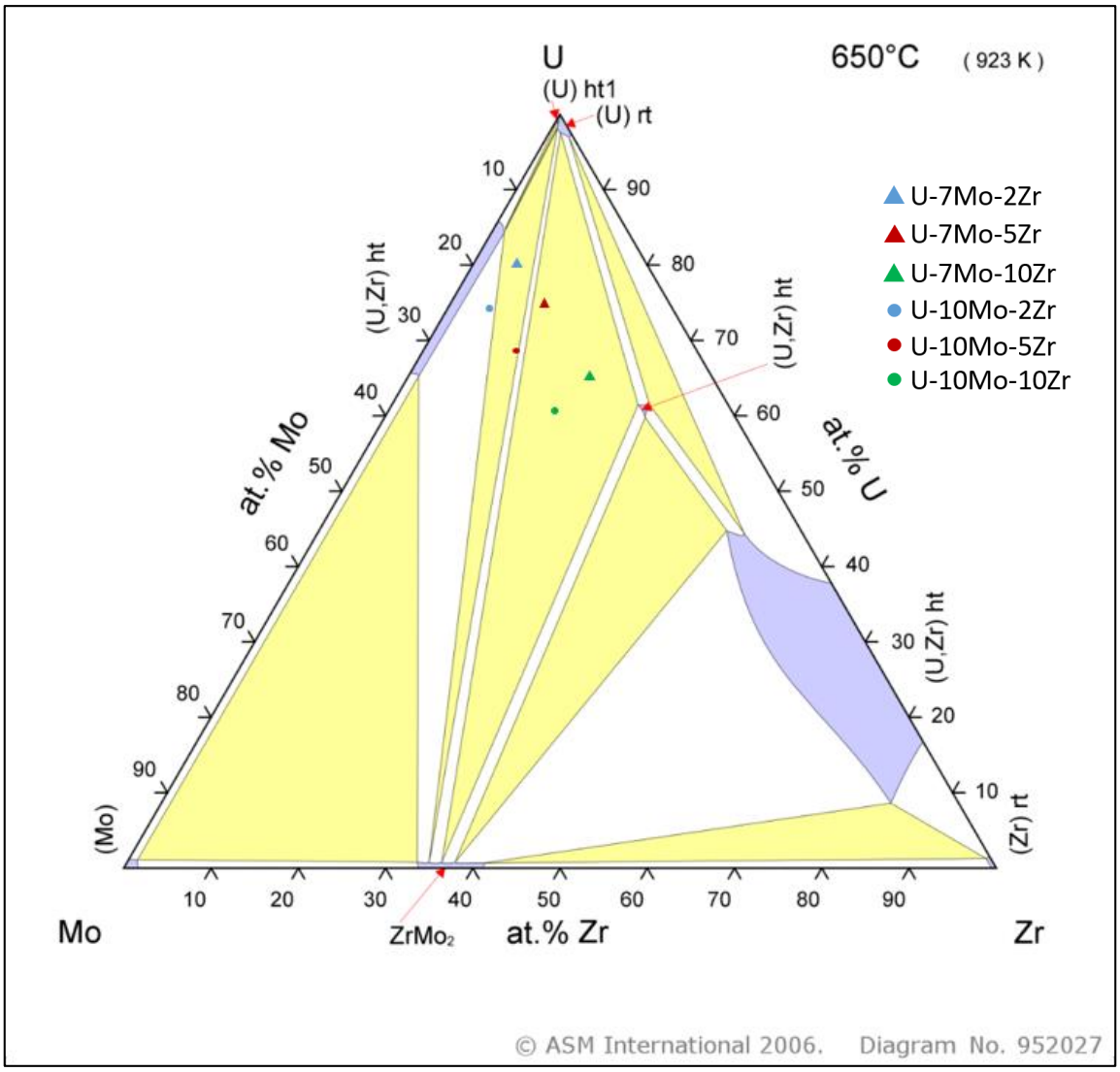

Figure 2-7. Isothermal (650°C) ternary phase diagram for U-Mo-Zr. Note: Alloys compositions given in weight percent and diagram given in atom percent. [24].

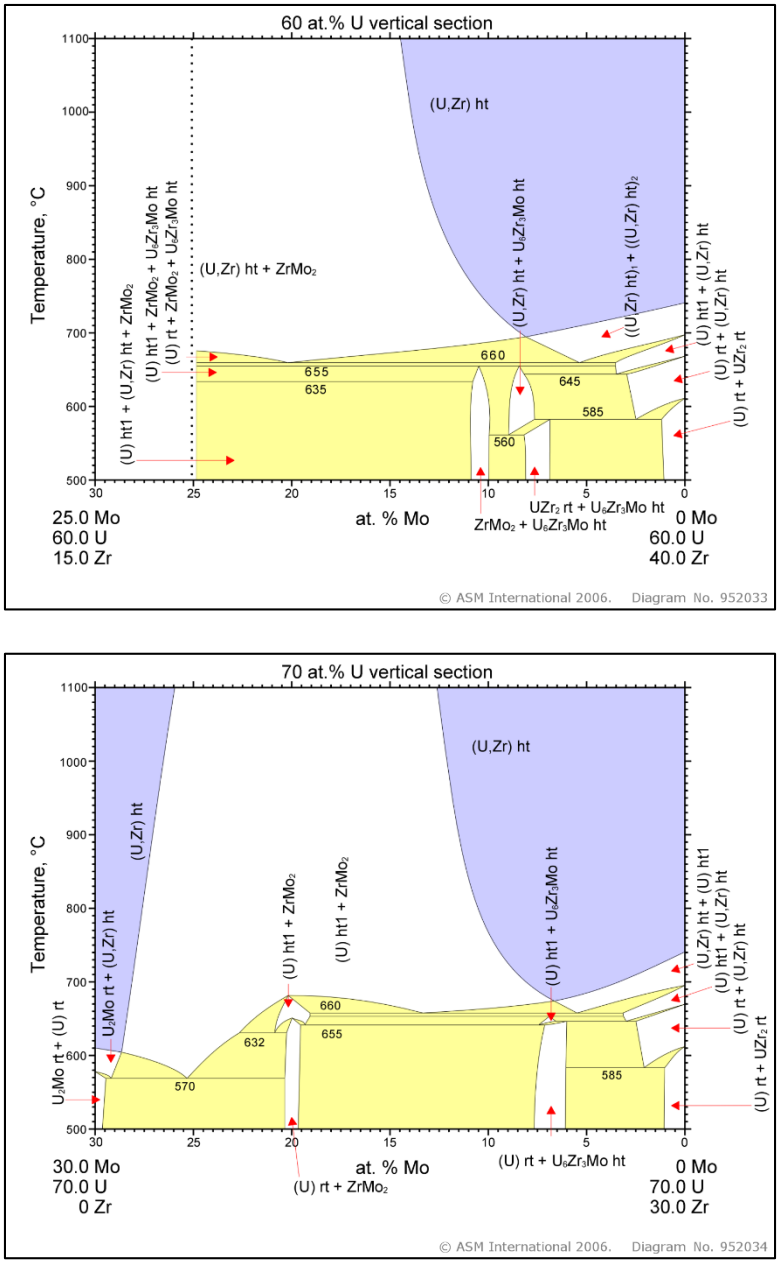

Figure 2-8. Partial composition range ternary phase diagrams (top: 60at% U, bottom: 70at% U) for U-Mo-Zr. [24].

The alloys fabricated using the procedures in Section 3.1.1 were annealed at 650°C; the phase diagram presented in Figure 2-7 indicates phases that may be present

after annealing. A partial composition range phase diagram is shown in Figure 2-8 for alloys of 60 at% and 70 at% uranium. These two compositions are similar to those of U-10Mo-5Zr (68.93 at% U) and U-10Mo-10Zr (60.90 at% U) alloys that are presented later. Based on these diagrams, it is apparent that the following phases may be observed after annealing: α-U, γ-U, and the Mo_2Zr intermetallic phase.

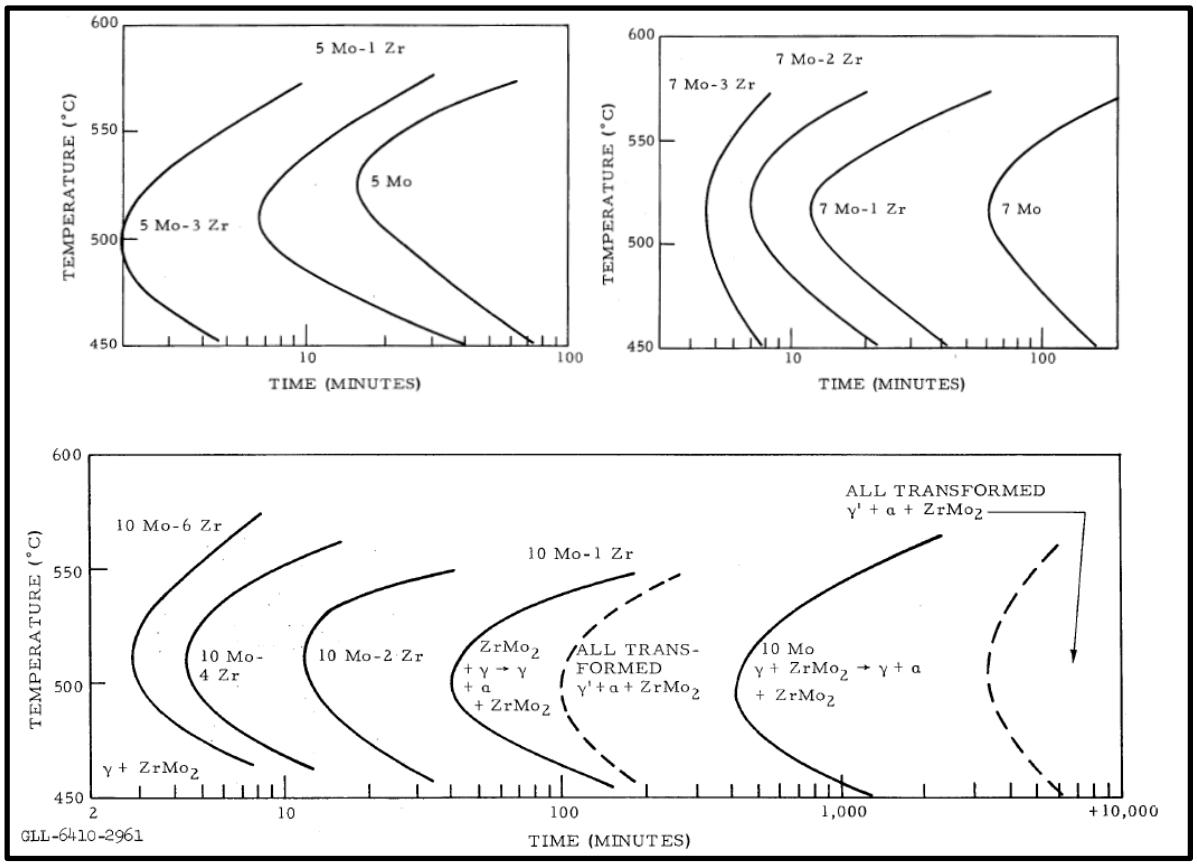

Figure 2-9. TTT diagrams for various U-Mo-Zr alloys (compositions given in wt%) [14].

The TTT diagrams presented in Figure 2-9 show that the addition of even a small amount of zirconium tends to decrease the amount of time it takes for γ-phase alloys to

decompose. This decomposition occurs most rapidly at or slightly above 500°C and is only on the order of minutes to hours.

2.2. Standard RERTR Fuel Plate Fabrication

In order to provide context throughout the remainder of this document, a brief overview of the standard fuel plate fabrication procedure is presented here. The U-10Mo fuel alloy is fabricated by arc melting uranium and molybdenum in a three step flip procedure within an argon atmosphere glove box [26]. The resulting ingot is cleaned using nitric acid and laminated with zirconium foil on both sides in a carbon steel can. The ingot is roughly 3000 μm thick and the zirconium foil is 2 μm thick. This assembly is placed in a furnace at 650°C then co-rolled until the zirconium foil reaches a thickness of roughly 25 μm. This results in a total foil thickness of roughly 300 μm and takes approximately 20-30 passes through the rolling mill. Throughout the rolling process, the foil sees about 130 minutes at 650°C then is annealed for an additional 45 minutes [27].

The foil is then removed from the carbon steel can and the outer surface is polished in preparation for cladding [27]. The foil is placed within a small pocket of a ~1000 μm thick Al6061 sheet and topped with a ~600 μm thick Al6061 sheet. This fuel plate assembly is then bonded using a hot isostatic press (HIP) at 560°C and 100MPa for 90 minutes [28].

2.3. X-Ray Diffraction

X-ray diffraction was used for qualitative structural analysis of the alloys fabricated in this study to determine what phases may be present. XRD analysis identifies

the spacing between planes of atoms by utilizing Bragg's law. Constructive interference occurs when Bragg's law is satisfied and the spacing between planes can be calculated, given the incident angle of X-rays. XRD can be used to assist in determination of the atomic structure of a material, or as in this case, it can be used to determine the presence of various phases.

There are many factors that can influence the peak width of the XRD data or slightly shift the peaks. This can include a lack of long range order, which would have an effect on the ratio of peak heights for a given phase. Residual stresses in the alloy can cause all peaks of a given stressed phase to shift. If the atoms of a phase are compressed or in tension, this could cause the peaks to shift to the left or right, respectively. If the sample surface is not exactly parallel to the stage, this can also cause a slight shift to the left or right of all the peaks.

Reference data exists that specifies what peaks should be present for a given uranium phase, or uranium alloy of interest. Comparison of data generated through analysis with the reference data can provide an idea of what phases may be present in the alloys. It was expected that α-U, γ-U, an intermetallic δ, an intermetallic γ', and an intermetallic Mo_2Zr phase may be present. Reference angles for these phases are presented in Appendix A, with the exception of δ-phase.

3. EXPERIMENTAL DESIGN

This section includes details on alloy fabrication and preparation techniques for the U-Mo-Zr alloys. Analysis techniques utilized include an electron-probe micro-analyzer (EPMA) with wavelength dispersive spectroscopy (WDS), X-ray diffraction (XRD), and differential scanning calorimetry (DSC).

3.1. Alloy Fabrication

3.1.1. Alloy Casting

All alloys were prepared in the same manner using the procedure described in this section. Depleted uranium (DU) pieces were cut to suitable sizes and weighed to determine the appropriate amount of molybdenum and zirconium required to create the desired alloys. Nuclear grade zirconium crystal bars were cut using a diamond saw to correct proportions and cleaned in ethanol using an ultrasonic cleaner. Molybdenum was prepared the same way. Molybdenum without an analysis certificate was used for the U-2Mo and U-5Mo series of alloys, and 99.96% certified pure molybdenum from Alfa Aesar was used for the U-7Mo and U-10Mo alloys. The DU was cleaned in a solution of ~40% nitric acid in water. Additional nitric acid was added when the reaction was observed to slow down or stop. Once the removable surface oxidation was eliminated, the DU pieces were rinsed in water then placed in ethanol and cleaned in an ultrasonic cleaner.

Final alloy constituent masses were recorded and the DU, molybdenum, and zirconium were loaded into yttrium oxide crucibles which were immediately placed in the furnace. Table 3-1 shows the recorded constituent masses for the cast alloys prepared for

this project and Table 3-2 shows the calculated weight and atom percent of the constituents of a given alloy based on the values in Table 3-1.

Table 3-1. Mass of alloy constituents.

Nominal Alloy	Mass (grams)			
	DU	Mo	Zr	Total
U-2Mo-1Zr	17.53	0.366	0.185	18.1
U-2Mo-2Zr	21.86	0.466	0.458	22.8
U-5Mo-1Zr	11.11	0.589	0.118	11.8
U-5Mo-2Zr	16.55	0.879	0.352	17.8
U-5Mo-5Zr	13.45	0.736	0.724	14.9
U-7Mo-2Zr	14.39	1.108	0.315	15.8
U-7Mo-5Zr	13.04	1.039	0.736	14.8
U-7Mo-10Zr	9.658	0.824	1.170	11.7
U-10Mo-2Zr	13.07	1.484	0.298	14.9
U-10Mo-5Zr	10.52	1.251	0.628	12.4
U-10Mo-10Zr	10.13	1.281	1.275	12.7

Table 3-2. Weight percent and atomic percent distributions for alloys based on alloy constituent masses.

	Weight Percent			Atom Percent		
Alloy	DU	Mo	Zr	DU	Mo	Zr
U-2Mo-1Zr	97.0%	2.02%	1.02%	92.7%	4.80%	2.54%
U-2Mo-2Zr	95.9%	2.05%	2.01%	90.3%	4.78%	4.94%
U-5Mo-1Zr	94.0%	4.99%	1.00%	86.3%	11.4%	2.39%
U-5Mo-2Zr	93.1%	4.95%	1.98%	84.2%	11.1%	4.67%
U-5Mo-5Zr	90.2%	4.93%	4.85%	78.4%	10.6%	11.0%
U-7Mo-2Zr	91.00%	7.01%	1.99%	80.12%	15.31%	4.57%
U-7Mo-5Zr	88.0%	7.01%	4.97%	74.4%	14.7%	11.0%
U-7Mo-10Zr	82.9%	7.07%	10.0%	65.5%	13.9%	20.7%
U-10Mo-2Zr	88.0%	9.99%	2.01%	74.6%	21.0%	4.43%
U-10Mo-5Zr	84.9%	10.1%	5.06%	68.9%	20.3%	10.7%
U-10Mo-10Zr	79.85%	10.10%	10.05%	60.90%	19.10%	19.99%

All alloys were melted and furnace cooled in a Materials Research Furnace (MRF) high-temperature tungsten-mesh furnace using a two-step flip procedure. The furnace was evacuated and backfilled with argon three times, then argon was allowed to flow through the furnace while maintaining a positive pressure of roughly 2 psi. Table 3-3 contains the heating profiles used to cast the alloys. The profile labeled (a) was used for the U-2Mo and U-5Mo series of alloys. The profile labeled (b) was used during the casting of the U-7Mo and U-10Mo alloys.

Table 3-3. Temperature profiles for casting U-Mo-Zr alloys.

(a)

Temperature Step (°C)	Step Time (Minutes)
Hold 20	1
20 → 1700	50
Hold 1700	60
1700 → 1150	30
1150 → 600	55
600 → 20	25

(b)

Temperature Step (°C)	Step Time (Minutes)
Hold 20	1
20 → 300	30
300 → 1700	48
Hold 1700	60
1700 → 1150	30
1150 → 600	55
600 → 20	25

After the first melting in the furnace, the samples were removed from their respective yttrium oxide crucibles and surface oxidation was removed to the extent possible using sandpaper. The ingots were then cleaned using ethanol in an ultrasonic cleaner and placed in a new yttrium oxide crucible; oriented in such a way that what was previously the top, was on bottom. The same temperature profiles were again followed for

the second melt of the ingots. This two-step casting procedure was used to generate bulk homogeneity. Figure 3-1 shows an ingot (U-10Mo-10Zr) being removed from its crucible after casting.

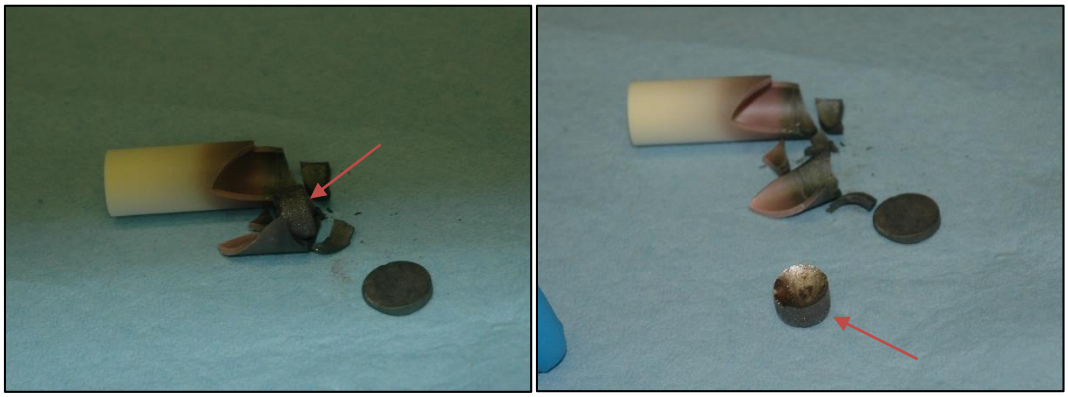

Figure 3-1. Example of ingot (U-10Mo-10Zr) as it is removed from the crucible after casting.

3.1.2. Ingot Sectioning

After the casting procedure in Section 3.1.1, the alloy samples were sectioned as a necessary part of sample preparation for annealing and the various analyses. Sectioning was performed on a LECO VC50 Diamond Saw. The cast ingots were sectioned on two different occasions: initially a piece of the ingot was cut to allow for as-cast characterization, afterwards the alloy was sectioned prior to homogenization and annealing.

Figure 3-2 (a) shows a sketch of how the ingot was initially sectioned. The smaller piece was mounted in a phenolic ring mount for EPMA analysis of the as-cast alloys, discussed in Section 3.2.1.

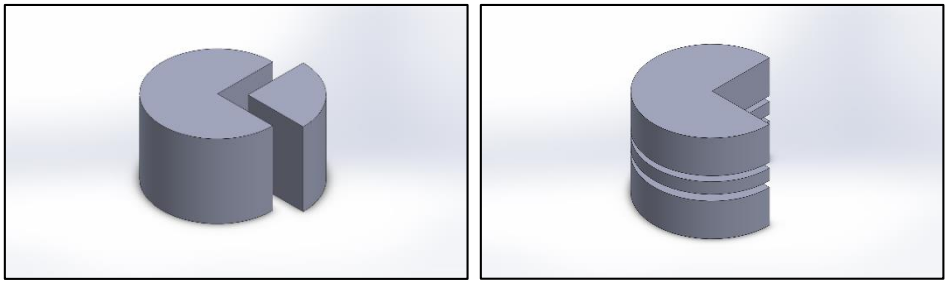

(a) **(b)**

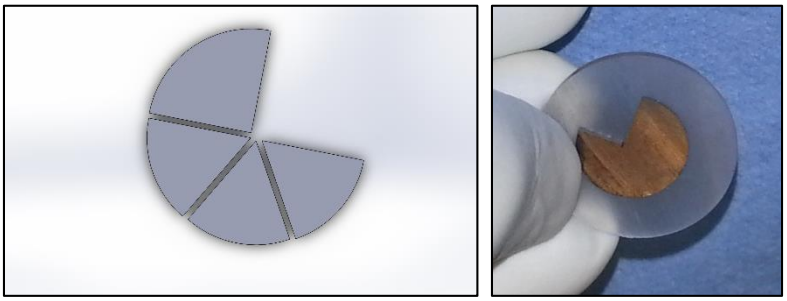

(c) (d)

Figure 3-2. Ingot sections.

The ingots were further sectioned as shown in Figure 3-2 (b) and (c) after reviewing the initial EPMA data and determining a homogenization and annealing schedule. This allowed for the sample to be utilized most efficiently. The ingots had to be mounted in epoxy in order to make the precise cuts in Figure 3-2 (b). Figure 3-2 (d) shows a disc ~1mm in thickness from the center of an ingot prior to removal from epoxy. Small cuts were made along the edges of the final wedge shaped pieces to allow them to be identified after heat treatments. The bottom section was used for XRD and EPMA analyses, the middle section was used for DSC analyses, and the top section was saved for archive purposes or to be used as a spare.

3.1.3. Homogenization and Annealing

The alloys were sectioned as described in Section 3.1.2, then sanded to remove surface oxidation. Due to the sample geometry and small size, complete removal of oxidation by mechanical means was impossible. Sample sections were grouped by alloy, typically one piece each from the top, middle, and bottom of the alloy, and wrapped in tantalum foil. Four total quartz tubes were loaded with samples so that they contained one section from each alloy, as shown in Figure 3-3. Each quartz tube was then evacuated and sealed.

Figure 3-3. Sealed quartz tube before homogenization or annealing. Tube contains 3 samples each of 6 alloys (L to R: U-7Mo-2Zr, U-7Mo-5Zr, U-7Mo-10Zr, U-10Mo-2Zr, U-10Mo-5Zr, U-10Mo-10Zr).

All four quartz tubes were loaded into a Lindberg Blue Tube Furnace and homogenized at 950°C for one week. The furnace was then turned off and the alloys allowed to cool within the furnace over the course of 24 hours. One quartz tube was then separated to be used for analyses. Figure 3-4 shows the quartz tubes after the homogenization. The three remaining quartz tubes were annealed at 650°C, with one tube each being removed and air quenched after one hour, two hours, and five hours.

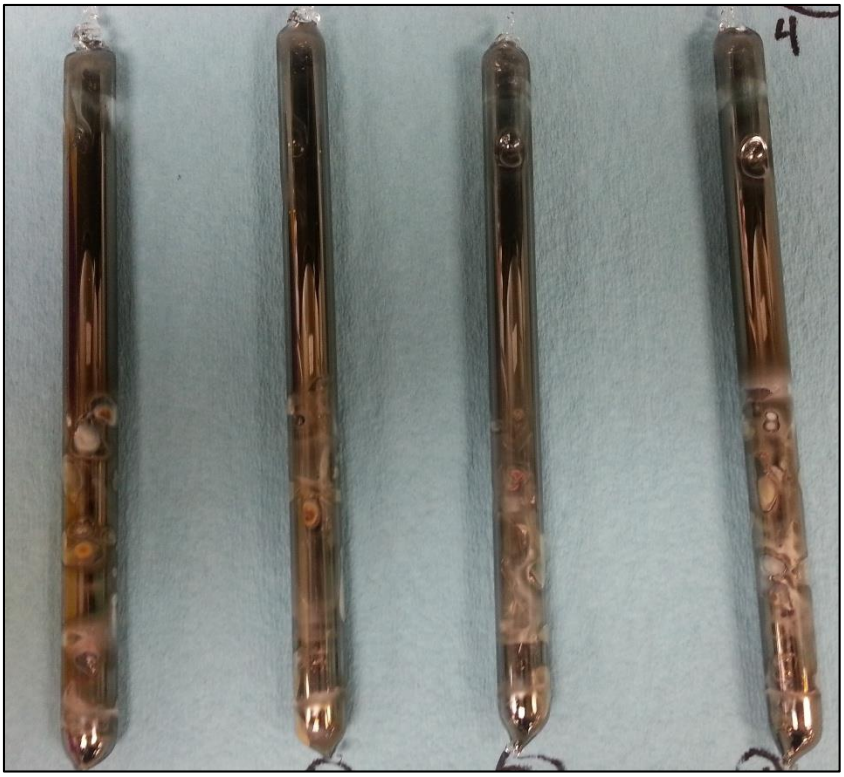

Figure 3-4. All four quartz tubes after homogenization and before annealing.

3.2. Alloy Characterization

3.2.1. Electron-probe Micro-analyzer Analysis

Electron-probe micro-analyzer analysis was performed on all as-cast, homogenized, and annealed alloys. The analyses were performed using a Cameca SX50 instrument operated by the Texas A&M Geology Department. Standard operating procedure included a carbon coating of the sample in order to avoid electrical charge buildup while the sample was in the instrument. This carbon coating also served to retard oxidation of the sample. Electron-probe micro-analyzer analysis included BSE imaging, capturing EDS spectra, and performing WDS analyses in various locations of the sample.

Images were acquired with an accelerating voltage of 15kV, and a beam current of either 3nA or 10nA. The current was varied to allow for the sample to be studied at different contrast levels, highlighting phases that may not be visible under all conditions. WDS data was collected with a beam current of 40nA and an accelerating voltage of 15kV. WDS analysis required standardization of the detectors in order to ensure accuracy.

While the instrument can detect oxygen, the results tend to be inaccurate. The alloys studied oxidize rapidly, and thus often have a layer of surface oxidation simply from the time it takes to transfer the samples between laboratories. The analysis software used in conjunction with the Cameca instrument calculates weight percentages based on the assumption that the top 1μm is completely homogenous, although the measurement does not analyze composition to that depth. Due to this, the software incorrectly assumes that surface oxidation is distributed throughout the sample and calculates a value higher than actuality. If the calculated oxygen content is subtracted from the total alloy weight percent of constituents given by the software, the value is often closer to 100%, a more realistic measurement.

The nitrogen and yttrium detected is also incorrect in the reported values. To demonstrate that the nitrogen and yttrium values given for WDS analyses are likely higher than reality, a WDS analysis was performed on a UO_2 standard, the results of which can be found in Table 3-1. Based on this, nitrogen and yttrium values presented throughout can be considered trivial unless noted otherwise.

Table 3-4. WDS analysis of UO_2 standard.

	Composition	
	wt%	**at%**
U	88.05	31.2
Mo	0.01	0.01
Zr	0.00	0.00
O	11.95	63.01
N	0.95	5.71
Y	0.08	0.08
Total	101.04	100.01

Electron-probe micro-analyzer analysis requires a very flat surface that is free of scratches in order to avoid influencing the scattering of x-rays. Sections of alloys were mounted and polished using standard metallographic techniques. A Buehler MiniMet™ 1000 was used to polish all sample mounts. A nominal polishing schedule is shown in Table 3-5, although this was not always followed explicitly. The 0.25 μm diamond suspension polishing step was performed immediately before carbon coating in order to minimize surface oxidation present on the sample.

Table 3-5. General polishing schedule for EPMA analysis.

Grit	Weight (pounds)	Time (minutes)
180	4	8-12
240	4	8-12
400	4	8
600	4	8
800	2	8
1200	2	8
3 μm	2	4
1 μm	2	4
0.25 μm	2	4

3.2.2. X-Ray Diffraction Analysis

X-ray diffraction analysis was performed on all homogenized and as-cast samples and used to determine what phases may be present for a given alloy and annealing treatment. Preparation for XRD was very similar to that of EPMA, described in Section 3.2.1. X-ray diffraction analysis does not require as flat of a surface as EPMA, so XRD was performed on the samples after the 800 grit polishing step. The similarities in sample prep for EPMA analysis and XRD allowed for the same sample to be used for both analyses. Utilizing the same sample for both EPMA and XRD allowed for integrity of analysis results and for alloy material to be used efficiently.

X-ray diffraction was performed on a Bruker D8 Discover instrument (Figure 3-5) within the Materials Science and Engineering Department at Texas A&M. Each sample was run under the same analysis conditions: 0.07° step size for 2Θ from 20° to 110° with 1 second counts at each step.

Figure 3-5. Bruker D8 Discover instrument used for XRD analysis.

3.2.3. Differential Scanning Calorimetry Analysis

Differential scanning calorimetry analysis of select samples was performed in order to gain an understanding of phase changes that may occur. All DSC measurements were performed on a Netzsch STA 409PC instrument. Alumina crucibles (Al_2O_3) were used for all measurements. Differential scanning calorimetry samples were cut from the middle section of the alloy ingots as seen in Figure 3-2 (c) and (d). Sample sizes for the DSC ranged from 20 mg to 50 mg. These samples were ground with 400 grit sandpaper to remove surface oxidation, however, the sample size again made it impossible to completely remove all surface oxidation. The samples were then washed in ethanol in an ultrasonic cleaner prior to loading into the crucibles. Upon generation of EPMA and XRD results, a heating schedule was decided upon and is shown in Table 3-6.

The temperature range of interest (500°C to 800°C) was chosen based on the phase diagrams of the uranium, molybdenum, and zirconium alloys. This range encompasses all of the potential phase changes that would be of interest for this research study. This

temperature cycle was repeated three times in order to help determine the stability of a given phase. A heating rate of 5°C through this range was used so that any phase changes would be clearly visible. A 10 hour anneal at 650°C was performed following the first three heating/cooling cycles. This annealing temperature was chosen to replicate fabrication conditions of fuel plates [27]. After the 10 hour anneal, an additional three cycles were performed in order to see if any different phases appeared.

Table 3-6. Heating profile for DSC analyses.

Temperature Step (°C)	Duration (minutes)	
20-500	48	
Hold 500	60	x3
500 to 800	60	
Hold 800	60	
800 to 500	60	
500-650	30	
Hold 650	600	
650-500	30	
Hold 500	60	x3
500 to 800	60	
Hold 800	60	
800 to 500	60	
500-20	48	

4. RESULTS

This section provides the data generated using the various analytical techniques described in Section 3.2. The EPMA and WDS data are presented separately for each alloy, organized by heat treatment. XRD data are presented by alloy so that the effect of annealing may be easily observed. All DSC data are presented together in order to allow for easier comparison. The overall test matrix in Table 4-1 shows an overview of the analyses performed for each alloy and heat treatment. In the table, the subheadings H, 1, 2, and 5 refer to homogenized, 1 hour annealed, 2 hour annealed, and 5 hour annealed alloys, respectively.

4.1. Sample Design

Analysis of initial as-cast alloys was completed to determine the homogenization and annealing schedule, along with additional alloy compositions. The U-2Mo and U-5Mo alloys were the first alloys cast and appeared to be macroscopically homogenous and solid solutions with various oxygen or zirconium impurities.

Table 4-1. Matrix highlighting the analyses performed on the U-xMo-yZr alloys.

Alloy	Final Casting	Initial EPMA *(As Cast)*	Anneal @ 950ºC *(Homogenize)*	Anneal @ 650ºC (1,2,5 hr)	EPMA				XRD				DSC			
					H	**1**	**2**	**5**	**H**	**1**	**2**	**5**	**H**	**1**	**2**	**5**
U-2Mo-1Zr	6/7/2013	✓														
U-2Mo-2Zr	6/7/2013	✓														
U-5Mo-1Zr	5/7/2013	✓														
U-5Mo-2Zr	5/7/2013	✓														
U-5Mo-5Zr	5/7/2013	✓														
U-7Mo-2Zr	12/11/2013	✓	✓	✓	✓	✓	✓	✓	✓	✓	✓	✓	✓			
U-7Mo-5Zr	12/11/2013	✓	✓	✓	✓	✓	✓	✓	✓	✓	✓	✓	✓			
U-7Mo-10Zr	12/11/2013	✓	✓	✓	✓	✓	✓	✓	✓	✓	✓	✓	✓			
U-10Mo-2Zr	12/11/2013	✓	✓	✓	✓	✓	✓	✓	✓	✓	✓	✓	✓			
U-10Mo-5Zr	12/11/2013	✓	✓	✓	✓	✓	✓	✓	✓	✓	✓	✓	✓			
U-10Mo-10Zr	12/11/2013	✓	✓	✓	✓	✓	✓	✓	✓	✓	✓	✓	✓	✓	✓	✓

Table 4-2 shows various WDS analysis data for U-2Mo and U-5Mo series of alloys that were cast initially. Figure 4-1 (a) is a U-2Mo-1Zr alloy and shows a zirconium based impurity (1) with a uranium oxide phase (2) within a solid solution. Figure 4-1 (b) is a U-2Mo-2Zr alloy and shows that the bulk of this alloy appears to be a solid solution. Figure 4-1 (c) is a U-5Mo-5Zr alloy and again shows a zirconium rich (1) impurity in a solid solution.

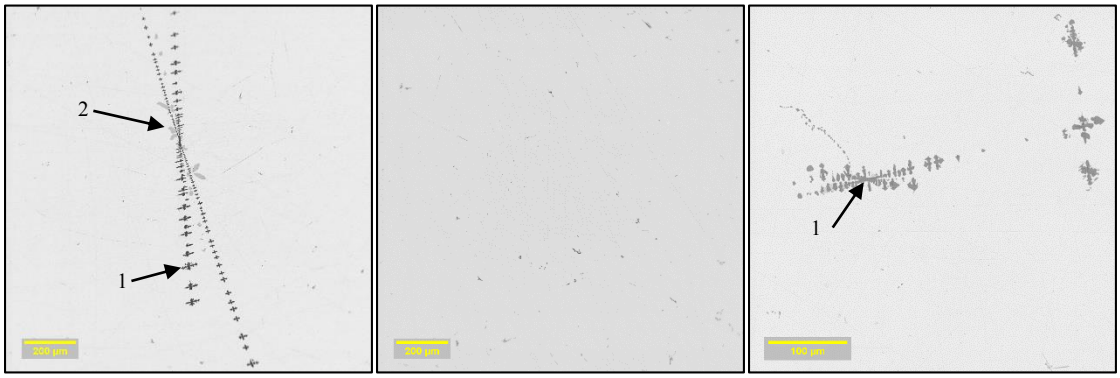

(a) (b) (c)

Figure 4-1. Example images of (a) U-2Mo-1Zr, (b) U-2Mo-2Zr, and (c) U-5Mo-5Zr.

Table 4-2. WDS analysis results for bulk area of U-2Mo and U-5Mo series of alloys.

		Composition (wt%)					Composition (at%)			
		U	Mo	Zr	O	Total	U	Mo	Zr	O
U-2Mo-1Zr	Average (Bulk)	96.75	2.05	0.90	3.19	103.82	57.86	3.05	1.41	28.28
	Standard Deviation (Bulk)	0.02	0.09	0.04	0.47	0.46	2.24	0.17	0.10	3.10
U-2Mo-2Zr	Average (Bulk)	95.69	2.15	1.97	3.01	103.73	57.65	3.22	3.10	26.99
	Standard Deviation (Bulk)	0.15	0.08	0.17	0.24	0.18	0.89	0.16	0.31	1.74
U-5Mo-1Zr	Average (Bulk)	93.56	5.26	0.90	2.13	102.73	60.13	8.40	1.51	20.34
	Standard Deviation (Bulk)	0.38	0.17	0.13	0.12	0.43	1.34	0.49	0.20	0.67
U-5Mo-2Zr	Average (Bulk)	92.74	5.33	1.89	1.78	102.46	61.97	8.83	3.30	17.67
	Standard Deviation (Bulk)	0.33	0.03	0.04	0.03	0.37	0.18	0.04	0.06	0.30
U-5Mo-5Zr	Average (Bulk)	89.63	5.28	4.94	3.34	103.86	50.73	7.41	7.30	28.12
	Standard Deviation (Bulk)	1.01	0.22	0.73	0.19	0.26	0.58	0.34	1.10	1.48

An increase in molybdenum content and zirconium content was decided upon for the next set of alloys, the U-7Mo and U-10Mo alloys. It was decided upon that a test matrix of 7 wt% and 10 wt% molybdenum, combined with 2 wt%, 5 wt% and 10 wt% zirconium would provide a wide range of data in an area that had not been widely studied (see Table 4-1).

The EPMA was used to characterize the morphology of the as-cast alloys and images were collected. No WDS data was collected on these samples since images revealed a lack of homogeneity. The images in Figure 4-2 show that the alloy constituents are relatively well mixed, although microscopically inhomogeneous and not in equilibrium.

The heat treatment schedule described in Section 3.1.3 that included homogenization was determined based on these images. The homogenization of these alloys was performed for 7 days at 950°C. The annealing treatment was determined based on fabrication conditions for actual fuel plates. The samples would be annealed at 650°C for a period of 1, 2, and 5 hours.

4.2. Electron-probe Micro-analyzer and X-ray Diffraction

The images and WDS data results are presented in this section for each alloy studied. Average composition for the bulk material is presented with the standard deviation, along with WDS analyses of various points of interest. Some of the features analyzed with WDS may have experienced an influence from "edge effects" due to their size (~2-3 μm) in comparison with beam diameter (1 μm). That is, the detectors may have picked up some counts from the area around the actual spot being analyzed. Alternatively,

some of the larger spots analyzed with WDS may not be representative of all features similar in appearance. There was often a size discrepancy in small features (1-3 μm or 5-15 μm) as is noticeable in BSE imaging and often only analysis of the larger features was possible, although it may not be representative of all features.

The images that were selected to be representative of the entire sample are presented at various magnifications and contrast levels. It is clear in some images (for example, Figure 4-6 (c) and (d)) that not all phases are necessarily visible at a given contrast level.

All XRD data is also presented by alloy composition. X-ray diffraction data was used to as a qualitative method to determine what phases may be present in these alloys. Tables following the XRD plots indicate what phases are likely present based on a comparison of XRD analytical data and reference data for the various phases. X-ray diffraction on solid samples has some potential problems which are described in Section 2.3 . Additional XRD comparisons highlighting the effect of varying molybdenum or zirconium content are available in Appendix B.

Throughout the XRD analyses performed, no UZr_2 characteristic peaks (20.4°, 28.9°, 46.6°, and 71.8°) were identified in the data [20].

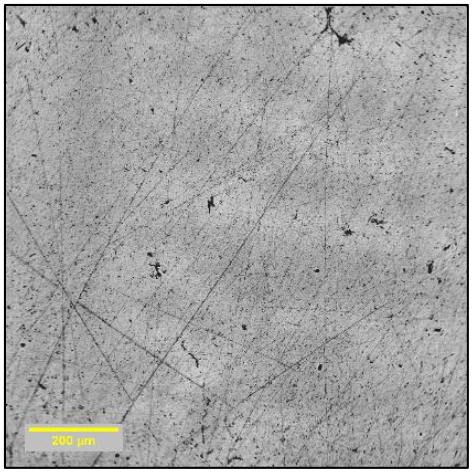

U-7Mo-2Zr

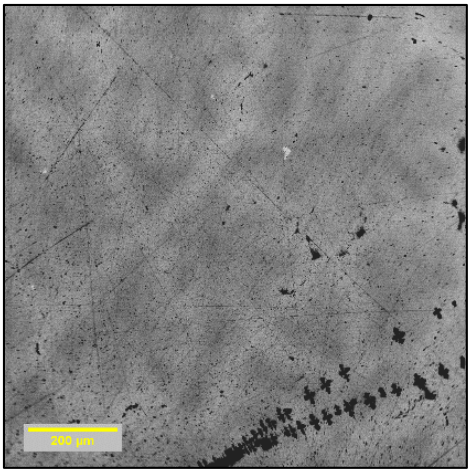

U-10Mo-2Zr

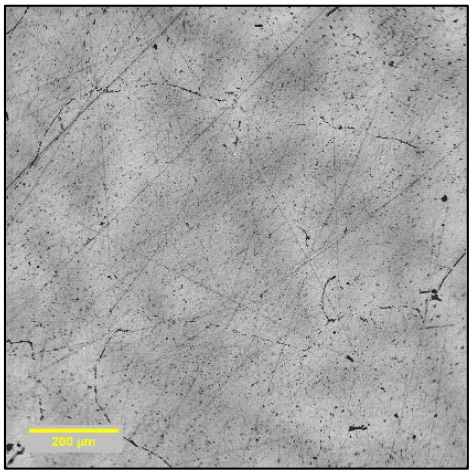

U-7Mo-5Zr

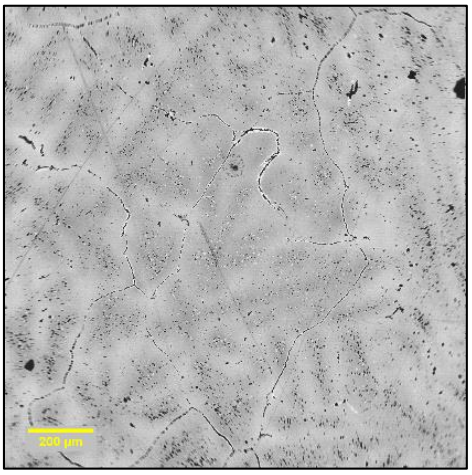

U-10Mo-5Zr

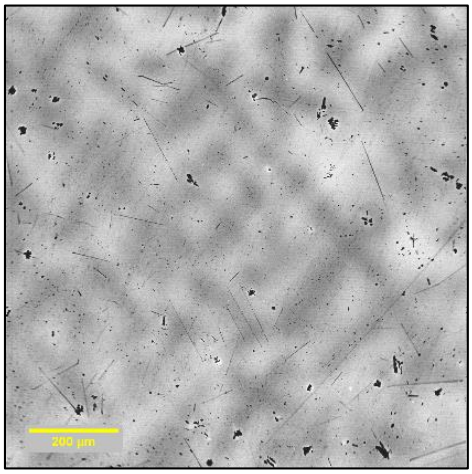

U-7Mo-10Zr

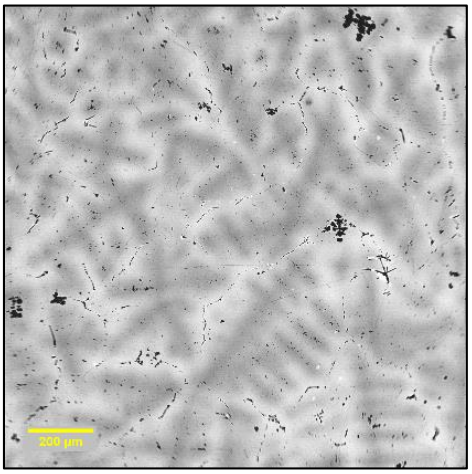

U-10Mo-10Zr

Figure 4-2. Images of as-cast alloys.

4.2.1. U-7Mo-2Zr

4.2.1.1. *Homogenized*

The images of the U-7Mo-2Zr homogenized alloy are presented in Figure 4-3 and WDS data is presented in Table 4-3, followed by a description of the WDS points analyzed.

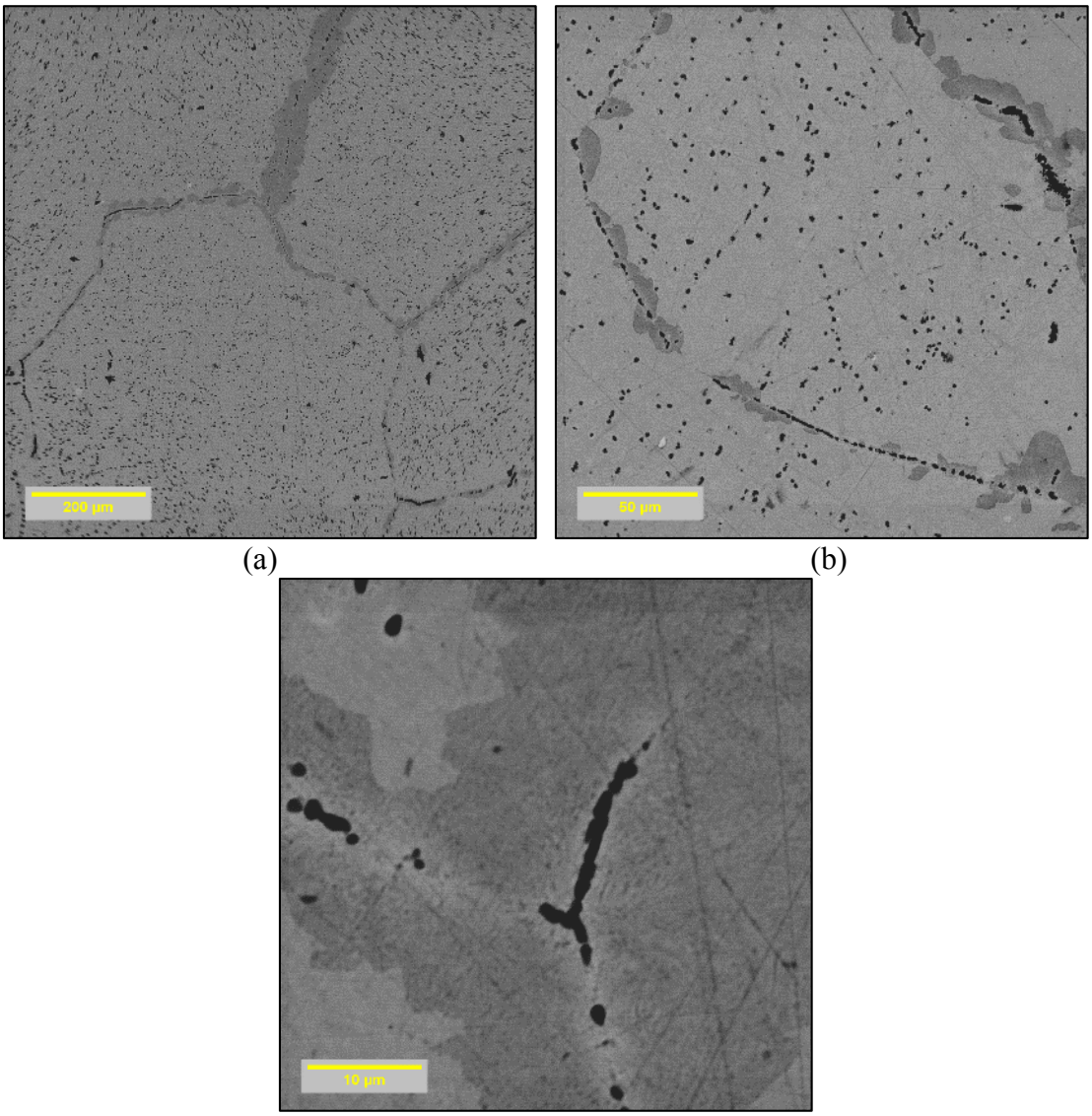

(a) (b)

(c)

Figure 4-3. Images of U-7Mo-2Zr homogenized alloy at (a) 100x, (b) 400x, and (c) 2000x magnifications.

Table 4-3. WDS analytical composition of U-7Mo-2Zr homogenized alloy.

	Composition (wt%)							Composition (at%)					
	U	**Mo**	**Zr**	**O**	**N**	**Y**	**Total**	**U**	**Mo**	**Zr**	**O**	**N**	**Y**
Average (Bulk)	91.01	7.42	1.76	1.53	1.19	0.00	102.91	58.01	11.74	2.93	14.50	12.82	0.00
Standard Deviation (Bulk)	0.20	0.08	0.08	0.18	0.09	0.00	0.22	1.40	0.37	0.18	1.39	0.78	0.00
Point 1	90.90	7.48	1.85	1.47	1.23	0.00	102.93	57.89	11.82	3.07	13.94	13.29	0.00
Point 2	5.75	22.11	63.03	0.81	0.00	0.00	91.69	2.43	23.14	69.38	5.06	0.00	0.00
Point 3	0.59	0.20	82.47	0.61	0.00	0.00	83.87	0.26	0.23	95.48	4.04	0.00	0.00

Point 1 Dark area near grain boundary; bulk

Point 2 Black spot within bulk

Point 3 Black spot within bulk

The composition of the grey area near the grain boundaries is relatively similar to that of the bulk of the sample based on Point 1. Point 2 and 3 however don't correspond to any particular phases or bulk area. They are both zirconium rich phases and are likely locations that the zirconium has gettered impurities.

Point 2 and Point 3 in Table 4-3 have a low total weight. EDS analysis determined this was due to silicon in the sample. This silicon may have been introduced during the homogenization of the alloy when the sample came into contact with the quartz tubing.

4.2.1.2. *1 hour annealed*

Images of the U-7Mo-2Zr 1 hour annealed alloy are presented in Figure 4-4 and WDS data is presented in Table 4-4, followed by a description of the WDS points analyzed.

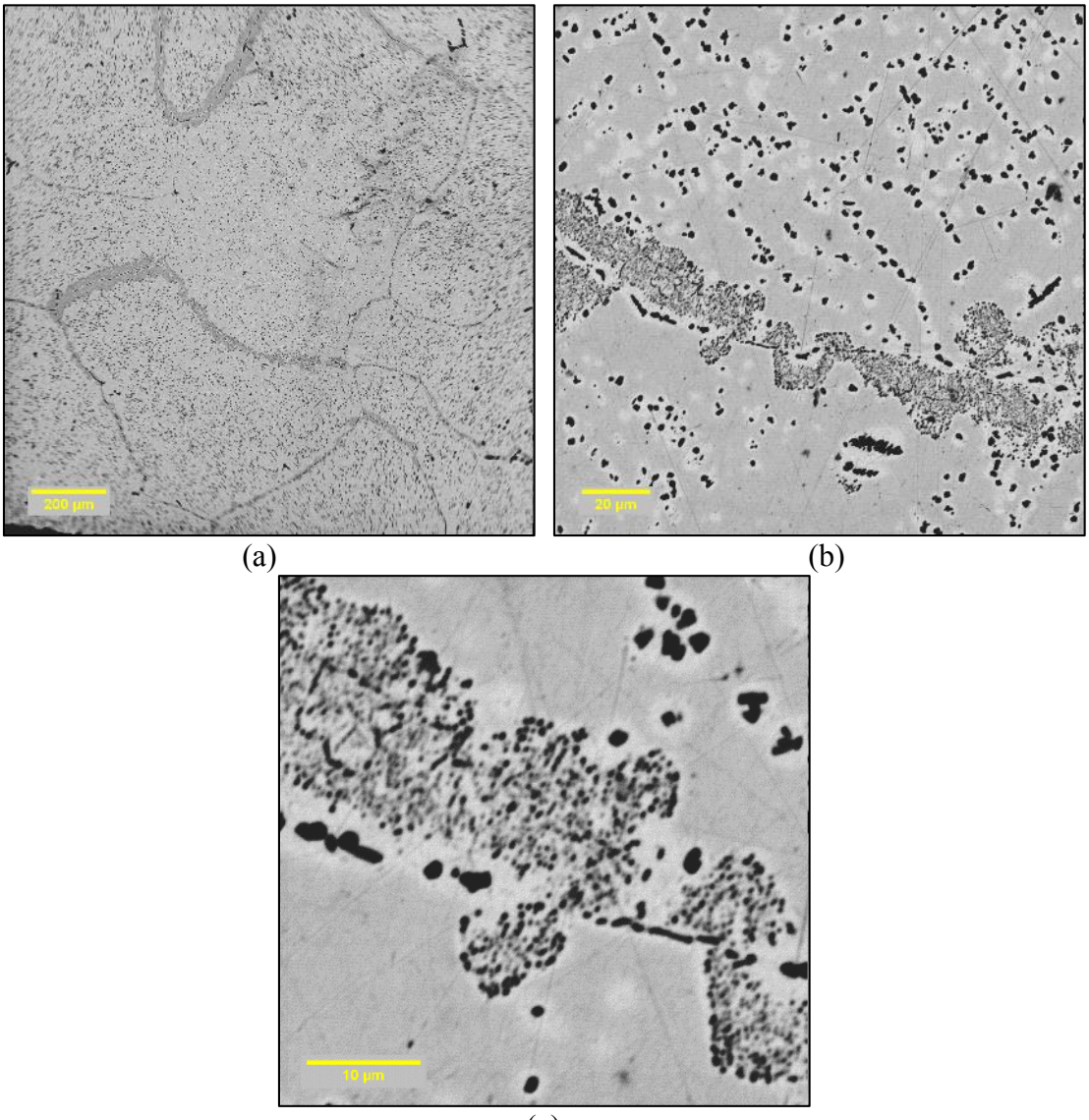

(a) (b)

(c)

Figure 4-4. Images of U-7Mo-2Zr 1hr annealed alloy at (a) 66x, (b) 600x, and (c) 2000x magnifications.

Table 4-4. WDS analytical composition of U-7Mo-2Zr 1hr annealed alloy.

	Composition (wt%)							Composition (at%)					
	U	**Mo**	**Zr**	**O**	**N**	**Y**	**Total**	**U**	**Mo**	**Zr**	**O**	**N**	**Y**
Average (Bulk)	90.90	7.44	1.76	1.45	1.04	0.01	102.60	59.33	12.05	3.00	14.08	11.53	0.03
Standard Deviation (Bulk)	0.09	0.09	0.07	0.19	0.16	0.02	0.05	0.26	0.16	0.10	1.85	1.78	0.03
Point 1	16.76	57.23	29.42	0.49	0.00	0.03	103.92	6.90	58.48	31.62	2.97	0.00	0.03
Point 2	93.24	5.71	1.24	1.70	1.25	0.00	103.14	59.32	9.01	2.06	16.10	13.52	0.00

Point 1: Black spot within bulk; Mo_2Zr intermetallic

Point 2: Bright region near small black spot; uranium enriched

Point 1 tends to correspond to a Mo_2Zr intermetallic phase composition while Point 2 is depleted of molybdenum and zirconium and enriched in uranium. The images show that these brighter regions only occur near grain boundaries or other features within the alloy. Bright phases that seem to appear in the bulk of the alloy likely have a black feature above or below them.

The homogenous grey region observed in the homogenized alloy near the grain boundaries appears to have segregated due to annealing. These small features are dark grey and black in color and are only a fraction of a micron in size. Unfortunately, due to their small size, no WDS data could be collected on these points.

4.2.1.3. *2 hour annealed*

Images of the U-7Mo-2Zr 2 hour annealed alloy are presented in Figure 4-5 and WDS data is presented in Table 4-5, followed by a description of the WDS points analyzed.

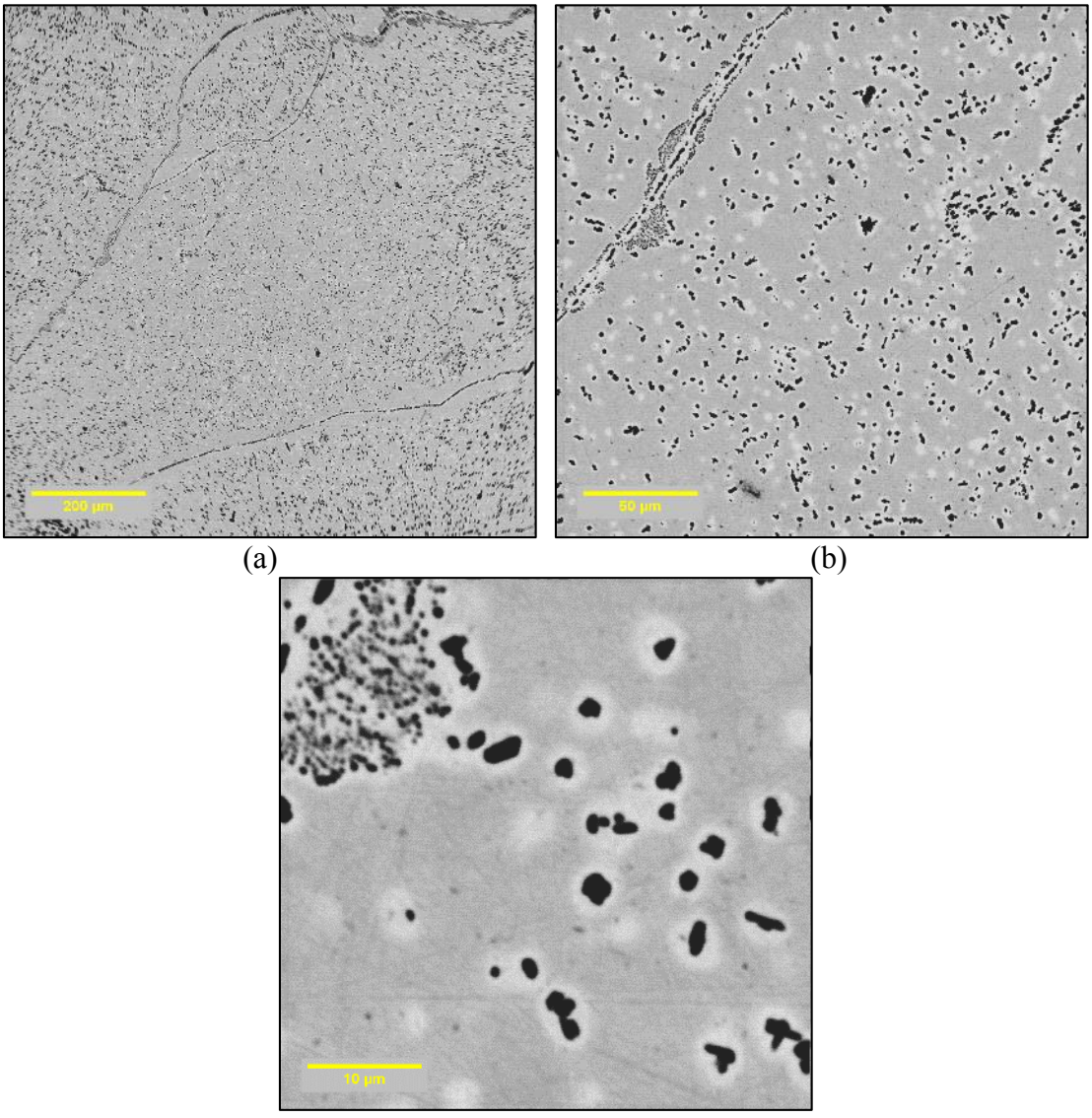

(a) (b)

(c)

Figure 4-5. Images of U-7Mo-2Zr 2hr annealed alloy at (a) 100x, (b) 400x, and (c) 2000x magnifications.

Table 4-5. WDS analytical composition of U-7Mo-2Zr 2hr annealed alloy.

	Composition (wt%)							Composition (at%)					
	U	**Mo**	**Zr**	**O**	**N**	**Y**	**Total**	**U**	**Mo**	**Zr**	**O**	**N**	**Y**
Average (Bulk)	90.43	7.53	1.76	1.46	0.85	0.02	102.05	60.31	12.45	3.06	14.47	9.68	0.03
Standard Deviation (Bulk)	0.15	0.04	0.05	0.11	0.06	0.02	0.13	0.61	0.11	0.07	0.96	0.71	0.04
Point 1	93.22	5.58	0.88	1.18	0.92	0.00	101.77	65.41	9.72	1.60	12.34	10.92	0.00
Point 2	94.08	4.94	0.75	1.80	0.93	0.00	102.50	62.35	8.12	1.30	17.74	10.50	0.00
Point 3	14.24	55.69	30.85	1.19	0.12	0.01	102.09	5.63	54.69	31.86	7.01	0.80	0.01

Point 1: Bright region near small grain boundary; uranium enriched

Point 2: Bright region near small black spot; uranium enriched

Point 3: Black spot within bulk; Mo_2Zr intermetallic

This two hour annealed sample appears similar in composition to the one hour annealed sample. Bright regions are present that are depleted in molybdenum and zirconium and enriched in uranium. Point 3 was an attempt to perform WDS on a small black feature within the bulk of the sample. Due to the size of the black spot, edge effects likely came into play and skewed the elemental ratios. This spot is likely a Mo_2Zr intermetallic phase. Small dark grey and black features again appear near grain boundaries and are roughly the same size as in the one hour annealed alloy.

4.2.1.4. *5 hour annealed*

Images of the U-7Mo-2Zr 5 hour annealed alloy are presented in Figure 4-6 and WDS data is presented in Table 4-6, followed by a description of the WDS points analyzed.

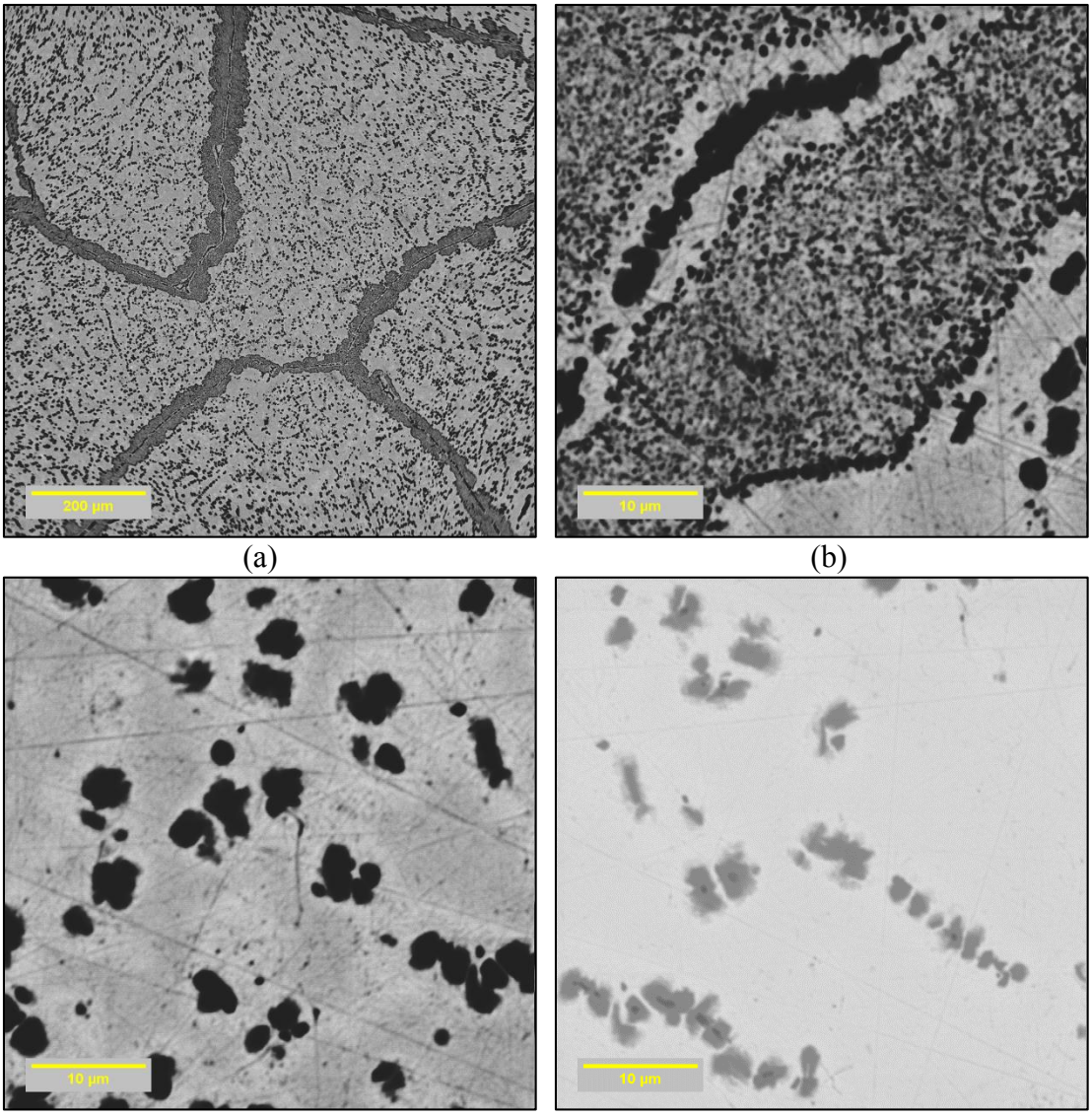

(a) (b)

(c) (d)

Figure 4-6. Images of U-7Mo-2Zr 5hr annealed alloy at (a) 100x, (b) 2000x, (c) 2000x, and (d) 2000x magnifications. Image (d) was taken at low contrast settings.

Table 4-6. WDS analytical composition of U-7Mo-2Zr 5hr annealed alloy.

	Composition (wt%)							Composition (at%)					
	U	**Mo**	**Zr**	**O**	**N**	**Y**	**Total**	**U**	**Mo**	**Zr**	**O**	**N**	**Y**
Average (Bulk)	90.57	7.27	1.82	2.49	0.80	0.00	102.95	55.26	11.00	2.90	22.56	8.27	0.00
Standard Deviation (Bulk)	0.26	0.15	0.09	0.08	0.09	0.00	0.15	1.06	0.23	0.10	0.38	0.81	0.01
Point 1	9.66	61.96	30.23	0.67	0.00	0.00	102.52	3.83	60.95	31.27	3.93	0.03	0.00
Point 2	93.01	5.28	0.81	2.70	0.87	0.01	102.68	56.99	8.02	1.29	24.58	9.10	0.02

Point 1: Black spot within bulk; Mo_2Zr intermetallic

Point 2: Bright region near small black spot; uranium enriched

This five hour annealed alloy appears to be similar to the one hour and two hour annealed alloys. The small black features appear to be a Mo_2Zr phase as indicated by Point 1. The brighter regions are depleted in molybdenum and zirconium while enriched in uranium. The dark grey and black features are still present along the grain boundaries and are still too small to be analyzed by WDS.

Figure 4-6 (c) and (d) are images taken at 2000x magnification with different contrasts. Lowering the contrast has the effect of showing tiny black spots within some of the Mo_2Zr features. These may be locations that a zirconium impurity acted as nucleation sites for the Mo_2Zr intermetallics.

4.2.1.5. *X-Ray Diffraction*

The XRD data collected for the U-7Mo-2Zr alloy is presented in Figure 4-7, along with reference data for the γ-U and γ' phases. The peaks of the samples tend to correspond well with these two phases. Due to the close proximity of these characteristic peaks, it is

impossible to report with certainty that the detected peaks are due solely to one phase or the other. The wider peaks at 52.6°/53.5°, 65.8°/66.7°, and 89°/89.2° likely include counts due to both γ-U and γ' phases being present.

It is interesting to note that WDS data for the annealed samples tends to suggest that Mo_2Zr is present, but it does not clearly show up in the XRD spectra. In all three annealed samples, a wide peak around 89° may include counts from a Mo_2Zr phase, but this cannot be reported with certainty. It is possible that peaks for Mo_2Zr are not visible due to a combination of effects. Poor counting statistics coupled with a phase lacking long range order may make the peaks invisible in the collected data.

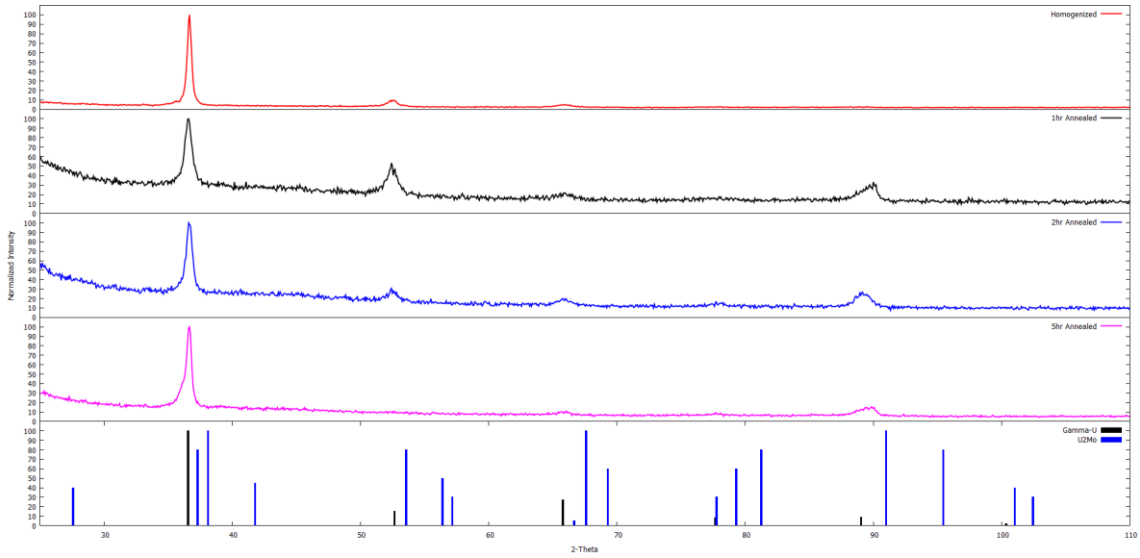

Figure 4-7. XRD spectra of U-7Mo-2Zr after various heat treatments. Reference spectrum data for γ and γ' phases is included as the bottom bar graph.

Table 4-7. Phases present in U-7Mo-2Zr.

Heat Treatment	Phases Present
Homogenized	γ and γ'
1-hour annealed	γ and γ'
2-hour annealed	γ and γ'
5-hour annealed	γ and γ'

4.2.2. U-7Mo-5Zr

4.2.2.1. *Homogenized*

Images of the U-7Mo-5Zr homogenized alloy are presented in Figure 4-8 and WDS data is presented in Table 4-8, followed by a description of the WDS points analyzed.

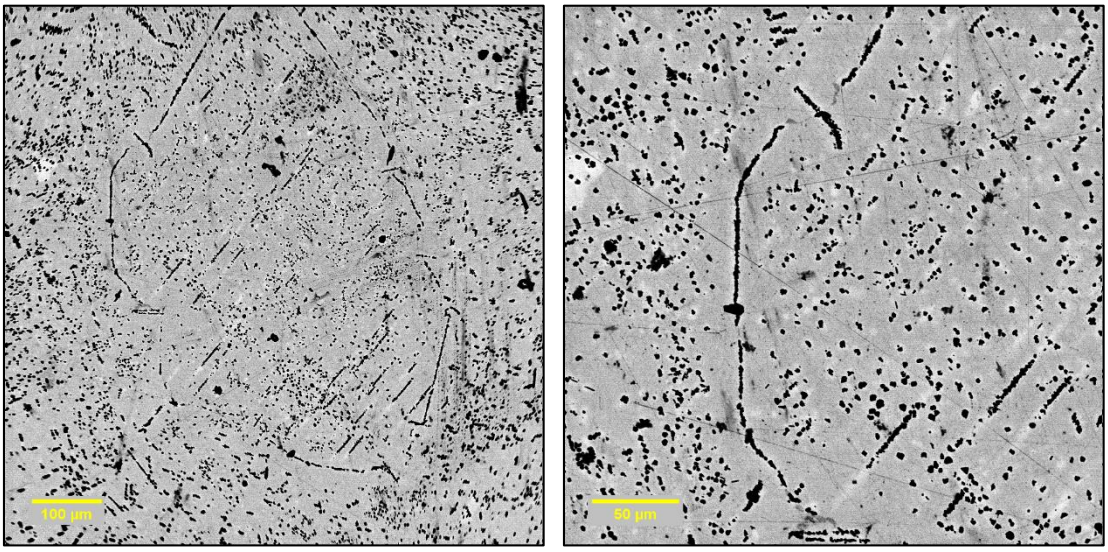

(a) (b)

Figure 4-8. Images of U-7Mo-5Zr homogenized alloy at (a) 120x and (b) 300x magnifications.

Table 4-8. WDS analytical composition of U-7Mo-5Zr homogenized alloy.

	Composition (wt%)							Composition (at%)					
	U	**Mo**	**Zr**	**O**	**N**	**Y**	**Total**	**U**	**Mo**	**Zr**	**O**	**N**	**Y**
Average (Bulk)	88.50	7.22	4.44	1.60	0.96	0.00	102.72	55.99	11.34	7.32	15.01	10.34	0.00
Standard Deviation (Bulk)	0.37	0.20	0.30	0.13	0.16	0.00	0.31	0.99	0.48	0.49	1.03	1.64	0.00
Point 1	3.92	29.11	63.48	4.05	0.34	0.00	100.89	1.27	23.47	53.82	19.58	1.86	0.00
Point 2	14.90	25.87	58.85	3.47	0.32	0.02	103.44	5.14	22.14	52.98	17.83	1.88	0.02

Point 1 Black spot within bulk

Point 2 Black spot within “line”

The composition of the bulk phase of the sample corresponds well with expectations, although molybdenum concentration is slightly high and zirconium concentration is slightly low. Point 1 and 2 are two different black spots that are enriched in zirconium and don’t correspond well to any particular expected phases. They have an elevated oxygen content but the total weight percent is not excessively low as would be likely if silicon was present. It is likely that these spots are zirconium that has gettered impurities from the bulk matrix, in this case oxygen. The depletion of zirconium in the bulk is likely due to the numerous zirconium rich features throughout the sample.

4.2.2.2. *1 hour annealed*

An image of the U-7Mo-5Zr 1 hour annealed alloy is presented in Figure 4-9 and WDS data is presented in Table 4-9, followed by a description of the WDS points analyzed.

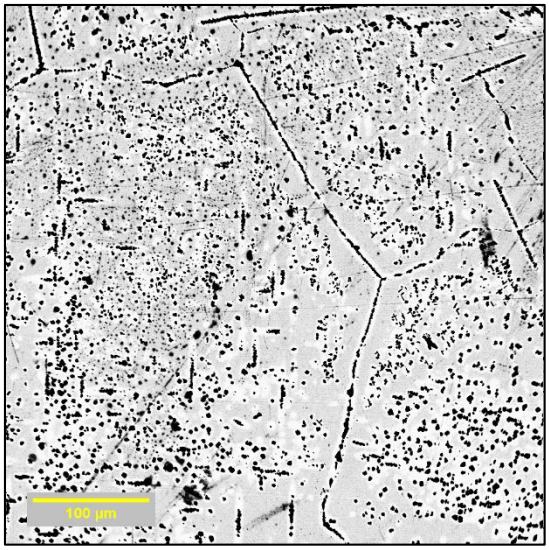

Figure 4-9. Image of U-7Mo-5Zr 1hr annealed alloy at 200x magnification.

Table 4-9. WDS analytical composition of U-7Mo-5Zr 1hr annealed alloy.

	Composition (wt%)							Composition (at%)					
	U	**Mo**	**Zr**	**O**	**N**	**Y**	**Total**	**U**	**Mo**	**Zr**	**O**	**N**	**Y**
Average (Bulk)	88.29	7.31	4.85	1.31	1.11	0.02	102.90	56.04	11.51	8.04	12.38	12.01	0.03
Standard Deviation (Bulk)	0.33	0.11	0.08	0.22	0.03	0.03	0.12	1.15	0.26	0.16	1.81	0.46	0.05
Point 1	93.93	3.70	2.50	2.30	1.28	0.07	103.79	56.64	5.54	3.93	20.63	13.14	0.12
Point 2	3.16	65.64	32.63	0.75	0.00	0.01	102.19	1.20	62.08	32.45	4.26	0.00	0.01
Point 3	1.08	65.71	32.89	0.60	0.00	0.03	100.30	0.42	62.97	33.15	3.44	0.00	0.03

Point 1: Bright region near small black “line”; uranium enriched

Point 2: Black spot within “line”; Mo_2Zr intermetallic

Point 3: Black spot within bulk; Mo_2Zr intermetallic

The composition of the bulk phase is similar to that of the homogenized sample, with slightly low zirconium values and slightly high molybdenum values. The bright phase at Point 1 is enriched in uranium and depleted in molybdenum and zirconium. The two black spots analyzed with WDS in this sample both appeared to be Mo_2Zr.

4.2.2.3. *2 hour annealed*

Images of the U-7Mo-5Zr 2 hour annealed alloy are presented in Figure 4-10 and WDS data is presented in Table 4-10, followed by a description of the WDS points analyzed.

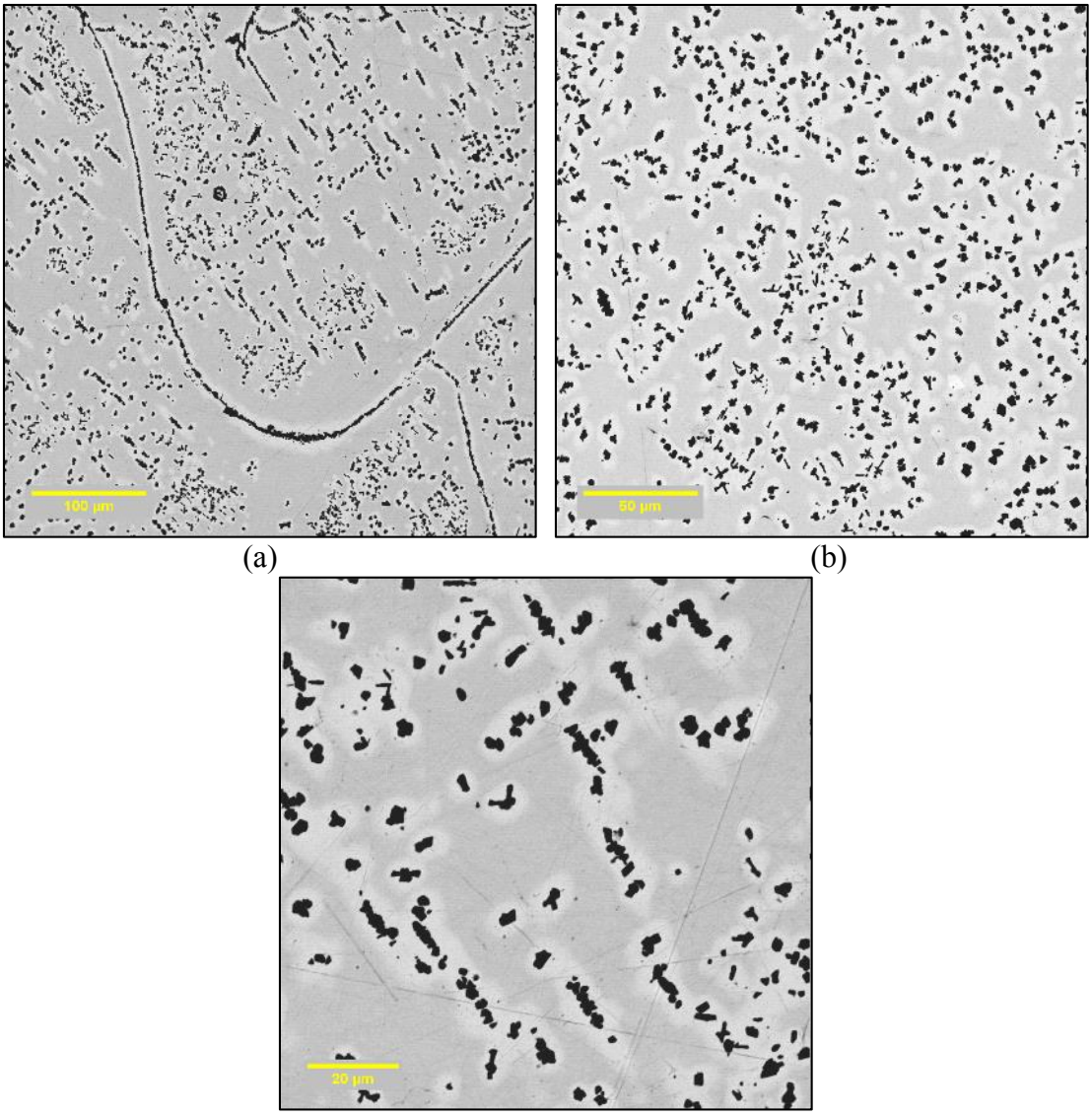

(a) (b)

(c)

Figure 4-10. Images of U-7Mo-5Zr 2hr annealed alloy at (a) 200x, (b) 400x, and (c) 800x magnifications.

Table 4-10. WDS analytical composition of U-7Mo-5Zr 2hr annealed alloy.

	Composition (wt%)							Composition (at%)					
	U	**Mo**	**Zr**	**O**	**N**	**Y**	**Total**	**U**	**Mo**	**Zr**	**O**	**N**	**Y**
Average (Bulk)	87.82	7.34	4.83	1.32	0.73	0.01	102.04	58.34	12.09	8.36	12.99	8.21	0.02
Standard Deviation (Bulk)	0.13	0.08	0.15	0.07	0.07	0.02	0.19	0.83	0.21	0.25	0.54	0.66	0.03
Point 1	10.31	54.12	35.37	0.77	0.00	0.00	100.56	4.15	54.09	37.17	4.59	0.00	0.00
Point 2	4.52	63.21	33.21	0.79	0.00	0.05	101.77	1.74	60.35	33.35	4.51	0.00	0.05
Point 3	93.00	3.90	2.69	2.13	0.92	0.04	102.68	59.20	6.15	4.47	20.13	9.97	0.07
Point 4	4.23	63.90	33.09	0.65	0.08	0.01	101.96	1.63	60.94	33.19	3.72	0.53	0.01

Point 1: Black spot within bulk

Point 2: Black spot within bulk; Mo_2Zr intermetallic

Point 3: Bright region near small black spot; uranium enriched

Point 4: Black spot within bulk; Mo_2Zr intermetallic

The composition of the two hour annealed sample is again roughly as expected for the bulk phase, although perhaps slightly depleted in zirconium and enriched in molybdenum. Point 1 may be an impurity similar to what was found in the homogenized sample, although this spot clearly had less oxygen. The total composition weight percent didn't indicate anything was missing such as silicon, and the molybdenum to zirconium ratio is opposite from what was observed in the homogenized sample. It is possible that this is a poorly formed Mo_2Zr intermetallic or a measurement was made near a true Mo_2Zr phase and an impurity phase so this includes counts from both areas. As before, the brighter phases are enriched in zirconium and some of the black features appear to be Mo_2Zr intermetallics.

4.2.2.4. *5 hour annealed*

Images of the U-7Mo-5Zr 5 hour annealed alloy are presented in Figure 4-11 and WDS data is presented in Table 4-11, followed by a description of the WDS points analyzed.

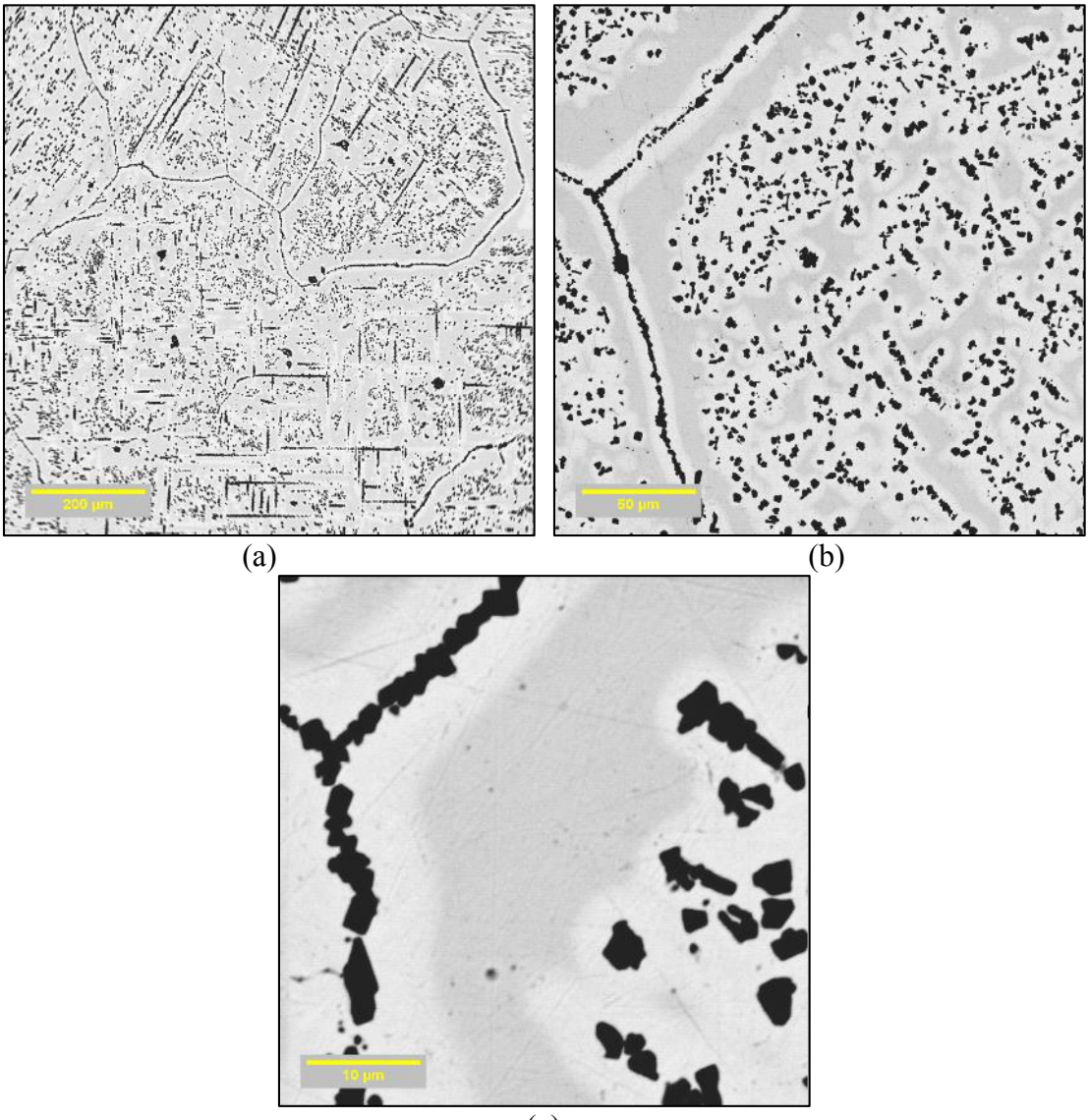

(a) (b)

(c)

Figure 4-11. Images of U-7Mo-5Zr 5hr annealed alloy at (a) 100x, (b) 400x, and (c) 2000x magnifications.

Table 4-11. WDS analytical composition of U-7Mo-5Zr 5hr annealed alloy.

	Composition (wt%)							Composition (at%)					
	U	**Mo**	**Zr**	**O**	**N**	**Y**	**Total**	**U**	**Mo**	**Zr**	**O**	**N**	**Y**
Average (Bulk)	87.92	7.36	4.85	1.49	0.80	0.00	102.40	56.94	11.82	8.19	14.31	8.74	0.01
Standard Deviation (Bulk)	0.18	0.13	0.13	0.11	0.10	0.01	0.10	1.16	0.41	0.08	0.85	0.94	0.01
Point 1	3.41	29.46	63.45	3.34	0.00	0.07	99.72	1.17	25.04	56.72	17.01	0.00	0.06
Point 2	3.66	63.54	33.53	0.59	0.01	0.00	101.33	1.42	61.18	33.96	3.38	0.06	0.00
Point 3	94.03	2.84	2.39	2.38	0.91	0.00	102.54	59.46	4.45	3.94	22.37	9.78	0.00

Point 1: Black spot within "line"

Point 2: Black spot within bulk; Mo_2Zr intermetallic

Point 3: Bright region near small black spot; uranium enriched

The composition of the bulk is consistent with measurements for the other samples in this series that were subjected to different heat treatments. Point 1 is similar to the potential impurity spot found in the homogenized sample where zirconium has gettered an oxygen impurity. The bright regions still tend to be enriched in uranium while depleted in molybdenum and zirconium and the small black features appear to be Mo_2Zr intermetallic inclusions.

4.2.2.5. *X-Ray Diffraction*

The XRD data collected for the U-7Mo-5Zr alloy is presented in Figure 4-12, along with reference data for the γ, γ', α, and Mo_2Zr phases. All samples appear somewhat similar in terms of composition, regardless of heat treatment. The main peak that occurs at 36.5° is indicative of the γ-phase. However, for all heat treatments, this phase is

somewhat broad and not well defined which may be due to the presence of α-U. Another smaller peak at 65.7° may also be from the γ-phase, but could also be from the α-phase which has a reference peak at 65.3° The peaks at 35.5° and 73° to 76° that are present for all samples seem to indicate the presence of α-phase. The main peak for the Mo_2Zr phase occurs at 39.4°, which is present in the data for all heat treatments, but it also overlaps with a peak from α-phase.

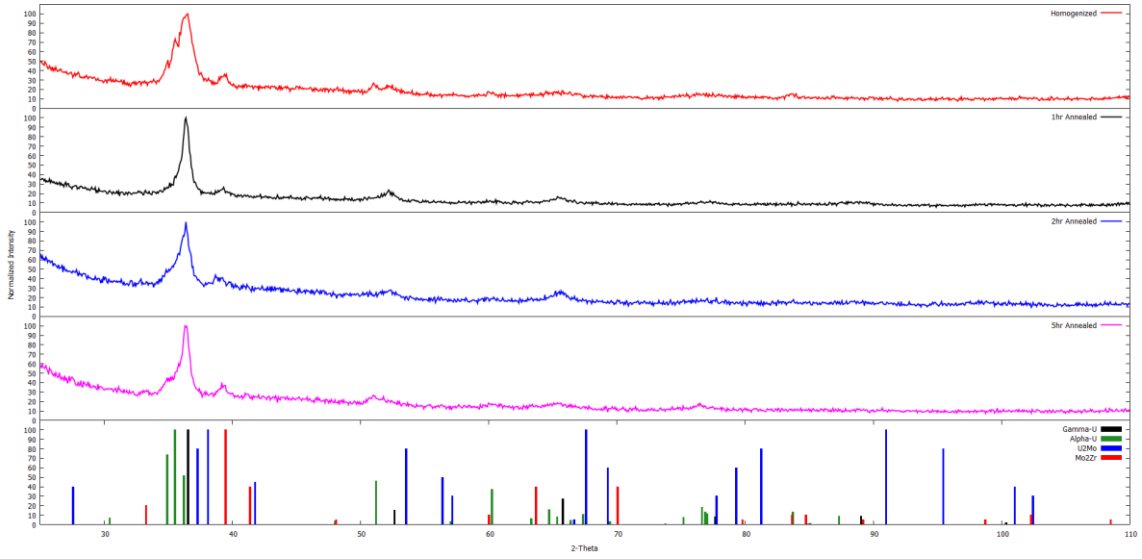

Figure 4-12. XRD spectra of U-7Mo-5Zr after various heat treatments. Reference spectrum data for γ, γ', α, and Mo_2Zr phases is included as the bottom bar graph.

Table 4-12. Phases present in U-7Mo-5Zr.

Heat Treatment	Phases Present
Homogenized	α, γ and Mo_2Zr
1-hour annealed	α, γ and Mo_2Zr
2-hour annealed	α, γ and Mo_2Zr
5-hour annealed	α, γ and Mo_2Zr

4.2.3. U-7Mo-10Zr

4.2.3.1. *Homogenized*

Images of the U-7Mo-10Zr homogenized alloy are presented in Figure 4-13 and WDS data is presented in Table 4-13, followed by a description of the WDS points analyzed.

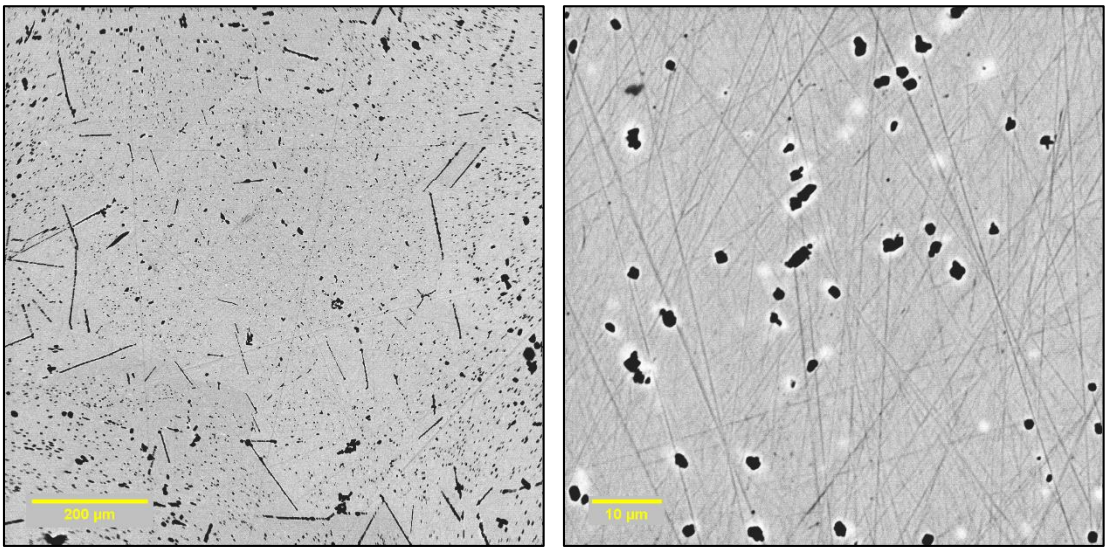

(a) (b)

Figure 4-13. Images of U-7Mo-10Zr homogenized alloy at (a) 100x and (b) 1200x magnifications.

Table 4-13. WDS analytical composition of U-7Mo-10Zr homogenized alloy.

	Composition (wt%)							Composition (at%)					
	U	**Mo**	**Zr**	**O**	**N**	**Y**	**Total**	**U**	**Mo**	**Zr**	**O**	**N**	**Y**
Average (Bulk)	83.31	7.46	9.58	1.51	0.92	0.00	102.77	50.59	11.24	15.18	13.58	9.42	0.00
Standard Deviation (Bulk)	0.22	0.17	0.20	0.12	0.16	0.00	0.76	1.36	0.15	0.37	0.79	1.34	0.00
Point 1	3.53	23.60	67.50	2.72	0.19	0.00	97.53	1.25	20.77	62.49	14.37	1.12	0.00
Point 2	18.57	21.36	53.95	0.66	0.00	0.00	94.54	8.36	23.85	63.36	4.43	0.00	0.00

Point 1 Black spot within bulk

Point 2 Black spot within bulk

This alloy shows similar characteristic to the previous U-7Mo series alloys in terms of bulk composition and zirconium rich impurity phases. Zirconium rich phases tend to deplete the bulk of zirconium so it is slightly enriched in uranium and molybdenum, although the bulk is of roughly the composition expected. Points 1 and 2 both have low total weight percent compositions as calculated by WDS, which is likely due to silicon impurities as observed previously. The bright phase observed directly around the darker zirconium rich features was too small to perform a WDS analysis but is likely a uranium rich phase, as indicated by the light contrast.

4.2.3.2. *1 hour annealed*

Images of the U-7Mo-10Zr 1 hour annealed alloy are presented in Figure 4-14 and WDS data is presented in Table 4-14, followed by a description of the WDS points analyzed.

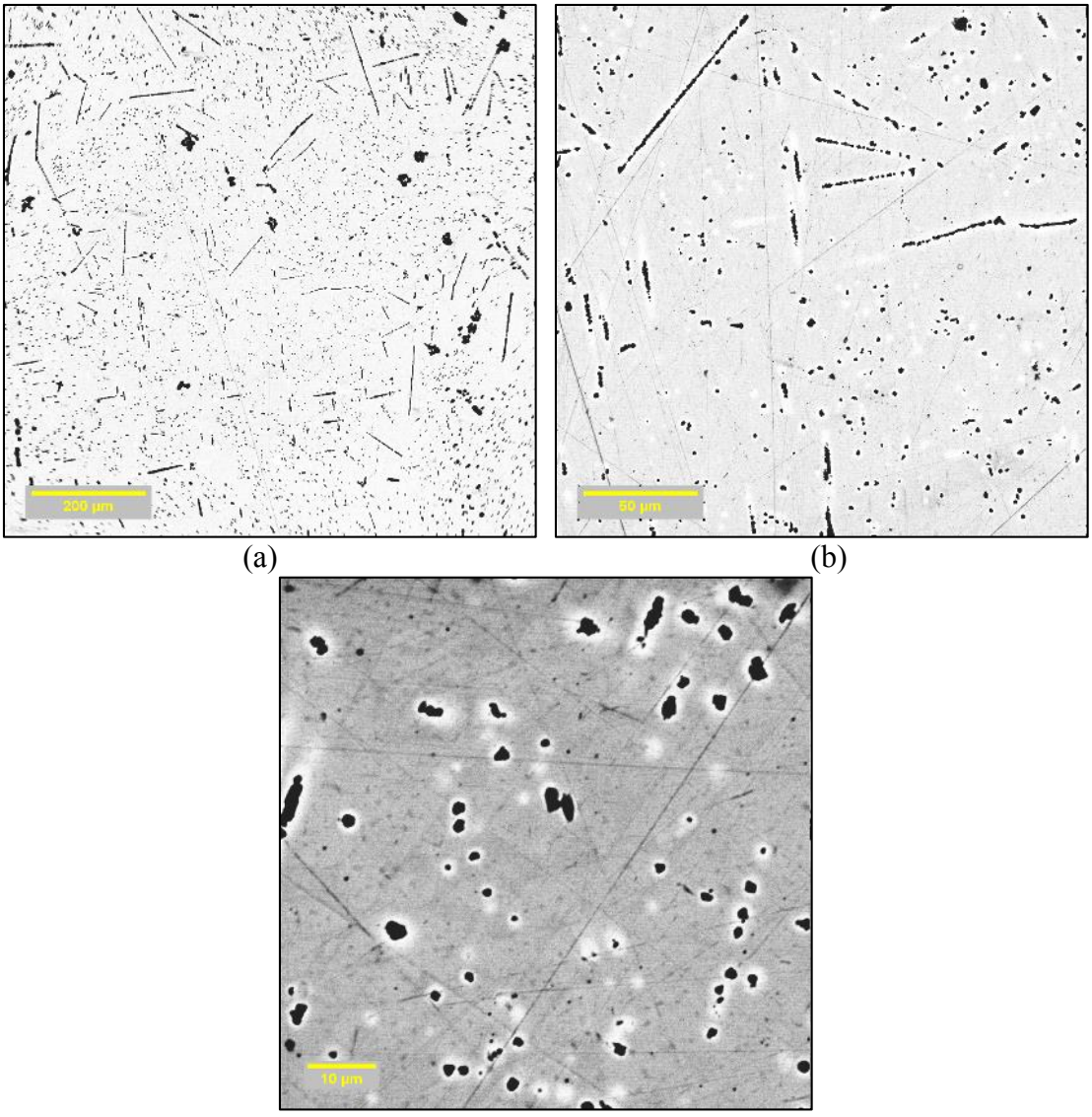

(a) (b)

(c)

Figure 4-14. Images of U-7Mo-10Zr 1hr annealed alloy at (a) 100x, (b) 400x, and (c) 1200x magnifications.

Table 4-14. WDS analytical composition of U-7Mo-10Zr 1hr annealed alloy.

	Composition (wt%)							Composition (at%)					
	U	**Mo**	**Zr**	**O**	**N**	**Y**	**Total**	**U**	**Mo**	**Zr**	**O**	**N**	**Y**
Average (Bulk)	83.80	7.50	9.31	1.13	0.93	0.02	102.69	52.62	11.68	15.25	10.55	9.86	0.04
Standard Deviation (Bulk)	0.39	0.06	0.15	0.13	0.13	0.02	0.44	1.16	0.31	0.47	1.05	1.22	0.03
Point 1	5.78	19.41	68.21	2.88	0.00	0.02	96.30	2.10	17.53	64.76	15.59	0.00	0.02

Point 1: Black spot within bulk

The one hour annealed sample had no obvious differences from the homogenized sample based on BSE imaging. The bulk phase is as expected with a slightly low zirconium concentration and high molybdenum concentration. Point 1 as analyzed by WDS indicates a zirconium rich impurity phase.

4.2.3.3. *2 hour annealed*

Images of the U-7Mo-10Zr 2 hour annealed alloy are presented in Figure 4-15 and WDS data is presented in Table 4-15, followed by a description of the WDS points analyzed.

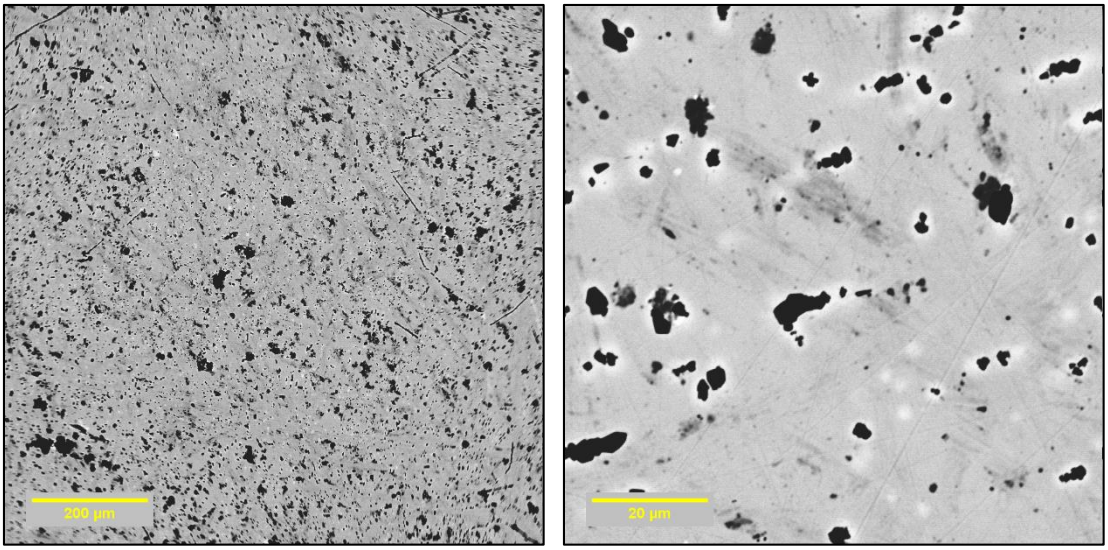

(a) (b)

Figure 4-15. Images of U-7Mo-10Zr 2hr annealed alloy at (a) 100x and (b) 1000x magnifications.

Table 4-15. WDS analytical composition of U-7Mo-10Zr 2hr annealed alloy.

	Composition (wt%)							Composition (at%)					
	U	**Mo**	**Zr**	**O**	**N**	**Y**	**Total**	**U**	**Mo**	**Zr**	**O**	**N**	**Y**
Average (Bulk)	83.10	7.47	9.61	1.42	0.72	0.00	102.33	51.91	11.58	15.67	13.16	7.69	0.00
Standard Deviation (Bulk)	0.32	0.04	0.20	0.05	0.07	0.00	0.23	0.61	0.10	0.23	0.46	0.65	0.00
Point 1	5.23	20.52	66.44	2.40	0.00	0.00	94.60	1.97	19.20	65.38	13.45	0.00	0.00
Point 2	2.57	16.50	77.09	3.38	0.00	0.00	99.53	0.87	13.89	68.22	17.03	0.00	0.00
Point 3	3.91	28.26	62.79	3.23	0.00	0.00	98.19	1.37	24.52	57.30	16.82	0.00	0.00
Point 4	3.49	23.39	65.63	2.74	0.00	0.04	95.29	1.28	21.20	62.59	14.89	0.00	0.04
Point 5	88.64	4.08	6.98	1.77	0.68	0.00	102.14	57.27	6.54	11.76	16.96	7.47	0.00

Point 1: Large black spot (~45μm)

Point 2: Black spot within "line"

Point 3: Black spot within bulk

Point 4: Black spot within bulk

Point 5: Bright region near small black "line"; uranium enriched

The U-7Mo-10Zr alloy that was annealed for two hours is similar to the homogenized and one hour annealed samples in terms of appearance. Based on previous results that indicated a low total weight percent concentration, four data points were taken at the black inclusions. They all followed the same general trend: zirconium rich features that appeared to have gettered impurities. A qualitative check for silicon using one of the WDS detectors showed a marked increase, which would indicate the low total concentration is due to the presence of silicon impurities. The bulk phase is still depleted

in zirconium content and enriched in molybdenum, and the bright phase surrounding precipitates is enriched in uranium.

4.2.3.4. *5 hour annealed*

Images of the U-7Mo-10Zr 5 hour annealed alloy are presented in Figure 4-16 and WDS data is presented in Table 4-16, followed by a description of the WDS points analyzed.

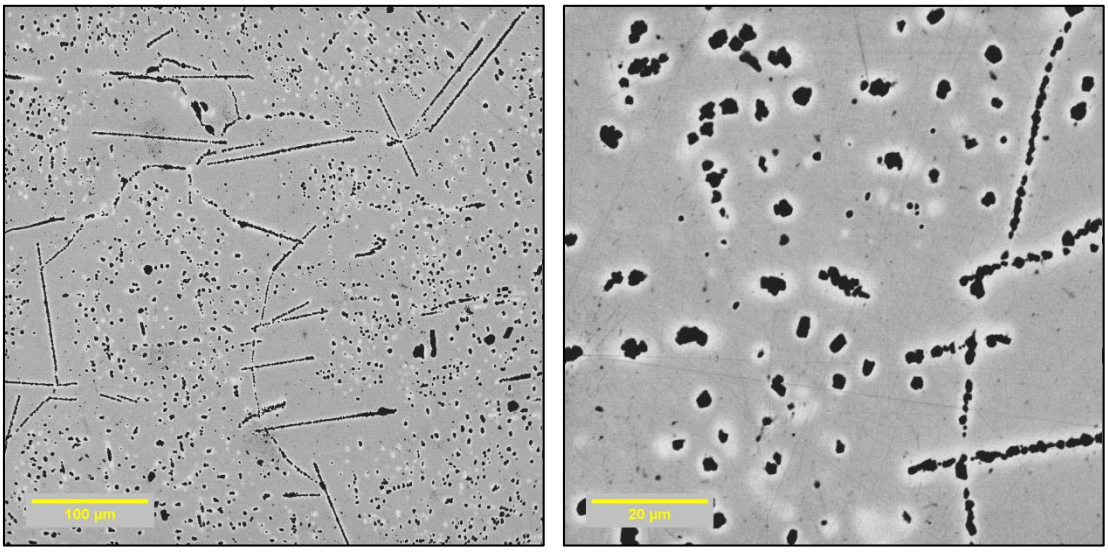

(a) (b)

Figure 4-16. Images of U-7Mo-10Zr 5hr annealed alloy at (a) 200x and (b) 1000x magnifications.

Table 4-16. WDS analytical composition of U-7Mo-10Zr 5hr annealed alloy.

	Composition (wt%)							Composition (at%)					
	U	**Mo**	**Zr**	**O**	**N**	**Y**	**Total**	**U**	**Mo**	**Zr**	**O**	**N**	**Y**
Average (Bulk)	82.94	7.49	9.64	1.50	0.64	0.02	102.23	51.84	11.62	15.73	13.96	6.83	0.03
Standard Deviation (Bulk)	0.38	0.07	0.33	0.15	0.08	0.02	0.21	0.73	0.22	0.66	1.25	0.79	0.04
Point 1	88.40	5.08	5.79	2.43	0.85	0.00	102.55	53.06	7.57	9.07	21.68	8.62	0.01
Point 2	4.15	28.78	63.60	3.24	0.00	0.00	99.77	1.43	24.65	57.29	16.63	0.00	0.00

Point 1: Bright region near small black "line"; uranium enriched

Point 2: Black spot within bulk

The same trends as detected previously were again observed with this five hour annealed alloy. A depletion of zirconium in the bulk, an increase in uranium content in the bright region around the black features, and zirconium rich impurities.

4.2.3.5. *X-Ray Diffraction*

The homogenized alloy is clearly different from the annealed alloys. Alpha-phase is present in the homogenized alloy, but not as well defined for the annealed alloys. It would appear that peaks generated for the annealed alloys don't correspond well with the reference peaks. In all cases for the annealed data, shifting the peaks to the right by 0.2° to 0.4° makes them all align with reference peaks fairly well. A peak is present for all three annealed samples at roughly 52.6° indicating γ-U. A peak at 65.7° also appears for all annealed alloys, which likely corresponds to γ-U. A peak around 65° to 67° is broad and not well defined for the homogenized alloy and may indicate the presence of α-U. A peak at roughly 89° appears for the two hour annealed alloy that is likely due to γ-U. A peak at

78° appears for the five hour annealed alloy that is not obvious for any other heat treatments; this peak is not near any known reference peaks. Based on the EPMA results it seems as if this alloy has several impurities in it which could have impacted the XRD analyses, thus the appearance of peaks that don't correspond well with any of the expected phases.

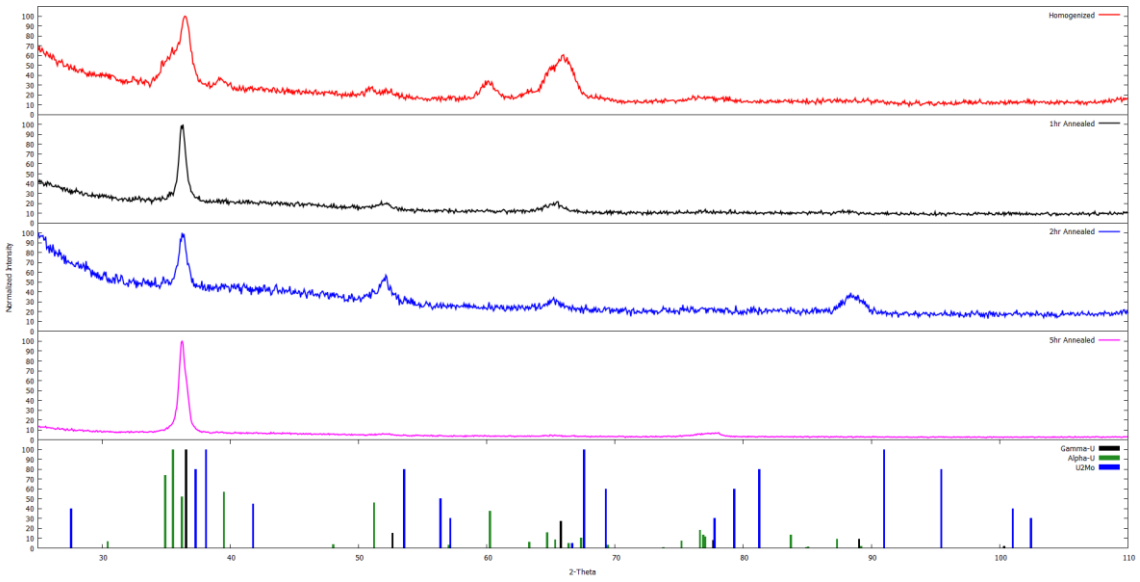

Figure 4-17. XRD spectra of U-7Mo-10Zr after various heat treatments. Reference spectrum data for γ, γ', and α phases is included as the bottom bar graph.

Table 4-17. Phases present in U-7Mo-10Zr.

Heat Treatment	Phases Present
Homogenized	α and γ
1-hour annealed	γ
2-hour annealed	γ
5-hour annealed	γ

4.2.4. U-10Mo-2Zr

4.2.4.1. *Homogenized*

Images of the U-10Mo-2Zr homogenized alloy are presented in Figure 4-18 and WDS data is presented in Table 4-18, followed by a description of the WDS points analyzed.

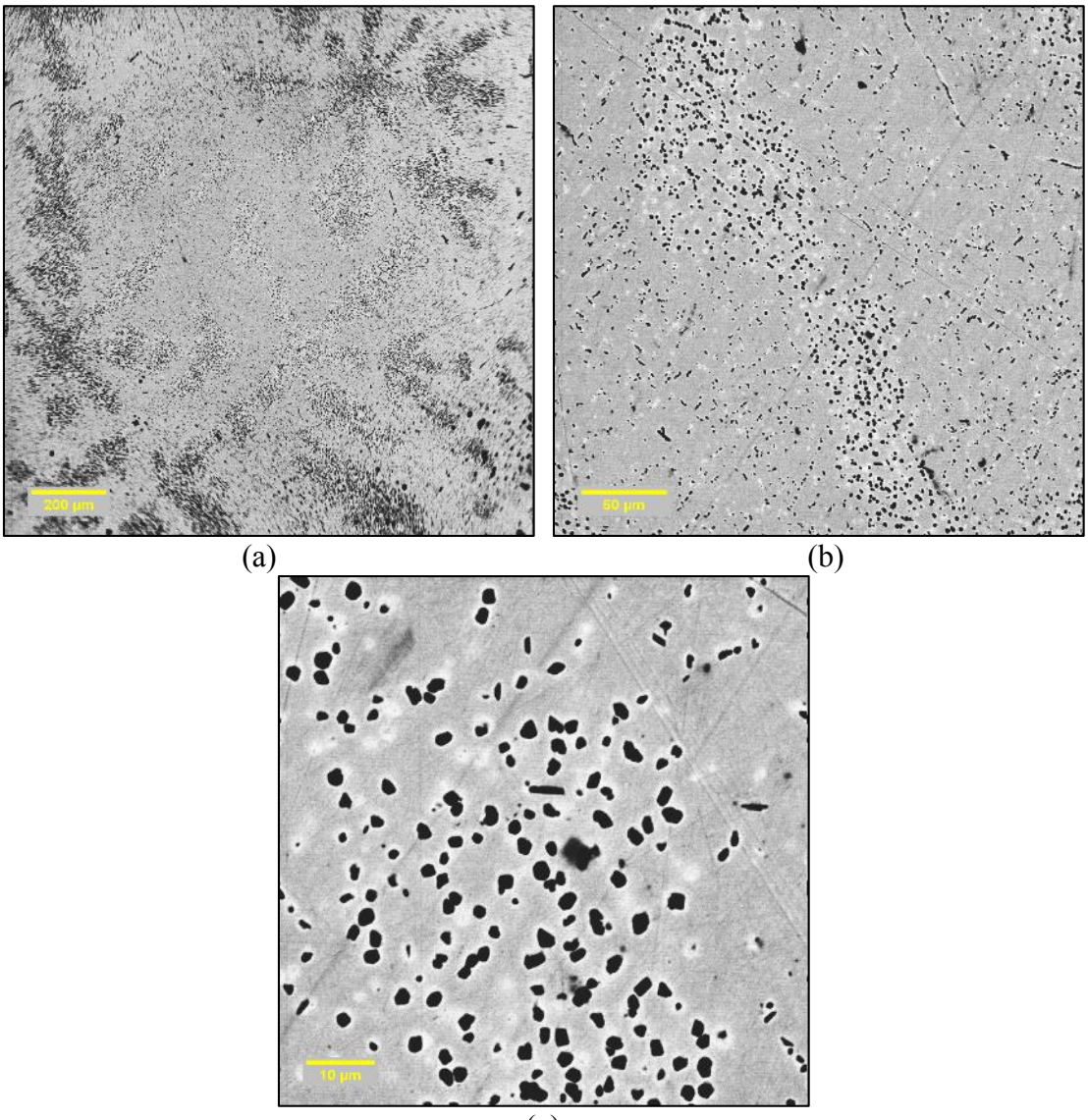

(a) (b)

(c)

Figure 4-18. Images of U-10Mo-2Zr homogenized alloy at (a) 66x, (b) 300x, and (c) 1200x magnifications.

Table 4-18. WDS analytical composition of U-10Mo-2Zr homogenized alloy.

	Composition (wt%)							Composition (at%)					
	U	**Mo**	**Zr**	**O**	**N**	**Y**	**Total**	**U**	**Mo**	**Zr**	**O**	**N**	**Y**
Average (Bulk)	88.47	10.23	1.44	1.21	1.08	0.03	102.45	57.49	16.49	2.44	11.64	11.88	0.05
Standard Deviation (Bulk)	0.46	0.23	0.23	0.11	0.20	0.02	0.09	1.74	0.60	0.42	0.77	1.81	0.04
Point 1	3.17	66.08	32.39	0.48	0.00	0.02	102.14	1.23	63.34	32.65	2.77	0.00	0.02

Point 1 Black spot within bulk; Mo_2Zr intermetallic

This U-10Mo-2Zr alloy clearly has different regions where the density of small black features varies. This variance has no obvious effect on the composition of the matrix material among the precipitate rich region or outside of it. Therefore, all WDS measurements of the bulk phase are included in the average. The bulk phase of this alloy exhibits the same trends observed thus far: depleted in zirconium while slightly enriched in molybdenum from the expected ratios. The black spots are consistent with Mo_2Zr intermetallics. No measurement was possible for the bright phase due to its small size throughout the sample.

4.2.4.2. *1 hour annealed*

Images of the U-10Mo-2Zr 1 hour annealed alloy are presented in Figure 4-19 and WDS data is presented in Table 4-19, followed by a description of the WDS points analyzed.

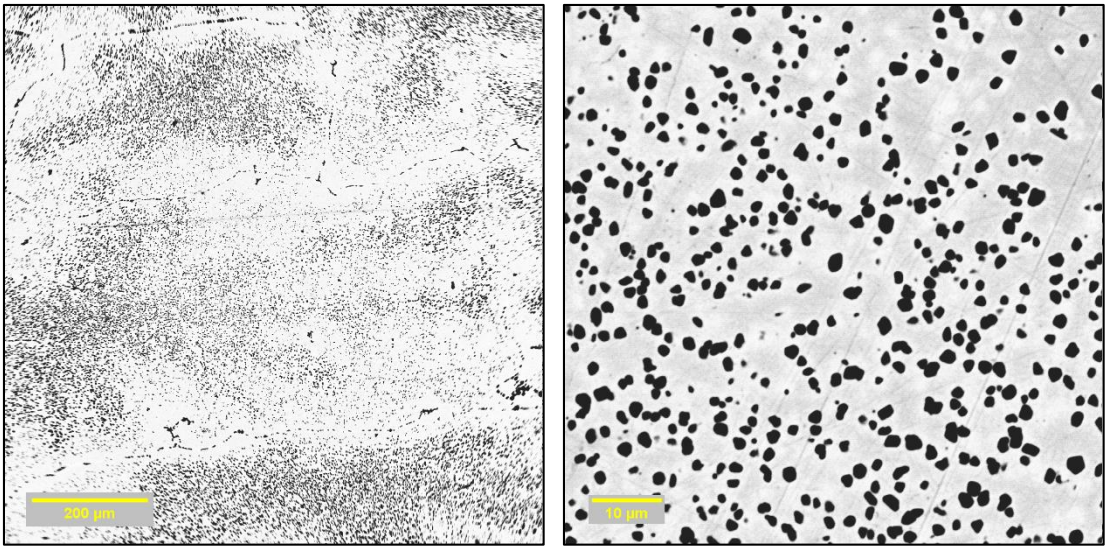

(a) (b)

Figure 4-19. Images of U-10Mo-2Zr 1hr annealed alloy at (a) 100x and (b) 1200x magnifications.

Table 4-19. WDS analytical composition of U-10Mo-2Zr 1hr annealed alloy.

	Composition (wt%)							Composition (at%)					
	U	**Mo**	**Zr**	**O**	**N**	**Y**	**Total**	**U**	**Mo**	**Zr**	**O**	**N**	**Y**
Average (Bulk)	88.77	10.06	1.50	1.14	1.01	0.01	102.49	58.50	16.45	2.57	11.20	11.25	0.02
Standard Deviation (Bulk)	0.52	0.27	0.20	0.05	0.06	0.02	0.25	0.45	0.40	0.34	0.45	0.72	0.03
Point 1	1.68	66.47	32.71	0.59	0.00	0.00	101.45	0.64	63.26	32.75	3.35	0.00	0.00
Point 2	1.06	67.04	32.45	0.57	0.00	0.04	101.17	0.41	63.81	32.49	3.25	0.00	0.04

Point 1: Black spot within bulk; Mo_2Zr intermetallic

Point 2: Black spot within bulk; Mo_2Zr intermetallic

As is evident in Figure 4-19 (a), there are obvious regions that are denser with dark black precipitates. Point 1 and 2 indicate that these phases are likely Mo_2Zr intermetallics. The bulk phase continues the trend of being depleted in zirconium. WDS points were taken of the bulk phase within the intermetallic dense region and outside of it. No notable difference was observed. The average bulk composition therefore includes all data points of the matrix phase. None of the brighter areas surrounding the black phases were large enough to allow for an accurate WDS measurement, although this region is likely a uranium rich phase as noted in all other alloys where measurement was possible.

4.2.4.3. *2 hour annealed*

Images of the U-10Mo-2Zr 2 hour annealed alloy are presented in Figure 4-20 and WDS data is presented in Table 4-20, followed by a description of the WDS points analyzed.

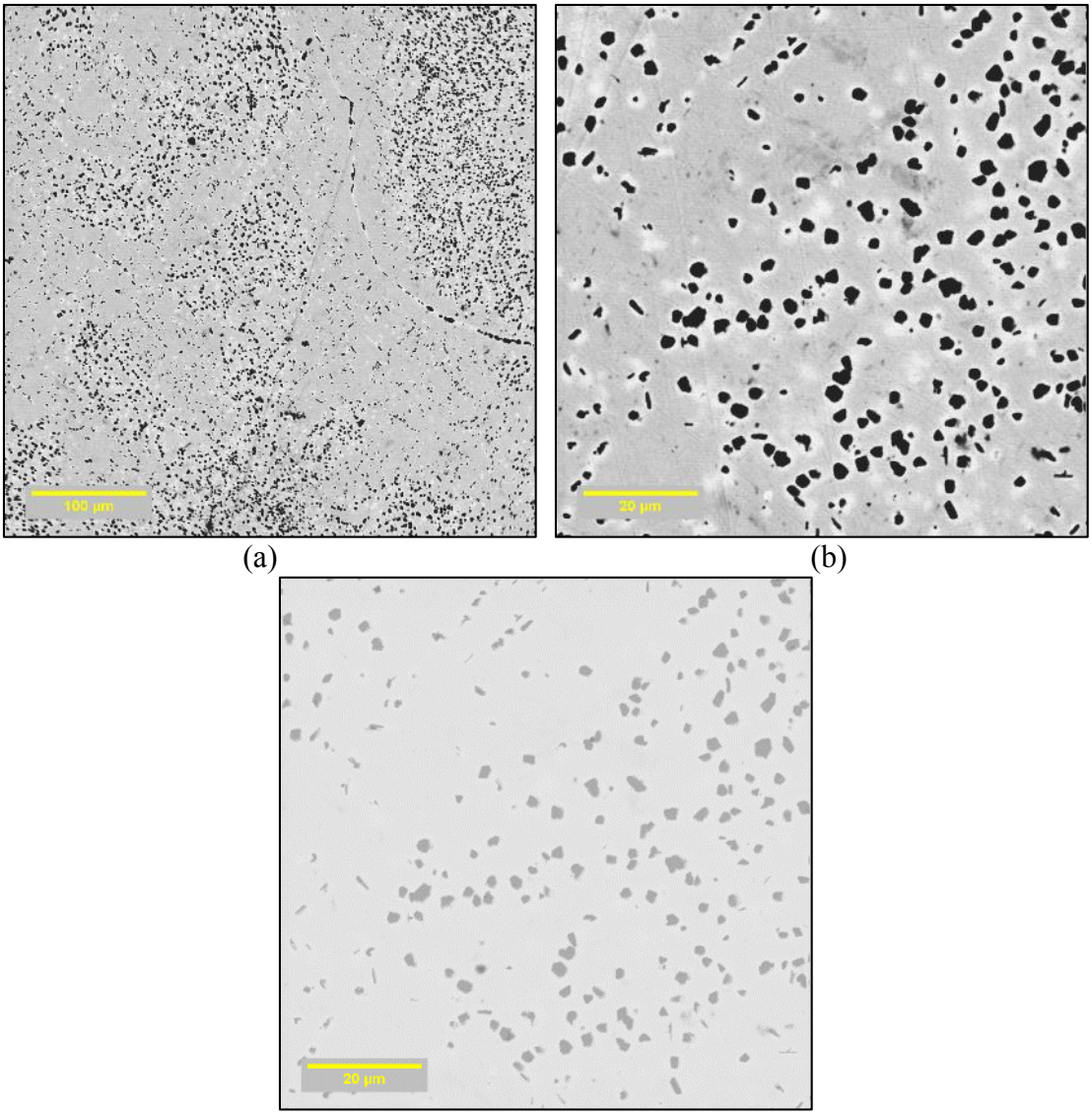

(a) (b)

(c)

Figure 4-20. Images of U-10Mo-2Zr 2hr annealed alloy at (a) 200x, (b) 1000x, and (c) 1000x magnifications. Image (c) was taken at low contrast settings.

Table 4-20. WDS analytical composition of U-10Mo-2Zr 2hr annealed alloy.

	Composition (wt%)							Composition (at%)					
	U	**Mo**	**Zr**	**O**	**N**	**Y**	**Total**	**U**	**Mo**	**Zr**	**O**	**N**	**Y**
Average (Bulk)	88.04	10.22	1.68	1.27	0.72	0.01	101.95	59.09	17.02	2.95	12.71	8.22	0.01
Standard Deviation (Bulk)	0.21	0.10	0.07	0.05	0.07	0.01	0.19	0.52	0.10	0.11	0.54	0.69	0.02
Point 1	3.01	66.12	31.57	0.67	0.00	0.01	101.39	1.16	63.22	31.75	3.87	0.00	0.01
Point 2	1.34	66.61	31.93	0.67	0.16	0.00	100.70	0.51	62.95	31.74	3.79	1.01	0.00
Point 3	92.48	6.76	0.45	1.18	1.01	0.03	101.91	63.71	11.56	0.82	12.05	11.81	0.05

Point 1: Black spot within bulk; Mo_2Zr intermetallic

Point 2: Black spot within grain boundary; Mo_2Zr intermetallic

Point 3: Bright region near small black spot; uranium enriched

The two hour annealed sample appears consistent with the one hour annealed sample and the homogenized alloy. Various regions are clearly visible that have a varying density of small black precipitates that Point 1 and 2 indicate are consistent with a Mo_2Zr phase. The bulk phase is again depleted in zirconium, and Point 3 indicates the bright phase around the intermetallics is a uranium rich phase.

4.2.4.4. *5 hour annealed*

Images of the U-10Mo-2Zr 5 hour annealed alloy are presented in Figure 4-21 and WDS data is presented in Table 4-21, followed by a description of the WDS points analyzed.

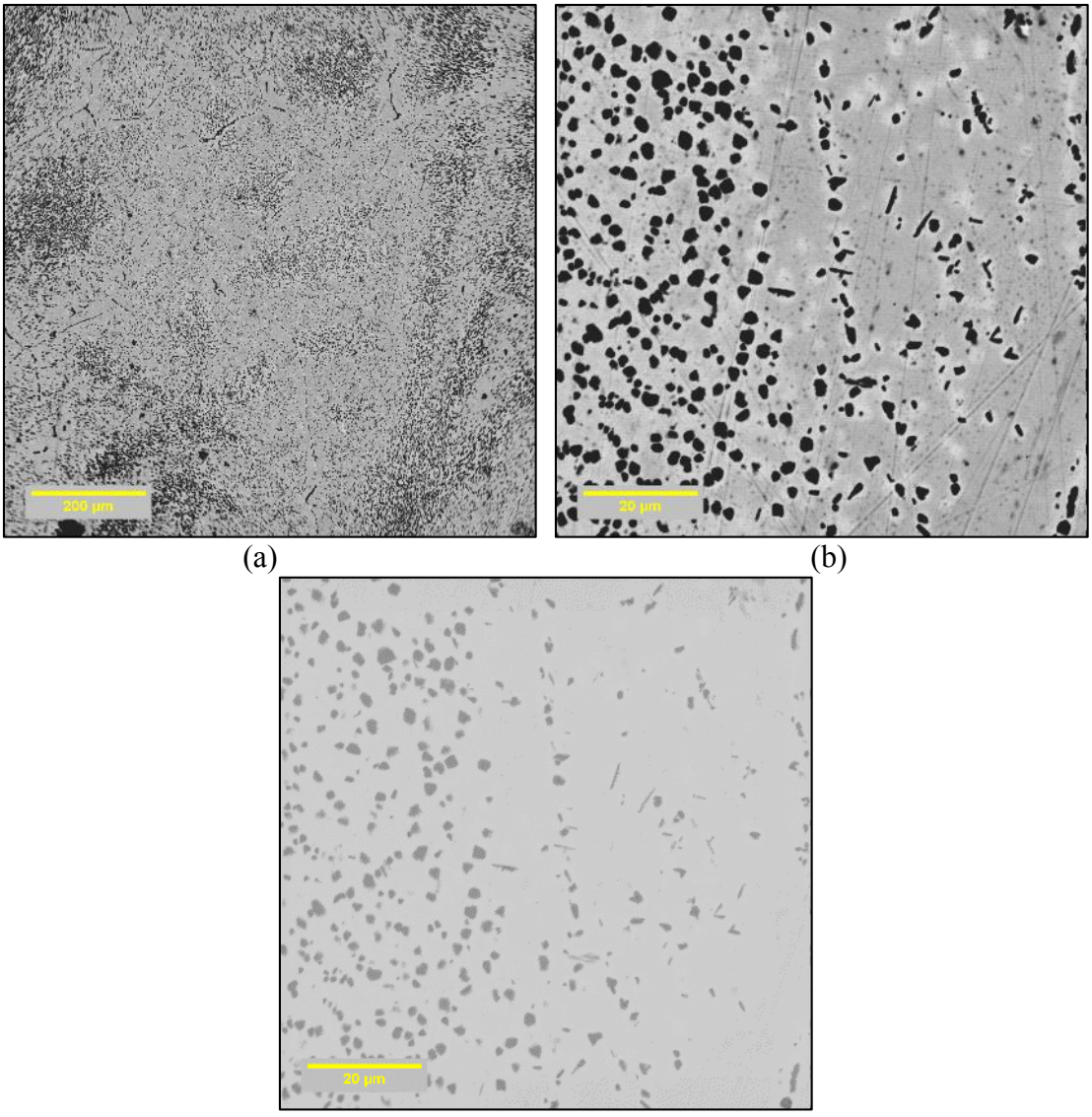

(a) (b)

(c)

Figure 4-21. Images of U-10Mo-2Zr 5hr annealed alloy at (a) 100x, (b) 1000x, and (c) 1000x magnifications. Image (c) was taken at low contrast settings.

Table 4-21. WDS analytical composition of U-10Mo-2Zr 5hr annealed alloy.

	Composition (wt%)							Composition (at%)					
	U	**Mo**	**Zr**	**O**	**N**	**Y**	**Total**	**U**	**Mo**	**Zr**	**O**	**N**	**Y**
Average (Bulk)	87.90	10.19	1.58	1.44	0.85	0.02	101.98	57.38	16.50	2.70	14.00	9.40	0.04
Standard Deviation (Bulk)	0.33	0.10	0.22	0.13	0.09	0.04	0.31	1.26	0.26	0.40	1.01	0.76	0.07
Point 1	93.12	6.53	0.56	1.59	0.97	0.00	102.76	61.74	10.75	0.96	15.66	10.89	0.00
Point 2	2.55	66.09	32.34	0.96	0.00	0.04	101.98	0.96	61.81	31.81	5.38	0.00	0.04
Point 3	1.51	66.71	32.17	0.72	0.00	0.00	101.10	0.58	63.27	32.09	4.07	0.00	0.00

Point 1: Bright region near small black spot; uranium enriched

Point 2: Black spot within bulk; Mo_2Zr intermetallic

Point 3: Black spot within bulk; Mo_2Zr intermetallic

The five hour annealed U-10Mo-2Zr alloy continues to follow the same trends observed for the previous heat treatments. The intermetallic dense regions are still very apparent on images for this alloy after being annealed for five hours, although the matrix phase within the dense region has the same composition as outside of the intermetallic dense region. The matrix phase is slightly depleted in zirconium, resulting in an enrichment in uranium and molybdenum. WDS analysis of various black inclusions seems to indicate this is a Mo_2Zr intermetallic. The bright region around these intermetallic phases is enriched in uranium.

4.2.4.5. *X-Ray Diffraction*

X-ray diffraction results for U-10Mo-2Zr are fairly consistent for all heat treatments. The data indicates that γ and γ' phases are present in all samples. WDS data

clearly indicates that Mo_2Zr is likely present in all samples; this is not obvious in the XRD data. The lack of an obvious Mo_2Zr phase in the XRD data may be attributable to some of the same factors described in section 4.2.1.5.

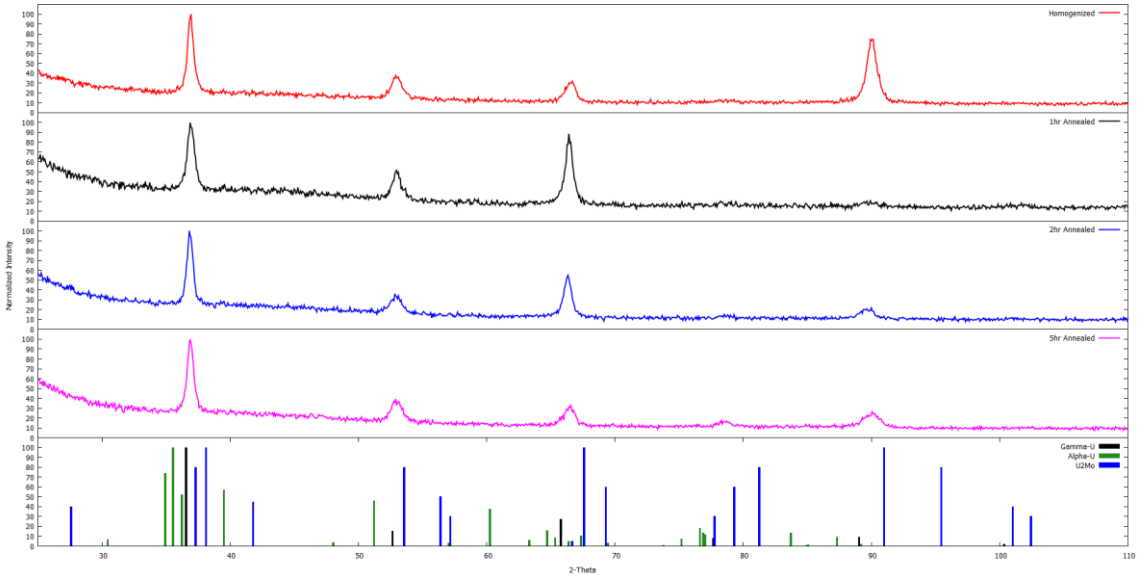

Figure 4-22. XRD spectra of U-10Mo-2Zr after various heat treatments. Reference spectrum data for γ, γ', and α phases is included as the bottom bar graph.

Table 4-22. Phases present in U-10Mo-2Zr.

Heat Treatment	Phases Present
Homogenized	γ and γ'
1-hour annealed	γ and γ'
2-hour annealed	γ and γ'
5-hour annealed	γ and γ'

4.2.5. U-10Mo-5Zr

4.2.5.1. *Homogenized*

Images of the U-10Mo-5Zr homogenized alloy are presented in Figure 4-23 and WDS data is presented in Table 4-23, followed by a description of the WDS points analyzed.

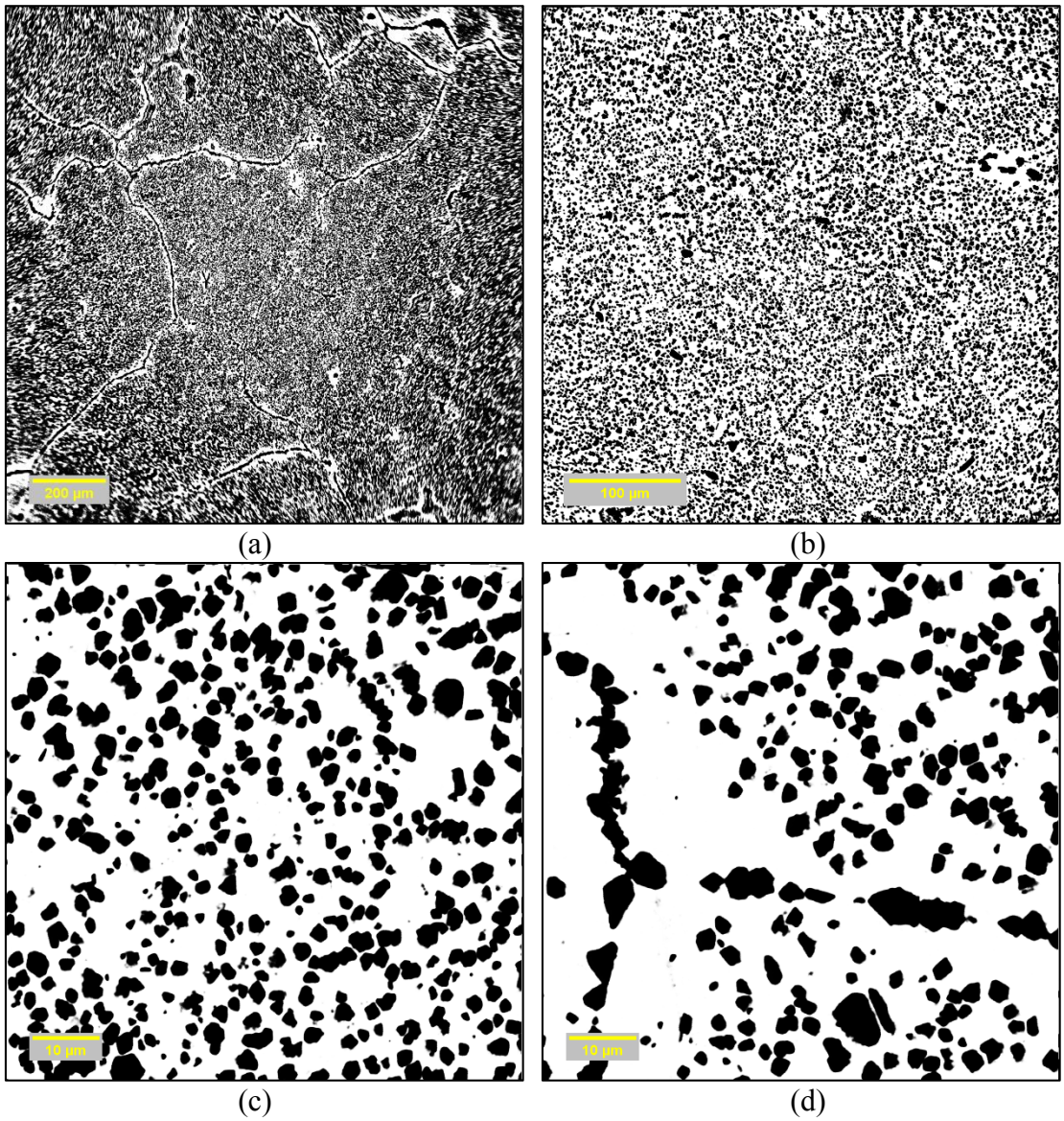

(a) (b)

(c) (d)

Figure 4-23. Images of U-10Mo-5Zr homogenized alloy at (a) 66x, (b) 200x, (c) 1200x, and (d) 1200x magnifications.

Table 4-23. WDS analytical composition of U-10Mo-5Zr homogenized alloy.

	Composition (wt%)							Composition (at%)					
	U	**Mo**	**Zr**	**O**	**N**	**Y**	**Total**	**U**	**Mo**	**Zr**	**O**	**N**	**Y**
Average (Bulk)	93.43	4.66	1.45	2.82	1.23	0.00	103.59	54.46	6.73	2.19	24.43	12.18	0.00
Standard Deviation (Bulk)	0.15	0.31	0.22	0.25	0.02	0.00	0.62	1.55	0.27	0.28	1.52	0.52	0.00
Point 1	5.01	64.20	31.35	2.28	0.86	0.00	103.69	1.70	54.07	27.76	11.51	4.96	0.00
Point 2	2.25	66.55	32.89	0.61	0.00	0.03	102.33	0.86	62.93	32.72	3.47	0.00	0.03

Point 1 Black spot within bulk; Mo_2Zr intermetallic

Point 2 Black spot within grain boundary; Mo_2Zr intermetallic

The U-10Mo-5Zr homogenized alloy has a very dense distribution of small black features that Point 1 and 2 indicate are consistent with Mo_2Zr intermetallics. The matrix phase of this alloy is not as expected based on composition. It is very depleted in zirconium, with an average of 1.45 wt% instead of closer to 5 wt%. It is also more depleted in molybdenum than previously observed, with only 4.66 wt% in the bulk when it should have closer to 10 wt%. These depletions are due to the abundance of Mo_2Zr intermetallic phases that deplete the bulk of molybdenum and zirconium.

4.2.5.2. *1 hour annealed*

Images of the U-10Mo-5Zr 1 hour annealed alloy are presented in Figure 4-24 and WDS data is presented in Table 4-24, followed by a description of the WDS points analyzed.

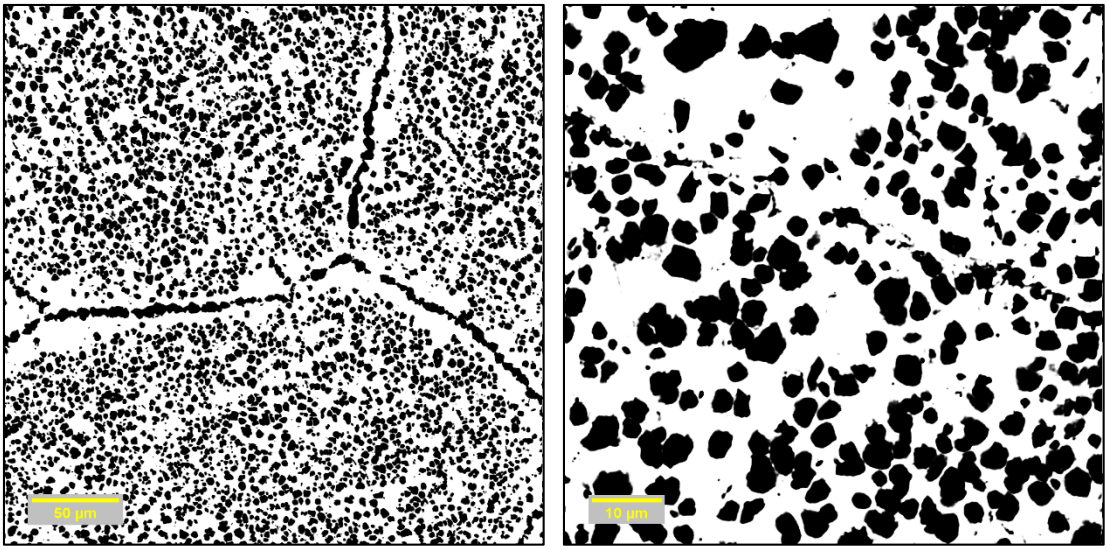

(a) (b)

Figure 4-24. Images of U-10Mo-5Zr 1hr annealed alloy at (a) 300x and (b) 1200x magnifications.

Table 4-24. WDS analytical composition of U-10Mo-5Zr 1hr annealed alloy.

	Composition (wt%)							Composition (at%)					
	U	**Mo**	**Zr**	**O**	**N**	**Y**	**Total**	**U**	**Mo**	**Zr**	**O**	**N**	**Y**
Average (Bulk)	93.84	4.07	1.48	3.37	1.22	0.00	103.98	52.63	5.66	2.17	27.94	11.60	0.00
Standard Deviation (Bulk)	0.25	0.19	0.08	0.60	0.07	0.00	0.53	3.12	0.06	0.24	3.46	0.04	0.00
Point 1	1.47	67.19	32.34	0.67	0.10	0.00	101.76	0.56	63.11	31.95	3.77	0.61	0.00
Point 2	1.64	66.81	32.80	0.65	0.26	0.05	102.21	0.61	62.04	32.03	3.64	1.62	0.05

Point 1: Black spot within bulk; Mo_2Zr intermetallic

Point 2: Black spot within bulk; Mo_2Zr intermetallic

A one hour anneal seems to have little effect on the alloy composition based on WDS data. The black phases still appear to be Mo_2Zr intermetallics while the bulk phase has roughly 1.5 wt% zirconium and 4 wt% molybdenum. The appearance in images is also very similar to that of the homogenized alloy.

4.2.5.3. *2 hour annealed*

Images of the U-10Mo-5Zr two hour annealed alloy are presented in Figure 4-25 and WDS data is presented in Table 4-25, followed by a description of the WDS points analyzed.

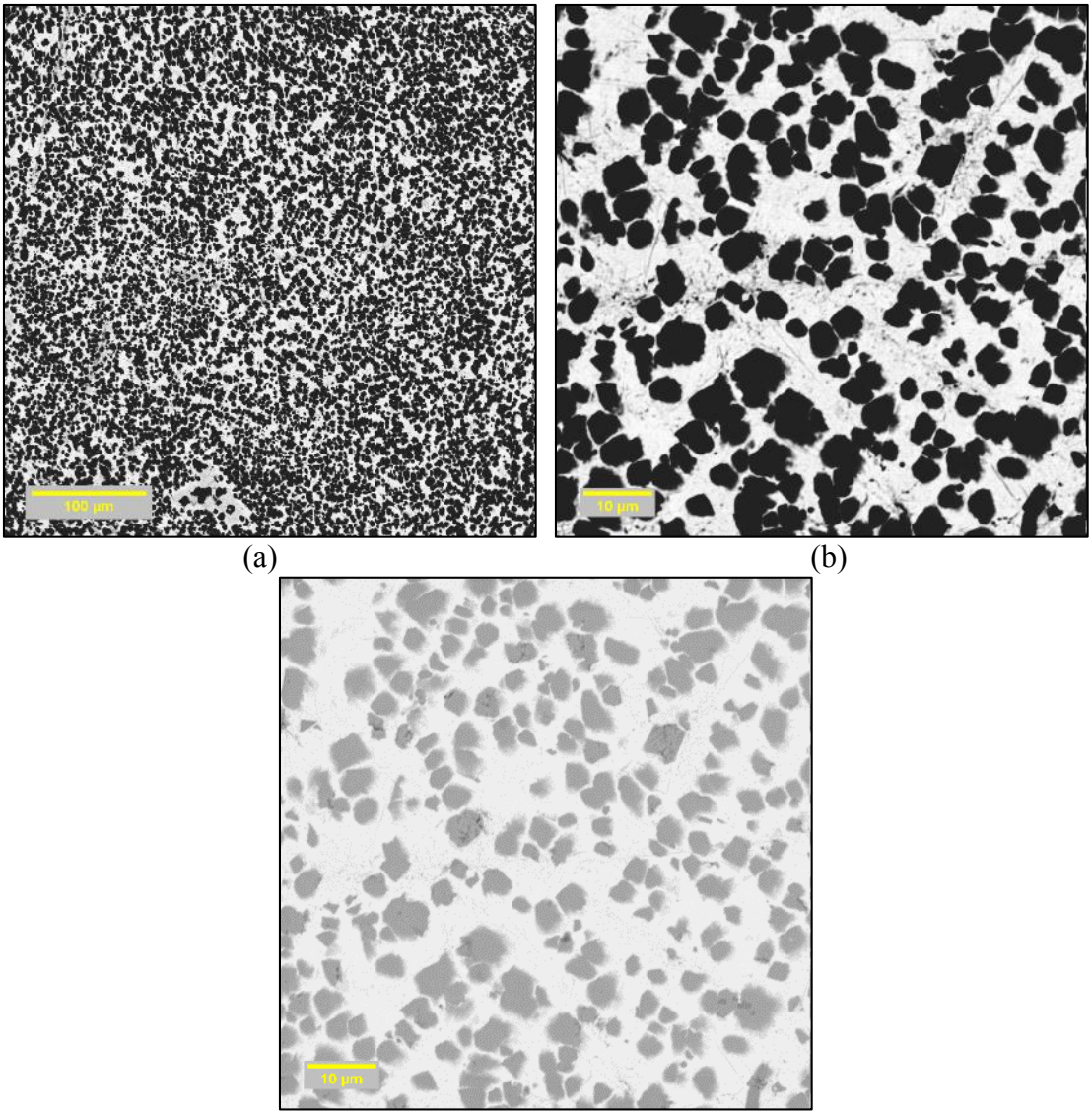

(a) (b)

(c)

Figure 4-25. Images of U-10Mo-5Zr 2hr annealed alloy at (a) 200x, (b) 1200x, and (c) 1200x magnifications. Image (c) was taken at low contrast settings.

Table 4-25. WDS analytical composition of U-10Mo-5Zr 2hr annealed alloy.

	Composition (wt%)							Composition (at%)					
	U	**Mo**	**Zr**	**O**	**N**	**Y**	**Total**	**U**	**Mo**	**Zr**	**O**	**N**	**Y**
Average (Bulk)	88.98	7.68	3.46	2.07	0.81	0.01	103.00	55.10	11.80	5.59	19.02	8.48	0.02
Standard Deviation (Bulk)	0.51	0.19	0.10	0.24	0.06	0.01	0.36	0.75	0.46	0.24	1.87	0.72	0.02
Point 1	93.15	4.80	2.02	2.83	1.09	0.02	103.91	54.47	6.96	3.09	24.62	10.84	0.03
Point 2	4.08	65.52	32.13	0.75	0.00	0.00	102.48	1.56	62.12	32.04	4.28	0.00	0.00
Point 3	1.22	67.74	33.11	0.77	0.00	0.01	102.85	0.46	62.91	32.33	4.29	0.00	0.01

Point 1: Bright region near grain boundary; uranium enriched

Point 2: Black spot within bulk; Mo_2Zr intermetallic

Point 3: Black spot within “line”; Mo_2Zr intermetallic

The two hour annealed U-10Mo-5Zr alloy has a drastically different average bulk composition. The zirconium content increases to roughly 3.5 wt% and molybdenum content to a little over 7.5 wt%, a significant increase from the homogenized or one hour annealed alloy. The presence of apparent Mo_2Zr intermetallics is still clearly evident and a few brighter phases surrounding the intermetallics are enriched in uranium, following the same trends noted previously. The low contrast image (Figure 4-25 (c)) shows that another phase is present within some of the small black features; however, this phase is too small to perform an analysis on. It may be an impurity rich location or some other feature. These phases within the apparent intermetallics do not appear frequently, but are present in various locations. As noted previously, these are likely nucleation sites for the intermetallics.

4.2.5.4. *5 hour annealed*

Images of the U-10Mo-5Zr five hour annealed alloy are presented in Figure 4-26 and WDS data is presented in Table 4-26, followed by a description of the WDS points analyzed.

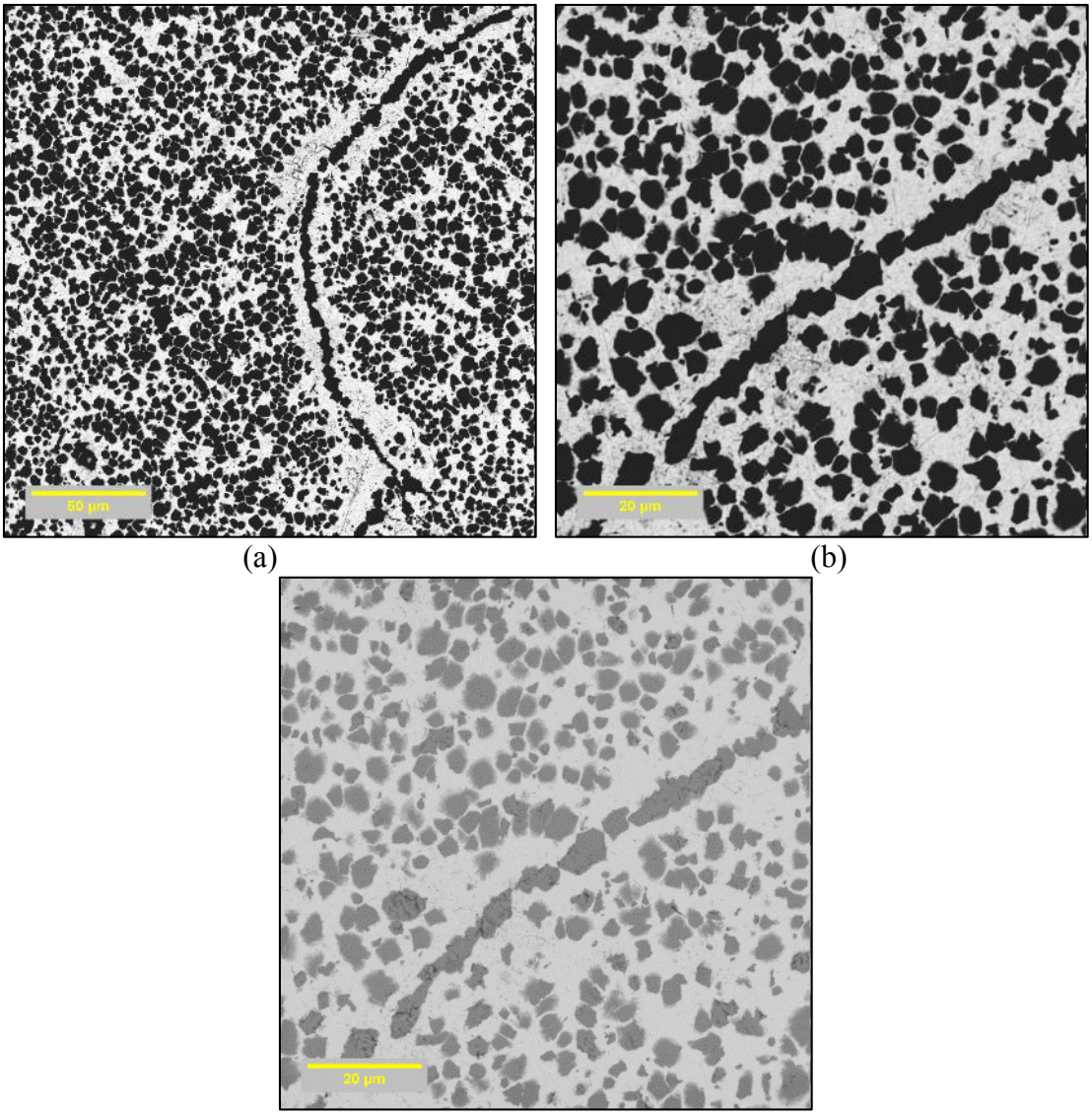

(a) (b)

(c)

Figure 4-26. Images of U-10Mo-5Zr 5hr annealed alloy at (a) 400x, (b) 1000x, and (c) 1000x magnifications. Image (c) was taken at low contrast settings.

Table 4-26. WDS analytical composition of U-10Mo-5Zr 5hr annealed alloy.

	Composition (wt%)							Composition (at%)					
	U	**Mo**	**Zr**	**O**	**N**	**Y**	**Total**	**U**	**Mo**	**Zr**	**O**	**N**	**Y**
Average (Bulk)	89.32	7.34	3.30	2.47	0.87	0.00	103.31	53.27	10.87	5.14	21.92	8.81	0.00
Standard Deviation (Bulk)	0.93	0.74	0.36	0.25	0.03	0.00	0.08	0.65	1.18	0.61	1.90	0.30	0.00
Point 1	2.09	66.89	31.91	0.81	0.00	0.02	101.72	0.79	62.99	31.61	4.59	0.00	0.02
Point 2	1.05	65.94	33.08	0.83	0.02	0.01	100.93	0.40	62.02	32.73	4.70	0.15	0.01
Point 3	94.31	3.50	1.34	4.36	1.17	0.00	104.67	49.35	4.54	1.83	33.91	10.38	0.00

Point 1: Black spot within bulk; Mo_2Zr intermetallic

Point 2: Black spot within "line"; Mo_2Zr intermetallic

Point 3: Bright region near small black spot; uranium enriched

This sample is somewhat similar to the two hour annealed sample. The matrix phase sees a marked increase in zirconium and molybdenum content from the homogenized and one hour annealed samples. It is however, still depleted from what would be expected based on the ratio of constituents when the alloy was fabricated. An abundance of what are likely Mo2Zr intermetallics can be found throughout the sample. Some of the small second phases that are found within the Mo_2Zr intermetallics are again found in this sample as indicated by the low contrast image in Figure 4-26. Their frequency is roughly the same as they are found in the two hour annealed sample.

4.2.5.5. *X-Ray Diffraction*

X-ray diffraction analysis indicated that all samples are composed of α-phase and Mo_2Zr intermetallics, which tends to agree with EPMA data. A peak at 101° in the

homogenized alloy suggests γ' may be present. This phase is not as obvious in the annealed alloys, but a poorly defined peak around 67° may indicate its presence in these samples. This determination, however, cannot be made with certainty. As before, the peak at 39.4° is characteristic of both α-phase and a Mo2Zr intermetallic. Other characteristic peaks for both of these phases are present in all heat treatments so the peak at this angle is likely a combination of counts from both phases. What is not apparent in the normalized XRD data is the change in composition of the bulk matrix phase between the homogenized and one hour annealed samples and the two and five hour annealed samples where the molybdenum and zirconium content see an obvious increase. However, the raw data shows a general trend of decreasing counts as annealing time increases.

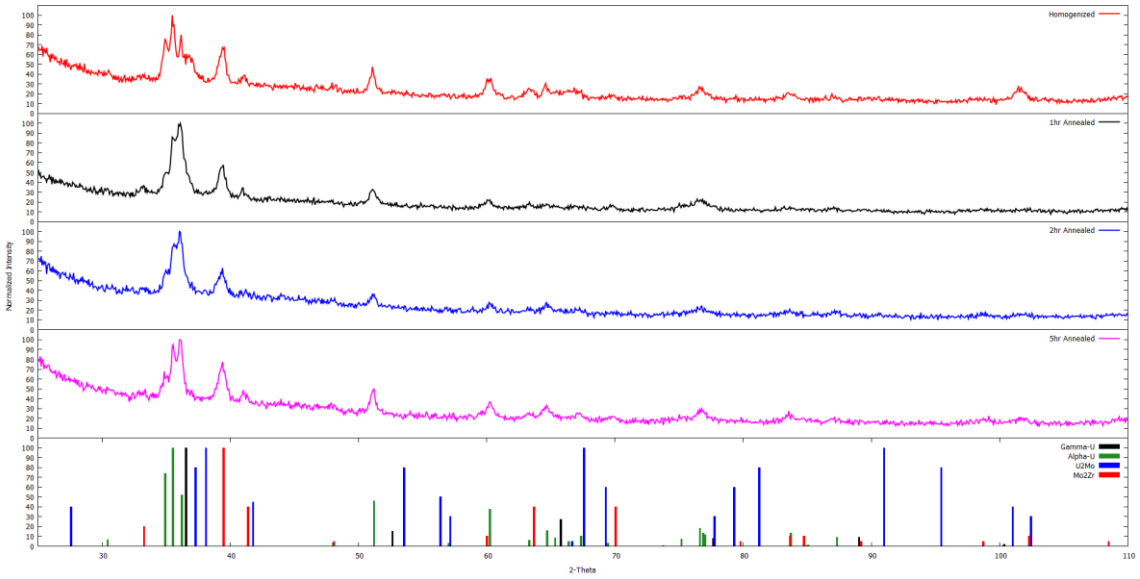

Figure 4-27. XRD spectra of U-10Mo-5Zr after various heat treatments. Reference spectrum data for γ, γ', α, and Mo_2Zr phases is included as the bottom bar graph.

Table 4-27. Phases present in U-10Mo-5Zr.

Heat Treatment	Phases Present
Homogenized	γ', α and Mo_2Zr
1-hour annealed	α and Mo_2Zr
2-hour annealed	α and Mo_2Zr
5-hour annealed	α and Mo_2Zr

4.2.6. U-10Mo-10Zr

4.2.6.1. *Homogenized*

Images of the U-10Mo-10Zr homogenized alloy are presented in Figure 4-28 and WDS data is presented in Table 4-28, followed by a description of the WDS points analyzed.

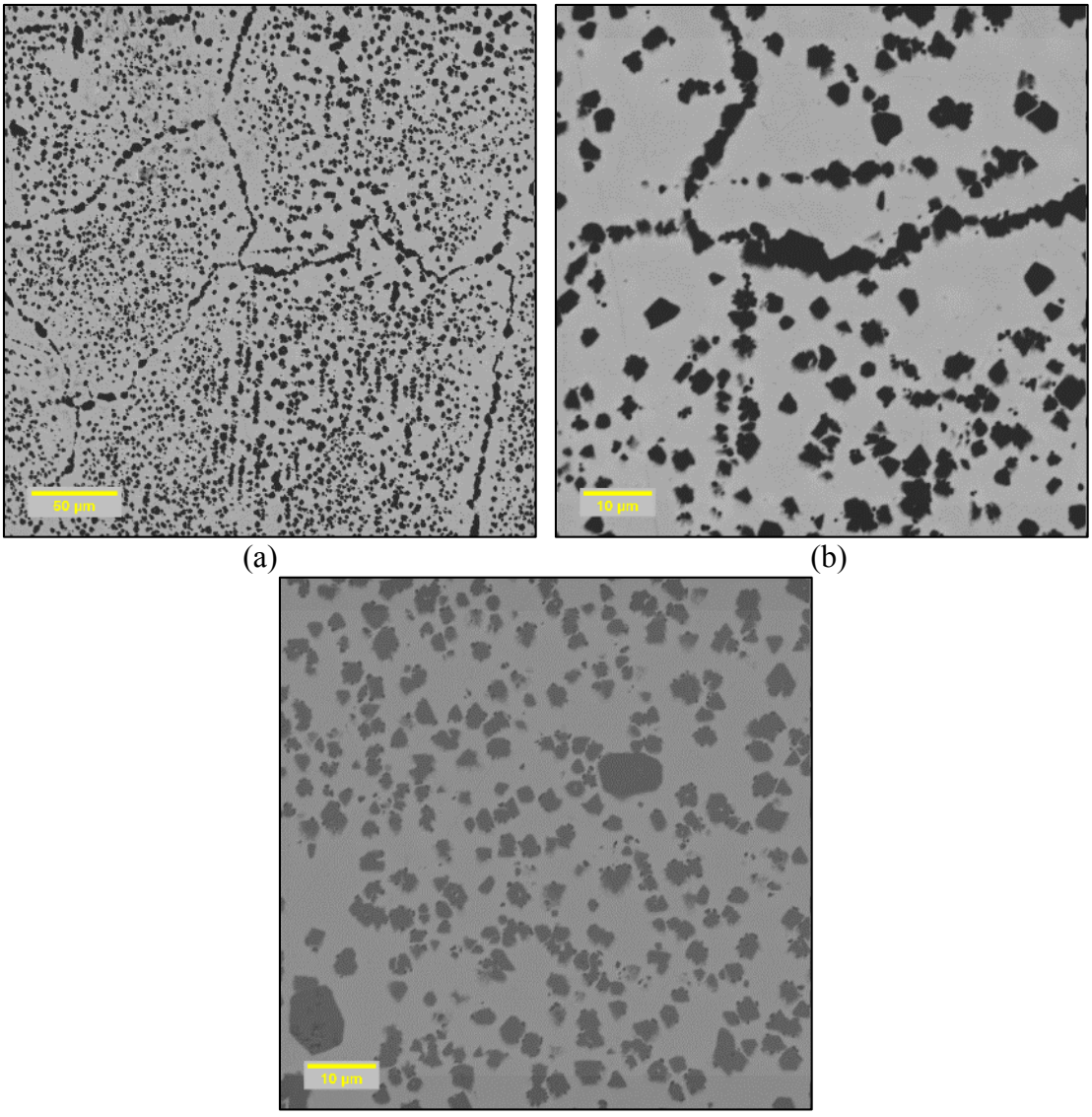

(a) (b)

(c)

Figure 4-28. Images of U-10Mo-10Zr homogenized alloy at (a) 300x, (b) 1200x, and (c) 1200x magnifications. Image (c) was taken at low contrast settings.

Table 4-28. WDS analytical composition of U-10Mo-10Zr homogenized alloy.

	Composition (wt%)							Composition (at%)					
	U	**Mo**	**Zr**	**O**	**N**	**Y**	**Total**	**U**	**Mo**	**Zr**	**O**	**N**	**Y**
Average (Bulk)	86.27	6.15	7.94	1.90	1.02	0.01	103.29	51.39	9.09	12.36	16.79	10.35	0.02
Standard Deviation (Bulk)	0.79	0.37	0.72	0.15	0.09	0.02	0.32	0.39	0.56	1.23	1.13	0.83	0.03
Point 1	3.21	52.38	46.24	1.67	0.00	0.03	103.52	1.15	46.63	43.30	8.89	0.00	0.02
Point 2	1.32	67.06	32.63	0.54	0.00	0.00	101.56	0.51	63.77	32.64	3.08	0.00	0.00
Point 3	4.21	29.51	63.67	3.28	0.00	0.00	100.68	1.44	25.05	56.83	16.68	0.00	0.00

Point 1: Black spot within bulk

Point 2: Black spot within grain boundary; Mo_2Zr intermetallic

Point 3: Black spot within bulk

The homogenized U-10Mo-10Zr alloy is similar in some ways to the U-10Mo-5Zr alloy in that the matrix phase is more depleted in zirconium and molybdenum than would be expected. It is very dense with what appear to be Mo_2Zr intermetallics based on the WDS analysis at Point 2. Both Point 1 and 3 have somewhat unusual compositions. The constituents add up to at least 100 wt%, but when the oxygen content is removed Point 1 is the only one that is still greater than 100 wt%. Point 1 may be an impurity phase containing silicon or it may be a phase without silicon that is not in equilibrium. Point 2 only adds up to 97.4 wt% so may be an impurity phase that contains some silicon.

Based on the low contrast image, it is clear that there are some second phases present in the apparent intermetallics, at their boundaries, or within the matrix. These darker regions are typically 0.25 μm to 0.5 μm in size and too small for any WDS point analysis. This phase is more abundant in this homogenized U-10Mo-10Zr sample than the U-10Mo-5Zr alloy.

4.2.6.2. *1 hour annealed*

Images of the U-10Mo-10Zr 1 hour annealed alloy are presented in Figure 4-29 and WDS data is presented in Table 4-29, followed by a description of the WDS points analyzed.

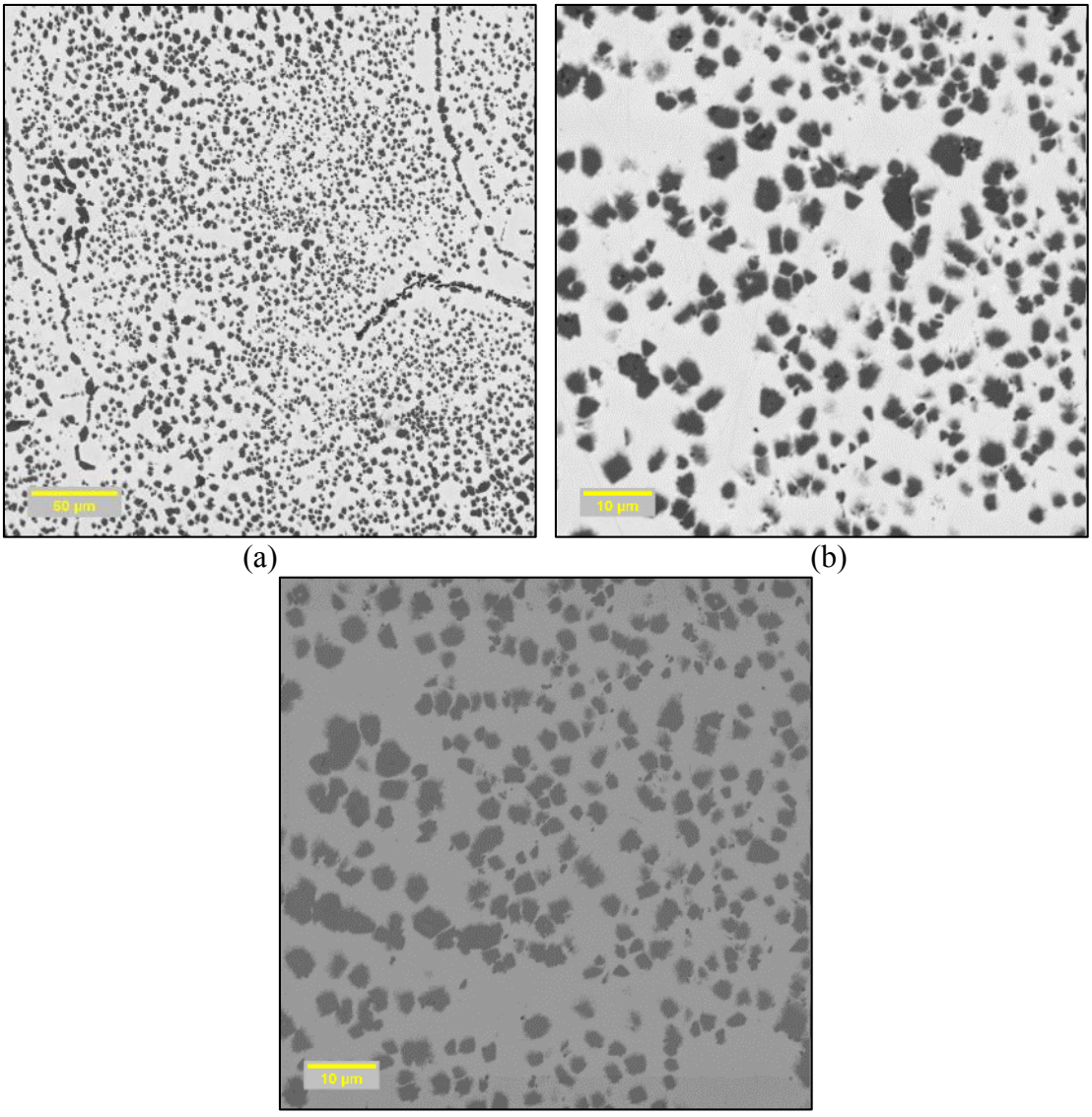

(a) (b)

(c)

Figure 4-29. Images of U-10Mo-10Zr 1hr annealed alloy at (a) 300x, (b) 1200x, and (c) 1200x magnifications. Image (c) was taken at low contrast settings.

Table 4-29. WDS analytical composition of U-10Mo-10Zr 1hr annealed alloy.

	Composition (wt%)							Composition (at%)					
	U	**Mo**	**Zr**	**O**	**N**	**Y**	**Total**	**U**	**Mo**	**Zr**	**O**	**N**	**Y**
Average (Bulk)	84.34	7.43	8.80	1.53	0.94	0.02	103.05	51.27	11.20	13.95	13.81	9.74	0.02
Standard Deviation (Bulk)	0.25	0.14	0.20	0.10	0.10	0.03	0.30	1.08	0.30	0.28	0.70	0.89	0.05
Point 1	3.33	63.49	34.41	0.79	0.00	0.00	102.02	1.27	60.03	34.22	4.48	0.00	0.00
Point 2	2.50	66.56	32.85	0.55	0.28	0.01	102.75	0.94	62.04	32.20	3.05	1.77	0.02

Point 1: Black spot within bulk; Mo_2Zr intermetallic

Point 2: Black spot within grain boundary; Mo_2Zr intermetallic

This sample that has been annealed for an hour contains a higher average content of molybdenum and zirconium in the bulk than the homogenized sample. The molybdenum increases by roughly 1.3 wt% while zirconium increases by about 0.8 wt%. The alloy still seems to contain many Mo_2Zr intermetallic precipitates throughout the matrix, resulting in an overall depletion of molybdenum and zirconium from the matrix. The low contrast image again shows the presence of a second phase that is typically in or around the intermetallics, although not exclusively.

4.2.6.3. *2 hour annealed*

Images of the U-10Mo-10Zr 2 hour annealed alloy are presented in Figure 4-30 and WDS data is presented in Table 4-30, followed by a description of the WDS points analyzed.

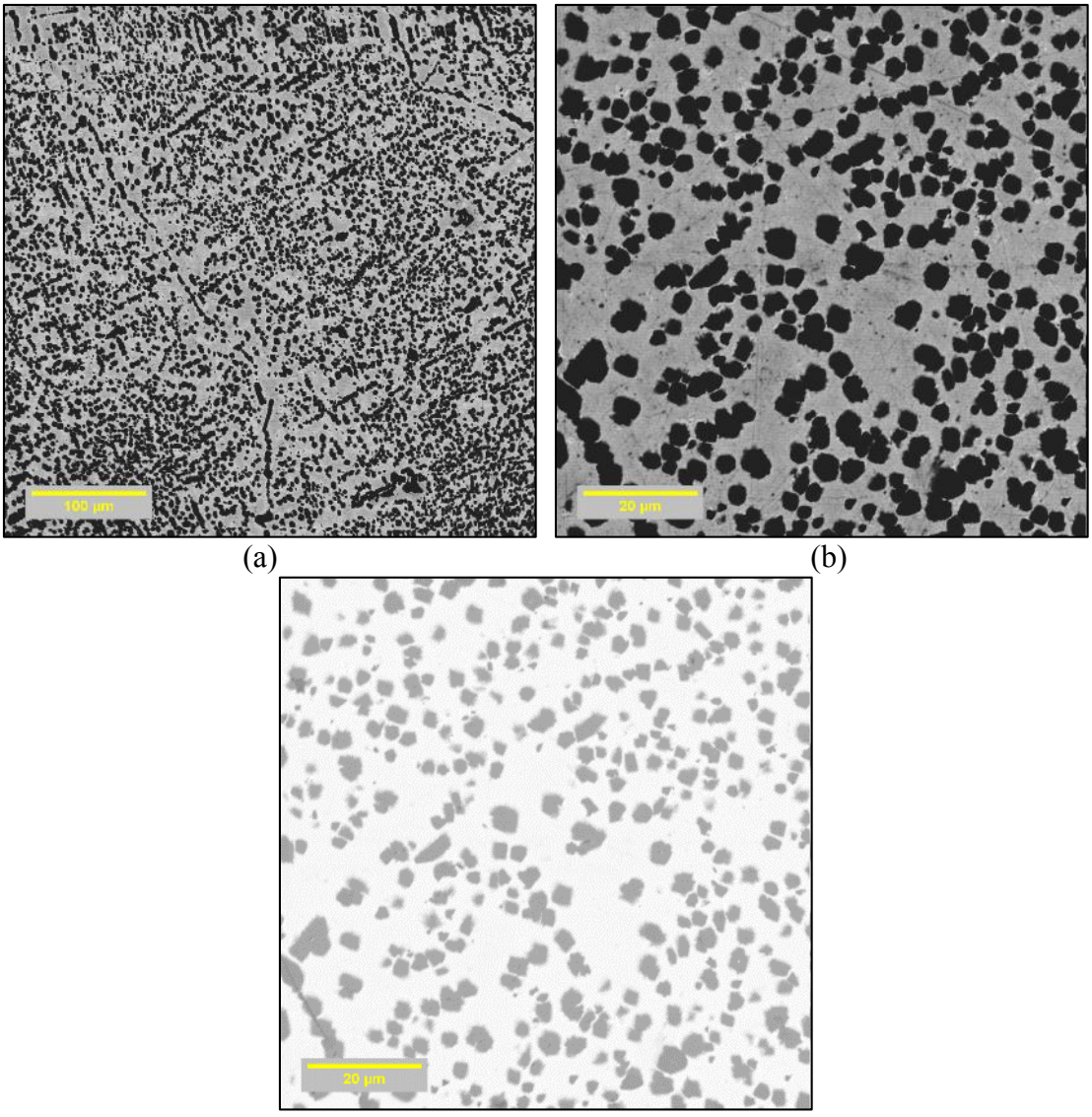

(a) (b)

(c)

Figure 4-30. Images of U-10Mo-10Zr 2hr annealed alloy at (a) 200x, (b) 1000x, and (c) 1000x magnifications. Image (c) was taken at low contrast settings.

Table 4-30. WDS analytical composition of U-10Mo-10Zr 2hr annealed alloy.

	Composition (wt%)							Composition (at%)					
	U	**Mo**	**Zr**	**O**	**N**	**Y**	**Total**	**U**	**Mo**	**Zr**	**O**	**N**	**Y**
Average (Bulk)	84.79	6.69	8.84	1.75	0.68	0.02	102.77	52.29	10.25	14.25	16.04	7.14	0.03
Standard Deviation (Bulk)	1.58	0.98	0.65	0.33	0.10	0.03	0.40	0.84	1.69	1.32	2.63	0.91	0.04
Point 1	2.58	65.10	34.77	0.65	0.00	0.00	103.11	0.98	61.06	34.30	3.66	0.00	0.00
Point 2	2.61	66.46	33.39	0.78	0.03	0.02	103.28	0.98	61.81	32.66	4.36	0.17	0.02
Point 3	88.80	4.48	6.99	2.11	0.72	0.08	103.18	54.83	6.87	11.26	19.40	7.53	0.13

Point 1: Black spot within bulk; Mo_2Zr intermetallic

Point 2: Black spot within grain boundary; Mo_2Zr intermetallic

Point 3: Bright region near small black spot; uranium enriched

The alloy that has been annealed for two hours still exhibits low molybdenum and zirconium content from what is expected. The small black spots are consistent with Mo_2Zr intermetallic phases. The bright phase that appears around these intermetallics is a uranium rich phase. As with the other two heat treatments for this alloy, a second phase is visible when the contrast is lowered; this phase is still too small to allow for WDS analysis.

4.2.6.4. *5 hour annealed*

Images of the U-10Mo-10Zr 5 hour annealed alloy are presented in Figure 4-31 and WDS data is presented in Table 4-31, followed by a description of the WDS points analyzed.

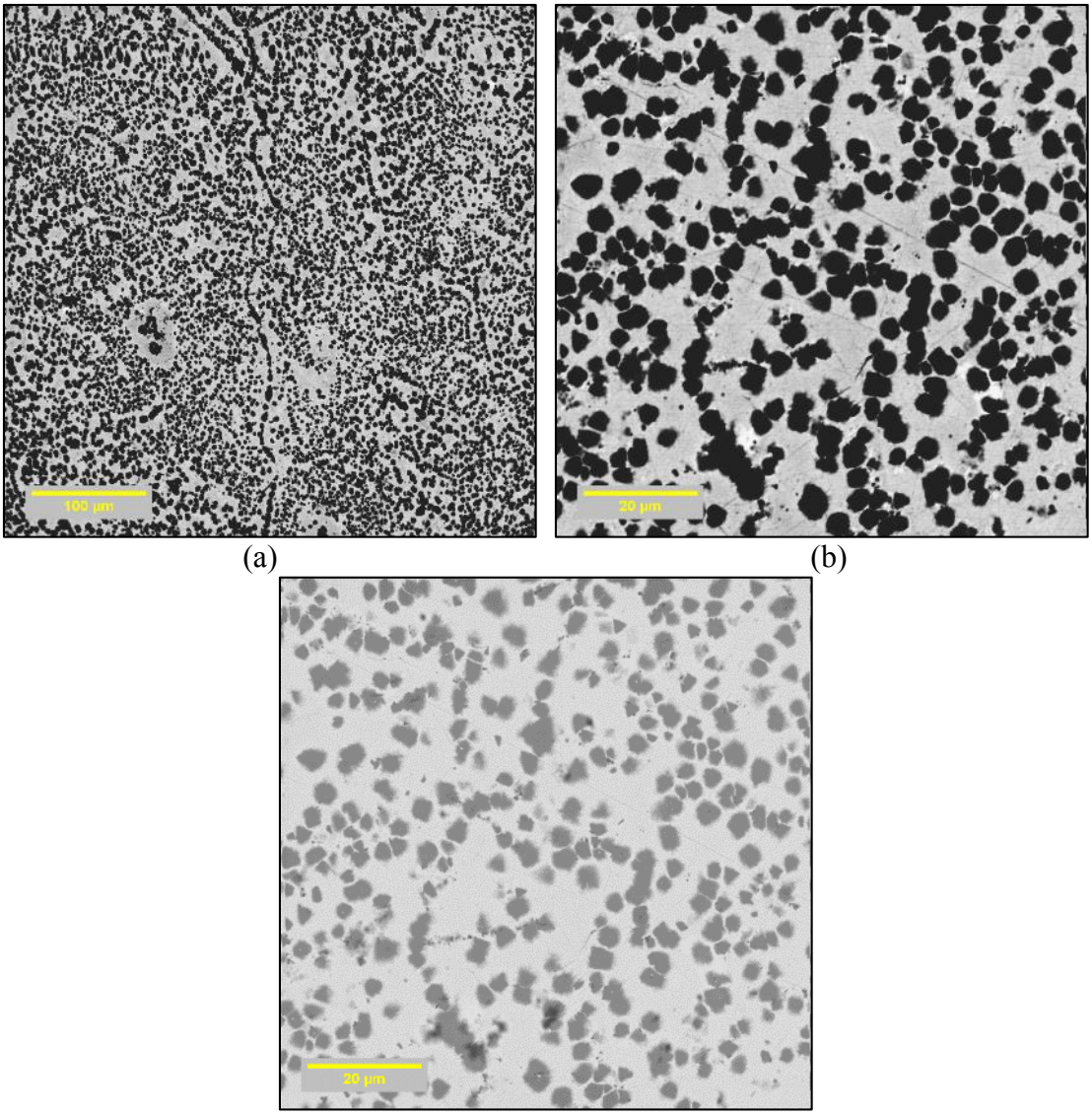

(a) (b)

(c)

Figure 4-31. Images of U-10Mo-10Zr 5hr annealed alloy at (a) 400x, (b) 1000x, and (c) 1000x magnifications. Image (c) was taken at low contrast settings.

Table 4-31. WDS analytical composition of U-10Mo-10Zr 5hr annealed alloy.

	Composition (wt%)							Composition (at%)					
	U	Mo	Zr	O	N	Y	Total	U	Mo	Zr	O	N	Y
Average (Bulk)	83.66	7.59	8.67	2.26	0.64	0.03	102.85	49.31	11.10	13.33	19.76	6.45	0.04
Standard Deviation (Bulk)	0.21	0.28	0.06	0.24	0.05	0.02	0.36	0.79	0.57	0.17	1.81	0.55	0.03
Point 1	8.10	59.11	34.13	0.58	0.00	0.01	101.92	3.21	58.10	35.29	3.39	0.00	0.01
Point 2	2.35	66.19	33.12	0.65	0.10	0.00	102.40	0.89	62.13	32.70	3.66	0.62	0.00
Point 3	90.34	3.43	5.60	3.09	0.78	0.01	103.25	52.28	4.93	8.46	26.61	7.72	0.02

Point 1: Black spot within bulk; Mo_2Zr intermetallic

Point 2: Black spot within bulk; Mo_2Zr intermetallic

Point 3: Bright region near small black spot; uranium enriched

The five hour annealed alloy continues the trend of having a low molybdenum and zirconium content in the matrix material. The black inclusions still appear to be Mo_2Zr intermetallics, and the bright region surrounding them is a uranium rich phase. Consistent with the rest of the alloys of the same composition, a second phase is visible within the intermetallics, at their boundary, or within the matrix material.

4.2.6.5. *X-Ray Diffraction*

The homogenized alloy may have minute amounts of γ-U present based on the XRD data presented in Figure 4-32, although the peaks that would indicate such are small and may be due to inaccuracies in the data. It is clear, however, that both α-uranium and a Mo_2Zr phase are present in all of the heat treatments. The appearance of Mo_2Zr is consistent with the EPMA analysis.

U_2Mo may be present in all samples, but an absolute determination cannot be made based on this data. For the homogenized sample, peaks that appear to be present at 56.4°, around 67°, or 101° could suggest the presence of γ' phase. These same peaks can be observed to a greater or lesser extent for the homogenized alloys which would suggest the same conclusion.

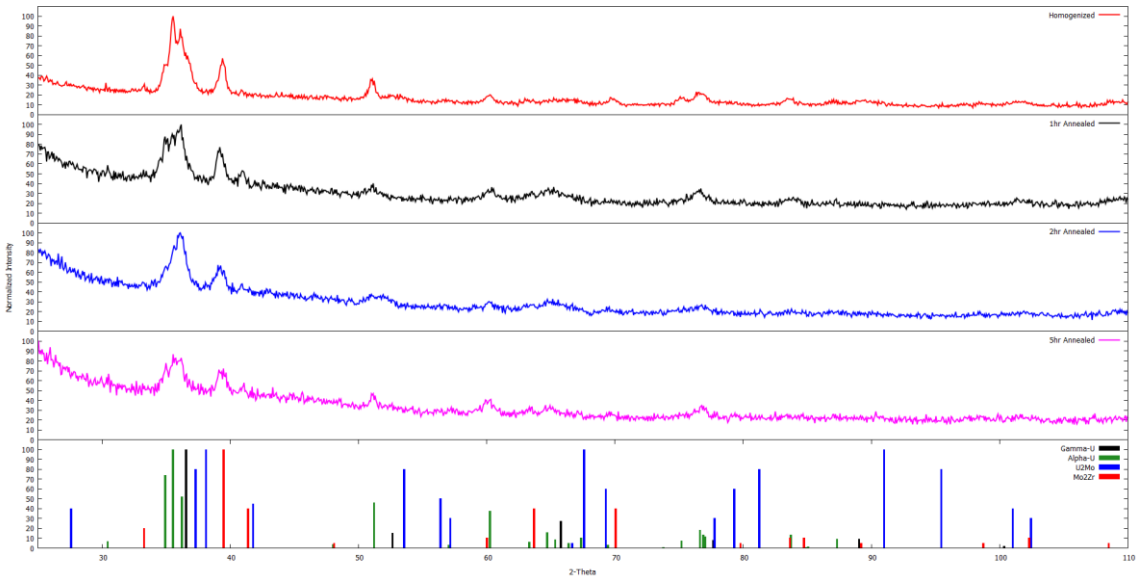

Figure 4-32. XRD spectra of U-10Mo-10Zr after various heat treatments. Reference spectrum data for γ, γ', α, and Mo_2Zr phases is included as the bottom bar graph.

Table 4-32. Phases present in U-10Mo-10Zr.

Heat Treatment	Phases Present
Homogenized	α and Mo_2Zr
1-hour annealed	α and Mo_2Zr
2-hour annealed	α and Mo_2Zr
5-hour annealed	α and Mo_2Zr

4.3. Differential Scanning Calorimetry

Differential scanning calorimetry analysis was performed on all homogenized samples and one sample (U-10Mo-10Zr) for the full set of heat treatments as noted in Table 4-1. These analyses were not intended to provide a full thermodynamic study of these alloys, but instead represent a preliminary glimpse for future work that may be useful to carry out with these alloys. The results included here should be considered a baseline and not a full analysis. (The primary focus of this work was the microscopy and phase identification presented in the previous section.)

Each DSC test sequence took over 36 hours, and resulted in the generation of 6 heating and 6 cooling curves for each of 9 samples tested. Plots are included in Appendix C and the results are summarized in Table 4-33. The first character of the sample name (h, 1, 2, 5) denotes the heat treatment received. The heat cycle number corresponds with the DSC heating program that contains 6 heating and cooling cycles from 500°C to 800°C, with a hold at 650°C between cycle 3 and 4. When multiple transitions were observed within the same cycle, the second transition onset temperature is included below the first.

Table 4-33. DSC transition onset temperatures (°C).

	Heat Cycle					
Sample	**1**	**2**	**3**	**4**	**5**	**6**
H-U-7Mo-2Zr	604.7	604.9	602.3	607.2 647.0	611.7	613.7
H-U-7Mo-5Zr	610.7 632.2	615.7	618.5	648.2	619.4	621.2 643.1
H-U-7Mo-10Zr	597.9	605.3	607.8	635.0	618.5	629.3
H-U-10Mo-2Zr	n/a	n/a	n/a	n/a	n/a	n/a
H-U-10Mo-5Zr	595.6	n/a	n/a	n/a	n/a	n/a
H-U-10Mo-10Zr	609.6 657.3	607.4	605.9	634.8 661.2	605.1	607.9
1-U-10Mo-10Zr	608.2 641.4	609.7	608.2	661.7	n/a	n/a
2-U-10Mo-10Zr	607.3 644.1	600.9	607.4	635.9 659.6	601.3	605.7
5-U-10Mo-10Zr	609.9 643.6	599.6	606.9	613.0 660.8	601.6	611.9

All samples had a very oxidized appearance upon completion of the analysis. Oxygen was likely introduced during the 10 hour anneal at 650°C from the argon supply or potentially from leaks in the sample chamber. This had the effect of adding noise to the signal, especially for the three curves after the prolonged anneal. This made the determination of onset temperature much more difficult, and some had to be determined manually. Each sample was only run once.

Some variations in slope of the DSC curve were noticed, while for other samples the DSC curves were very similar. H-U-7Mo-5Zr exhibited a notable decrease in slope from the first heating to the second. Thereafter, all curves had similar slopes. H-U-10Mo-2Zr was a fairly interesting sample in that no phase changes were observed using DSC. The slope of the first heating cycle was greater than that of the remaining heating cycles however. Sample H-U-10Mo-5Zr also exhibited interesting behavior in the DSC. The slope started much steeper for the first heating cycle then decreased in magnitude around 640°C. A possible phase change occurred that began at 595.6°C but this would need to be confirmed with more precise DSC runs.

The U-10Mo-10Zr alloy exhibited an increased slope for the first heating cycle for all heat treatments of the alloy. Typically, two phase transitions were observed on the first and fourth heating cycles, although measuring exact onset temperatures was difficult due to their proximity and signal noise. The remaining transitions for each successive heating cycle occurred at similar temperatures for all heat treatments.

5. DISCUSSION

Table 5-1 summarizes the findings reported in Chapter 4 and trends for the various alloys after the heat treatments is presented. All alloys were composed of a solid solution matrix phase containing intermetallic precipitates within the matrix or at grain boundaries. No discernable difference could be observed between α-U and γ-U in the images but XRD indicated the presence of both phases under different conditions. U-10Mo-5Zr and U-10Mo-10Zr displayed a significant depletion of molybdenum and zirconium in the matrix, while the other alloys exhibited only a slight depletion of zirconium which can be accounted for in the intermetallics.

Table 5-1. Phases present as indicated by XRD analysis.

Alloy	Homogenized	1hr anneal	2hr anneal	5hr anneal
U-7Mo-2Zr	γ, γ'	γ, γ'	γ, γ'	γ, γ'
U-7Mo-5Zr	α, γ, Mo_2Zr	α, γ, Mo_2Zr	α, γ, Mo_2Zr	α, γ, Mo_2Zr
U-7Mo-10Zr	α, γ	γ	γ	Γ
U-10Mo-2Zr	γ, γ'	γ, γ'	γ, γ'	γ, γ'
U-10Mo-5Zr	α, γ', Mo_2Zr	α, Mo_2Zr	α, Mo_2Zr	α, Mo_2Zr
U-10Mo-10Zr	α, Mo_2Zr	α, Mo_2Zr	α, Mo_2Zr	α, Mo_2Zr

Due to relatively short counting times and the factors described in Section 2.3, it is difficult to interpret the results of XRD analyses with absolute certainty. Often, the same phases were observed to be present in the homogenized alloys and the annealed alloys. This would suggest that the phases present are stable due to the lack of changes after annealing. On the other hand, annealing did indeed coarsen the morphology of the phases.

In terms of fuel plate fabrication this means that the accompanying thermal processes of the hot rolling step are unlikely to further evolve new phases beyond the ones noted here, but the phase morphology will likely evolve over time.

The minimum beam diameter for WDS analyses is 1 μm and the sample stage moves in 1 μm increments. The stage is subject to shift ±1 μm on a given surface upon initializing a WDS measurement, meaning that any area 3 μm or smaller is virtually impossible to accurately measure. The smallest feature that can be measured with some amount of certainty is roughly 5 μm which posed challenges. Often the Mo_2Zr intermetallics found in the alloys appeared as precipitates right at the size limit for WDS analysis. This means that since only the larger spots were analyzed, some of the analyses may not be completely representative of all features. The larger spots were often not indicative of Mo_2Zr, but instead a zirconium rich impurity phase. Based on this it seems probable that, when impurities were present, a disproportionately high number of them were selected for WDS analyses. Table 5-2 presents a summary of alloys and heat treatments and whether Mo_2Zr was indicated via EPMA or XRD.

Table 5-2. Presence of Mo_2Zr (m), impurities (i), both (b), or none (n).

Alloy	EPMA				XRD			
	H	**1**	**2**	**5**	**H**	**1**	**2**	**5**
U-7Mo-2Zr	i	m	m	m	n	n	n	n
U-7Mo-5Zr	i	m	b	b	m	m	m	m
U-7Mo-10Zr	i	i	i	i	n	n	n	n
U-10Mo-2Zr	m	m	m	m	n	n	n	n
U-10Mo-5Zr	m	m	m	m	m	m	m	m
U-10Mo-10Zr	b	m	m	m	m	m	m	m

The data presented in Table 5-1 clearly shows the trends expected as a result of the TTT diagrams presented in Section 2.1. The alloys with a lower quantity of zirconium, namely U-7Mo-2Zr and U-10Mo-2Zr, exist in the γ-U and γ' phases without any apparent α-U.

The Mo_2Zr intermetallics are present in all alloys for all heat treatments with the exception of the U-7Mo-10Zr alloys which had unusual behavior. This was the only alloy that WDS points consistently did not add up to 100 wt% which indicated the presence of some unexpected component in the intermetallics. EDS suggested silicon may be present. Due to this, the results presented for the U-7Mo-10Zr alloy must not be taken as conclusive until further analysis is performed to determine the cause of this anomaly. Considering all

alloys were cast under the exact same conditions from the same stock materials, it was thought to be a reasonable assumption that all alloys had similar impurities present.

Although α-U and Mo_2Zr were observed in many of the samples, this does not immediately indicate poor performance of the fuel plate is to be expected. No detrimental effects of the U-Mo/Zr interdiffusion layer were observed to influence fuel performance in one iteration of irradiation experiments involving a U-Mo fuel with Zr foil barrier layer [29]. Fabrication methods and variables can have a significant effect on the interaction layer formation, which in turn could affect performance. This relationship among fabrication, interdiffusion layer formation, and irradiation performance will need to be further studied.

All alloys exhibited bright regions near darker impurity or intermetallic phases. This could indicate that the alloys still have not reached an equilibrium even after the 7 day homogenization at 950°C or being annealed. This same behavior was not noted in U-Mo vs. Zr diffusion couples [30]. This lack of equilibrium is notable with respect to fuel plate fabrication because these regions would have an unknown effect when irradiated at low temperatures for long periods of time.

The same trends were observed throughout all alloys and heat treatments for this bright region. This bright region is enriched in uranium and depleted in molybdenum and zirconium, presumably due to the continued growth of the nearby intermetallic phase. Identification of crystal structure was not possible without the use of another crystallographic technique such as TEM SAD (tunneling electron microscope-selected area diffraction) or neutron diffraction. Without knowing the crystal structure, no

determination was available to consider how this phase will further develop or behave under various thermal treatments or irradiations.

A notable difference was observed in images from the homogenized to the annealed samples for the U-7Mo-2Zr alloy. Along the grain boundaries a solid grey area is apparent within the homogenized alloy. All three annealed alloys appeared to have a region composed of multiple phases or precipitates along grain boundaries. These regions were too small to quantify with WDS, and would need further analysis to make a determination of composition or potential behavior.

As noted in Figure 2-3, slight decreases in molybdenum content have a significant effect on the decomposition onset time for γ-U. Where zirconium has formed an intermetallic with molybdenum and depleted the matrix phase of molybdenum, this decrease in γ-U decomposition time has important implications for fuel plates. Under standard operating conditions in a research reactor, the fuel plate is maintained at low temperatures (on the order of 100°C) [31]. However, in the case of a power excursion or accident scenario, or future use in a reactor of higher operating temperatures, this phase decomposition can affect fuel stability. If high temperatures are maintained for sufficient time, the fuel may undergo a phase decomposition from γ-U to α-U and Mo_2Zr or other phases, as indicated in the TTT diagrams. The behavior of these phases may be unstable in a reactor, or is, at best, not well characterized. The thickness of these interaction regions where the molybdenum content may be depleted is on the order of magnitude of a few microns [9]. Although small, these undesirable phases could potentially have a significant negative impact on fuel performance in terms of heat transfer if α-U develops and swells.

This would unfortunately be a self-propagating cycle whereby an increase in temperature increases swelling, which further decreases heat transfer.

The only alloys that exhibited a significant depletion of molybdenum in the matrix material were U-10Mo-5Zr and U-10Mo-10Zr, where the molybdenum content ranged from 4 wt% to 8 wt% according to WDS. There were no obvious relationships between molybdenum content and heat treatment. That is, the concentration of molybdenum was not observed to only increase or decrease with increasing annealing time.

Other than the U-10Mo-5Zr and U-10Mo-10Zr, the alloys actually exhibited a slight enrichment of molybdenum content in the bulk phase of the alloy. This would further stabilize the γ-U phase and increase the time necessary for the onset of phase decomposition to occur.

The alloys U-7Mo-2Zr, U-10Mo-5Zr, and U-10Mo-10Zr appeared to have a second phase that was visible only in low contrast images (for example, see Figure 4-6 (d)). These darker phases were too small to analyze with WDS. However, it was observed that most alloys had some level of impurities. These spots may be locations that zirconium has gettered impurities then acted as a nucleation site for other intermetallic phases (namely Mo_2Zr).

Phase decomposition of the metastable γ-phase was observed to begin at nucleation sites along grain boundaries, such as in Figure 4-3 (c). These nucleation processes are thermodynamically driven. Thermal motion can have the effect of causing clusters of atoms to form within the matrix that are compositionally different. These sites then act as nucleation sites for a new phase [4]. The formation of second phase precipitates,

often Mo_2Zr, is apparent in most alloys studied here. Where grain boundaries are present, they appear to be composed of these intermetallic precipitates, although the intermetallics don't form exclusively at grain boundaries. The difference in uranium phases (ie α-U or γ-U) is not readily apparent in images, though it is clear in the XRD data.

As noted in Section 2.1.4, Mo_2Zr intermetallic growth increases under irradiation [23]. Further investigation into these alloys and Mo_2Zr growth is necessary before any conclusions regarding behavior in a reactor can be made with certainty. It is plausible however, that irradiation could promote the formation of these intermetallics in the U-7Mo and U-10Mo alloys and cause a depletion effect of molybdenum in the matrix as observed in U-10Mo-5Zr and U-10Mo-10Zr.

The cursory DSC analysis described in Section 4.3 indicated that thermal cycling had significant effect on the phase transformations that occur in the alloys studied here. The first heating cycle and the fourth heating cycle (immediately after the ten hour anneal) often exhibited phase transformations occurring at temperatures that varied from that of the other four heating cycles (see Table 3-6).

The DSC data commonly revealed a phase change occurring between 595°C and 615°C on heating. This phase change was also observed in the work performed by Sandeep Irukuvarghula and Sangjoon Ahn with U-Zr alloys [20, 32] . This transformation may be attributed to a transformation of the δ-phase to γ-U. The research presented by Sandeep suggests that this may be better described as a diffusional ω-phase (ω_d) transforming to γ-phase [20]. The fact that this transition was often visible after thermal cycles would indicate that it is a stable phase. The fact that it was not always visible indicates that the

rate of transformation may be slow. Due to the complicated nature of these phases (δ and ω) and lack of additional analyses or relevant literature, further analysis is omitted here.

Other phase transformations were observed between 635°C and 665°C. These transformations may be attributed to α-U to β-U or γ-U phase change. These higher temperature changes were often only noticed on the initial heating cycle or after the ten hour anneal, if it all.

The increased slope for the first heating cycle of the homogenized U-10Mo-2Zr alloy would suggest it had an increased heat capacity. That is, the initial heating and cooling of the alloy caused some change that decreased its heat capacity, although no phase changes were obvious. It is interesting to note that for the U-10Mo-5Zr homogenized alloy, a transformation was initially visible on the first heating cycle but was not present in any successive heating cycles, either before or after an anneal at 650°C. A noticeable decrease in slope occurred around 640°C. This change in slope indicates a decreasing heat capacity.

6. SUMMARY AND CONCLUSIONS

Properties of the ternary U-Mo-Zr alloy system were investigated as part of the qualification process for fuel plates for various research and test reactors. Six U-xMo-yZr (x= 7, 10 wt%; y= 2, 5, 10 wt%) alloys were cast, then subjected to various heat treatments. Initially, they were homogenized at 950°C to ensure they were well mixed. They were then annealed at 650°C for 1, 2, and 5 hours in order to simulate a step of the fuel plate fabrication processes. These alloys were then characterized using EPMA, XRD, and DSC techniques.

All alloys exhibited somewhat similar characteristics in their images to a greater or lesser extent. A solid solution matrix phase that contained intermetallic precipitates in the matrix and along the grain boundaries was observed. WDS analysis determined that these intermetallics were typically consistent with Mo_2Zr, although some regions showed signs of zirconium rich impurity phases. With the exception of U-10Mo-5Zr and U-10Mo-10Zr, all alloys under all heat treatment conditions displayed a slight enrichment in molybdenum content in the matrix phase which should help maintain stability of the γ-U phase. The exceptions, U-10Mo-5Zr and U-10Mo-10Zr exhibited a significant depletion of molybdenum in the matrix phase and a marked increase in intermetallic precipitate density throughout the alloys and for all heat treatments. No clear relationship between heat treatment and molybdenum content could be determined.

Based on XRD analysis, α-U was present in alloys with zirconium content of 5 wt% or 10 wt% with the exception of U-7Mo-10Zr. However, this alloy seemed to have a

significant amount of zirconium rich impurities so the behavior of the bulk phase may have been influenced by this.

Differential scanning calorimetry analysis indicates a phase change around 595°C to 615°C that corresponds with a δ to γ-U transition for all homogenized alloys with the exception of U-10Mo-2Zr, which exhibited no phase changes. Often, a second phase change was observed during the first heating cycle and the fourth heating cycle, immediately after a 10 hour hold at 650°C. The onset temperature of this phase change suggests it is either an α-U to β-U or α-U to γ-U transition.

The results generated throughout this study, in conjunction with other literature, suggest that the interdiffusion layer between the U-Mo fuel meat and Zr barrier layer will not behave in a way detrimental to performance within a nuclear reactor. Further characterization of the ternary alloys containing 10 wt% molybdenum and a high concentration of zirconium will need to be performed in order to verify that intermetallics will not form in excess, resulting in a significant depletion of molybdenum from the matrix phase.

In order to address open issues and further investigate the U-Mo-Zr system as it relates to fuel development, the following recommendations are made:

1. Transmission electron microscopy should be utilized in order to allow for better resolution and subsequent analysis of microstructural characteristics of the alloys.
2. The homogenization time should be increased so that equilibrium can be ensured. A homogenization at 950°C for two to three weeks is recommended instead of a one week homogenization.

3. Additional DSC analyses should be performed in order to achieve higher fidelity results.
4. The effect of various thermal cycles should be examined. Temperature should be varied between 560°C and 650°C, along with the length of time the sample is annealed.

REFERENCES

1. Argonne National Laboratory. Lemont, IL. *RERTR: Currently-Qualified Fuels*. U.S. Department of Energy 2008. Retrieved 2014; Available from: http://www.rertr.anl.gov/QualFuel.html.
2. National Nuclear Security Administration, U.S. Department of Energy. *GTRI's Convert Program*. Retrieved 2014. Available from: http://nnsa.energy.gov/aboutus/ourprograms/dnn/gtri/convert.
3. National Nuclear Security Administration, U.S. Department of Energy. *GTRI's Convert Program: Minimizing the Use of Highly Enriched Uranium*. 2014. Retrieved 2014; Available from: https://nnsa.energy.gov/mediaroom/factsheets/gtri-convert.
4. Hofman, GL, MK Meyer, and AE Ray, *Design of High Density Gamma-Phase Uranium Alloys for LEU Dispersion Fuel Applications.* Conference Proceedings, The 1998 International Reduced Enrichment for Test Reactor Conference, Sao Paulo, Brazil. 1998.
5. Robinson, AB, GS Chang, DD Keiser Jr, DM Wachs, and DL Porter, *Irradiation Performance of U-Mo Alloy Based 'Monolithic'plate-Type Fuel–Design Selection.* Idaho National Laboratory Report INL/EXT-09-16807. 2009.
6. Oliveira, FBVd, EF Carvalho, and HG Riella, *Fabrication Results of Gamma Uranium-Molybdenum Alloys Fuels.* Conference Proceedings, 2009 International Nuclear Atlantic Conference, Rio de Janeiro, Brazil. 2009.

7. Park, Y, J Yoo, K Huang, DD Keiser Jr, JF Jue, et al., *Growth Kinetics and Microstructural Evolution During Hot Isostatic Pressing of U-10wt.% Mo Monolithic Fuel Plate in Al6061 Cladding with Zr Diffusion Barrier.* Journal of Nuclear Materials, 2014. **447**(1): p. 215-224.

8. Varela, CK, M Mirandou, S Aricó, S Balart, and L Gribaudo, *Interdiffusion between U (Mo, Pt) or U (Mo, Zr) and Al or Al A356 Alloy.* Journal of Nuclear Materials, 2009. **395**(1): p. 162-168.

9. Huang, K, CC Kammerer, DD Keiser Jr., and YH Sohn, *Diffusion Barrier Selection from Refractory Metals (Zr, Mo and Nb) Via Interdiffusion Investigation for U-Mo Rertr Fuel Alloy.* Journal of Phase Equilibria and Diffusion, 2014. **35**(2): p. 146-156.

10. U.S. Department of Energy, *DOE Fundamentals Handbook: Material Science.* 1993. **1**.

11. Parida, SC, S Dash, Z Singh, R Prasad, and V Venugopal, *Thermodynamic Studies on Uranium–Molybdenum Alloys.* Journal of Physics and Chemistry of Solids, 2001. **62**(3): p. 585-597.

12. Kittel, JH and SH Paine, *Effects of High Burnup on Natural Uranium*. Vol. 5539. 1957: Argonne National Laboratory.

13. Thewlis, J and H Steeple, *The β-Uranium Structure.* Acta Crystallographica, 1954. **7**(4): p. 323-328.

14. Peterson, CAW, WJ Steele, and SL DiGiallonardo, *Isothermal Transformation Study of Some Uranium-Base Alloys.* Lawrence Radiation Laboratory Report, UCRL-7824. 1964.

15. Dwight, AE, *The Uranium-Molybdenum Equilibrium Diagram Below 900 C.* Journal of Nuclear Materials, 1960. **2**(1): p. 81-87.

16. Halteman, EK, *The Crystal Structure of U2mo.* Acta Crystallographica, 1957. **10**(3): p. 166-169.

17. Murray, JL and TB Massalski, *Binary Alloy Phase Diagrams.* American Society for Metals, Metals Park, OH, 1986: p. 1642, 1649, 2151.

18. Sheldon, RI and DE Peterson, *The U-Zr (Uranium-Zirconium) System.* Bulletin of Alloy Phase Diagrams, 1989. **10**(2): p. 165-171.

19. Basak, CB, N Prabhu, and M Krishnan, *On the Formation Mechanism of Uzr_2 Phase.* Intermetallics, 2010. **18**(9): p. 1707-1712.

20. Irukuvarghula, S, *Solid State Phase Transformations in Uranium-Zirconium Alloys.* Texas A&M Doctoral Dissertation, 2013.

21. Akabori, M, T Ogawa, A Itoh, and Y Morii, *The Lattice Stability and Structure of Delta-Uzr_2 at Elevated Temperatures.* Journal of Physics: Condensed Matter, 1995. **7**(43): p. 8249.

22. Pérez, RJ and B Sundman, *Thermodynamic Assessment of the Mo–Zr Binary Phase Diagram.* Calphad, 2003. **27**(3): p. 253-262.

23. Liou, KY, P Wilkes, GL Kulcinski, and JH Billen, *Void Swelling and Phase Instability in Heavy Ion Irradiated Mo-Zr Alloy.* Journal of Nuclear Materials, 1979. **85**: p. 735-738.

24. Ivanov, OS and GN Bagrov, *Isothermal Cross Sections of the Triple System Uranium-Molybdenum-Zirconium at 1000 C-625 C.* Struct. Alloys Certain Syst. Cont. Uranium Thorium, 1963: p. 131-153.

25. Fizzotti, C and A Masperoni, *Study of Ternary Alloys of Uranium--Molybdenum--Niobium and Uranium--Molybdenum--Zirconium at Low Content of Binder.* EURATOM/CNEN/SNAM, translated for Oak Ridge National Laboratory RT/MET-68-5. 1968.

26. Huang, K, Y Park, DD Keiser Jr, and YH Sohn, *Interdiffusion between Zr Diffusion Barrier and U-Mo Alloy.* Journal of Phase Equilibria and Diffusion, 2012. **33**(6): p. 443-449.

27. Moore, GA and MC Marshall, *Co-Rolled U10mo/Zirconium-Barrier-Layer Monolithic Fuel Foil Fabrication Process.* Idaho National Laboratory Report INL/EXT-10-17774, 2010.

28. Moore, GA, JF Jue, BH Rabin, and MJ Nilles, *Full Size U-10Mo Monolithic Fuel Foil and Fuel Plate Fabrication-Technology Development.* Idaho National Laboratory Preprint INL/CON-09-17519. 2010.

29. Robinson, AB, DM Wachs, DE Burkes, and DD Keiser. *US RERTR Fuel Development Post Irradiation Examination Results*. Conference Proceedings,

Reduced Enrichment for Research and Test Reactors, 2008. Idaho National Laboratory INL/CON-08-14916. 2008.

30. Huang, K, Y Park, DD Keiser Jr, and YH Sohn, *Interdiffusion between Potential Diffusion Barrier Mo and U-Mo Metallic Fuel Alloy for Rertr Applications.* Journal of Phase Equilibria and Diffusion, 2013. **34**(4): p. 307-312.

31. World Nuclear Association. *Research Reactors*. 2014; Available from: http://www.world-nuclear.org/info/Non-Power-Nuclear-Applications/Radioisotopes/Research-Reactors/.

32. Ahn, S, *Comprehensive Investigation of the Uranium-Zirconium Alloy System: Thermophysical Properties, Phase Characterization and Ion Implantation Effects.* Texas A&M Doctoral Dissertation, 2013.

33. Smith et al., *Uranium (Gamma)*, Penn State University. Source of XRD reference data. 1973.

34. Lander, GH, MH Mueller *Uranium (Alpha)*, in Acta Crystallographica. Source of XRD reference data. 1970, 1997. p. 129.

35. Battelle Memorial Institute, *MoU2 (Molybdenum Uranium).* Source of XRD reference data. Private Communication.

36. Duwez, J, *Mo_2Zr (Molybdenum Zirconium)*, in California Institute of Technology. Private Communication. Source of XRD reference data.

Supplemental Sources Consulted

- Blatt, FJ, *On the Metastable γ-Phase Uranium-Molybdenum Alloys.* Journal of Physics and Chemistry of Solids, 1961. **17**(3): p. 177-187.
- Burkes, DE, T Hartmann, R Prabhakaran, and JF Jue, *Microstructural Characteristics of DU–xMo Alloys with x= 7–12wt%.* Journal of Alloys and Compounds, 2009. **479**(1): p. 140-147.
- Burkes, DE, CA Papesch, AP Maddison, T Hartmann, and FJ Rice, *Thermo-Physical Properties of DU–10wt.% Mo Alloys.* Journal of Nuclear Materials, 2010. **403**(1): p. 160-166.
- Burkes, DE, R Prabhakaran, T Hartmann, JF Jue, and FJ Rice, *Properties of DU–10wt% Mo Alloys Subjected to Various Post-Rolling Heat Treatments.* Nuclear Engineering and Design, 2010. **240**(6): p. 1332-1339.
- Burkes, DE, R Prabhakaran, JF Jue, and FJ Rice, *Mechanical Properties of DU-xMo Alloys with x= 7 to 12 Weight Percent.* Metallurgical and Materials Transactions A, 2009. **40**(5): p. 1069-1079.
- Craik, RL, D Birch, C Fizzotti, and F Saraceno, *Phase Equilibria in Uranium-Rich Binary Alloys Containing Molybdenum and Zirconium and the Effect of Ternary Additions of Carbon.* Journal of Nuclear Materials, 1962. **6**(1): p. 13-25.
- Creasy, J, *Thermal Properties of Uranium-Molybdenum Alloys: Phase Decomposition Effects of Heat Treatments.* Texas A&M Masters Thesis, 2011.

- Ewh, AE, E Perez, DD Keiser Jr, and YH Sohn, *Microstructural Characterization of U-Nb-Zr, U-Mo-Nb, and U-Mo-Ti Alloys Via Electron Microscopy.* Journal of Phase Equilibria and Diffusion, 2010. **31**(3): p. 216-222.
- Ewh, AE, *Effects of Allotropic Transformations on Interdiffusion Behavior in Binary Systems.* Masters Thesis at University of Central Florida, 2012.
- Gates, JE, WE Murr, AA Bauer, and FA Rough, *Irradiation Studies of Uranium-10 W/o Molybdenum Fuel Alloy*. 1961, Atomic Power Development Associates, Inc., Detroit; Battelle Memorial Inst., Columbus, Ohio.
- Goldstein, Y and A Bar-Or, *Decomposition of Gamma Phase in Uranium Alloys Containing 8, 10.8, and 14.3 Wt Percent Molybdenum*. 1967, Israel Atomic Energy Commission, Tel-Aviv.
- Howlett, BW, *A Study of the Shear Transformations from the Gamma-Phase in Uranium-Molybdenum Alloys Containing 6.0–12.5 at% Molybdenum.* Journal of Nuclear Materials, 1970. **35**(3): p. 278-292.
- Howlett, BW, AJ Eycott, IK Kang, and DRF West, *The Kinetics of the Isothermal Decomposition of a Gamma-Phase Uranium-6 Atomic% Molybdenum Alloy.* Journal of Nuclear Materials, 1963. **9**(2): p. 143-154.
- Ivanov, OS and YS Virgiliev, *The Decomposition of the γ-Uranium Base Solid Solutions as Revealed by X-Ray Investigations.* Journal of Nuclear Materials, 1962. **6**(2): p. 199-202.

- Ivanov, OS and GN Bagrov, *Isothermal Cross Sections at 600 C, 575 C, and 500 C, Polythermal Sections, and the Phase Diagram of the Triple System Uranium-Molybdenum-Zirconium.* ASM Alloy Phase Diagrams Center: p. 154-176.
- Ivanov, OS and GN Bagrov, *Isothermal Cross Sections of the Triple System Uranium-Molybdenum-Zirconium at 1000 C-625 C.* ASM Alloy Phase Diagrams Center: p. 131-153.
- Keskar, M, SK Sali, ND Dahale, K Krishnan, R Phatak, et al., *X-Ray and Thermal Studies of Mixed Valent Uranium Molybdates.* Journal of Nuclear Materials, 2012. **421**(1): p. 147-152.
- Kim, YS, GL Hofman, AB Robinson, DM Wachs, HJ Ryu, et al., *Irradiation Performance of U–Mo–Ti and U–Mo–Zr Dispersion Fuels in Al–Si Matrixes.* Journal of Nuclear Materials, 2012. **427**(1): p. 233-238.
- Kutty, TRG, S Dash, J Banerjee, S Kaity, A Kumar, et al., *Thermophysical Properties of U_2Mo Intermetallic.* Journal of Nuclear Materials, 2012. **420**(1): p. 193-197.
- Landa, A, P Söderlind, and PEA Turchi, *Density-Functional Study of U–Mo and U–Zr Alloys.* Journal of Nuclear Materials, 2011. **414**(2): p. 132-137.
- Massalaski, TB, *Binary Alloy Phase Diagrams*. Vol. 2. 1986. 1642, 1649, 2151.
- Meyer, MK. *A Global Overview of High Density U-Mo Fuel Development Efforts*. Conference Proceedings, International Symposium on Minimisation of Highly Enriched Uranium (HEU) in the Civilian Nuclear Sector : The Way Ahead. 2006. Oslo, Norway: Idaho National Laboratory.

- Meyer, MK, GL Hofman, SL Hayes, CR Clark, TC Wiencek, et al., *Low-Temperature Irradiation Behavior of Uranium–Molybdenum Alloy Dispersion Fuel.* Journal of Nuclear Materials, 2002. **304**(2): p. 221-236.
- Mirandou, MI, SF Aricó, SN Balart, and LM Gribaudo, *Characterization of the Interaction Layer in Diffusion Couples U-7 Wt.% Mo/Al 6061 Alloy at 550° C and 340° C.: Effect of the γ-U (Mo) Cellular Decomposition.* Materials Characterization, 2009. **60**(8): p. 888-893.
- Murphy, MM and DA Colling, *Uranium Alloy Metallurgy: An Annotated Bibliography*, in *Other Information: Orig. Receipt Date: 31-DEC-74*. 1974. p. Medium: X; Size: Pages: 109.
- Orlov, VK, VM Teplinskaya, and NT Chebotarev, *Decomposition of a Metastable Solid Solution in Uranium-Molybdenum Alloy.* Atomic Energy, 2000. **88**(1): p. 42-47.
- Park, JM, HJ Ryu, SJ Oh, DB Lee, Ch K Kim, et. al. *Interdiffusion Behaviors of U-Mo-Zr/Al-Si*. in *International Meeting on Reduced Enrichment for Research and Test Reactors. RERTR. 2006, Cape Town, South Africa*. 2006.
- Park, JM, HJ Ryu, SJ Oh, DB Lee, CK Kim, et al., *Effect of Si and Zr on the Interdiffusion of U–Mo Alloy and Al.* Journal of Nuclear Materials, 2008. **374**(3): p. 422-430.
- Perez, E, B Yao, DD Keiser Jr, and YH Sohn, *Microstructural Analysis of as-Processed U–10wt.% Mo Monolithic Fuel Plate in Al6061 Matrix with Zr Diffusion Barrier.* Journal of Nuclear Materials, 2010. **402**(1): p. 8-14.

- Raymond, S, J Bouchet, GH Lander, M Le Tacon, G Garbarino, et al., *Understanding the Complex Phase Diagram of Uranium: The Role of Electron-Phonon Coupling.* Physical review letters, 2011. **107**(13): p. 136401.
- Rechtien, JJ and RD Nelson, *Phase Transformations in Uranium, Plutonium, and Neptunium.* Metallurgical Transactions, 1973. **4**(12): p. 2755-2765.
- Rest, J, YS Kim, GL Hofman, MK Meyer, and SL Hayes, *U-Mo Fuels Handbook V. 1.0*, in *Argonne National Laboratory Internal Report*. 2006.
- Rhodes, CG and D Kramer, *On the Gamma to Gamma Prime Transformation in Uranium—33 at% Molybdenum.* Journal of Nuclear Materials, 1963. **9**(1): p. 114-115.
- Rothman, SJ, *Diffusion in Uranium, Its Alloys, and Compounds*. 1961, Argonne National Laboratory, Illinois.
- Rough, FA, AA Bauer, *Constitution of Uranium and Thorium Alloys*. 1958, Battelle Memorial Institute.
- Sinha, VP, PV Hegde, GJ Prasad, GK Dey, and HS Kamath, *Effect of Molybdenum Addition on Metastability of Cubic γ-Uranium.* Journal of Alloys and Compounds, 2010. **491**(1): p. 753-760.
- Snelgrove, JL, GL Hofman, MK Meyer, CL Trybus, and TC Wiencek, *Development of Very-High-Density Low-Enriched-Uranium Fuels.* Nuclear Engineering and Design, 1997. **178**(1): p. 119-126.

- Takahashi, Y, M Yamawaki, and K Yamamoto, *Thermophysical Properties of Uranium-Zirconium Alloys.* Journal of Nuclear Materials, 1988. **154**(1): p. 141-144.
- Tkach, I, N-TH Kim-Ngan, S Mašková, M Dzevenko, L Havela, et al., *Characterization of Cubic γ-Phase Uranium Molybdenum Alloys Synthesized by Ultrafast Cooling.* Journal of Alloys and Compounds, 2012. **534**: p. 101-109.
- Van den Berghe, Sven, A Leenaers, E Koonen, and L Sannen, *From High to Low Enriched Uranium Fuel in Research Reactors.* Advances in Science and Technology, 2011. **73**: p. 78-90.
- Varela, CL, SF Arico, M Mirandou, SN Balart, and LM Gribaudo, *Identification of Phases in the Interaction Layer between U-Mo-Zr/Al and U-Mo-Zr/Al-Si.* 2008.
- Yakel, HL, *Review of X-Ray Diffraction Studies in Uranium Alloys*. 1973, Oak Ridge National Laboratory, Tenn.(USA).
- Zweifel, T, H Palancher, A Leenaers, A Bonnin, V Honkimaki, et al., *Crystallographic Study of Si and Zrn Coated U–Mo Atomised Particles and of Their Interaction with Al under Thermal Annealing.* Journal of Nuclear Materials, 2013. **442**(1): p. 124-132.

APPENDIX A: X-RAY DIFFRACTION REFERENCE DATA

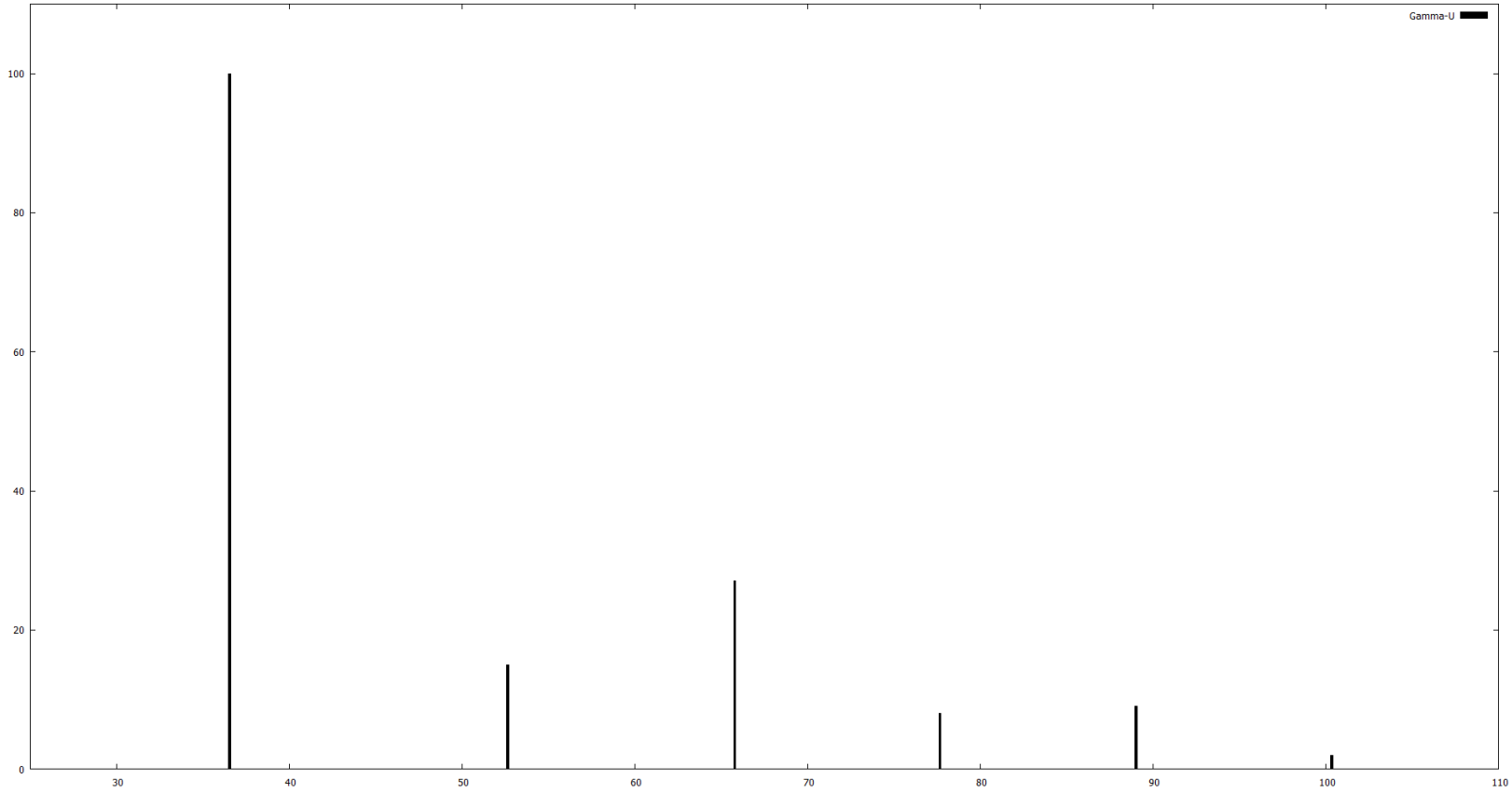

Appendix Figure 1. Reference XRD data for γ-U. [33].

Appendix Table 1. Reference XRD data for γ-U. [33].

2Θ	Intensity	h	k	l
36.555	100	1	1	0
52.647	15	2	0	0
65.792	27	2	1	1
77.678	8	2	2	0
89.034	9	3	1	0
100.35	2	2	2	2
112.1	9	3	2	1
140.34	5	3	3	0

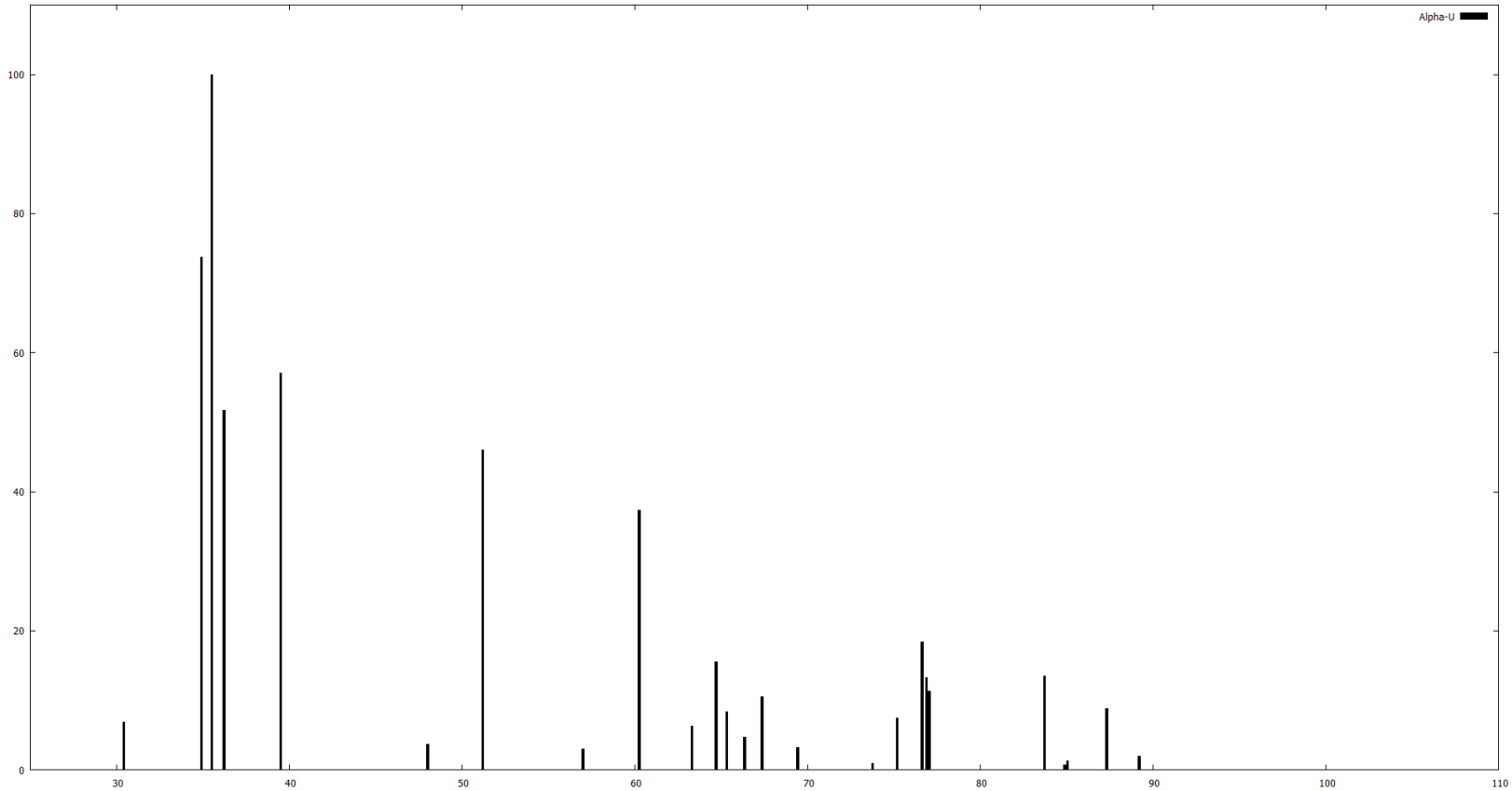

Appendix Figure 2. Reference XRD data for α-U. [34].

Appendix Table 2. Reference XRD data for α-U. [34].

2Θ	Intensity	h	k	l
30.431	68	0	2	0
34.928	737	1	1	0
35.52	999	0	2	1
36.228	517	0	0	2
39.508	570	1	1	1
48.017	36	0	2	2
51.204	459	1	1	2
57.019	30	1	3	0
60.262	373	1	3	1
63.322	63	0	4	0
64.707	155	0	2	3
65.339	83	2	0	0
66.381	47	0	4	1
67.364	105	1	1	3
69.45	32	1	3	2
73.77	9	2	2	0
75.188	74	0	4	2
76.634	184	2	2	1
76.898	132	0	0	4
77.06	113	2	0	2
83.721	135	1	3	3
84.899	7	0	2	4
85.057	13	2	2	2
87.332	88	1	1	4
89.199	20	0	4	3

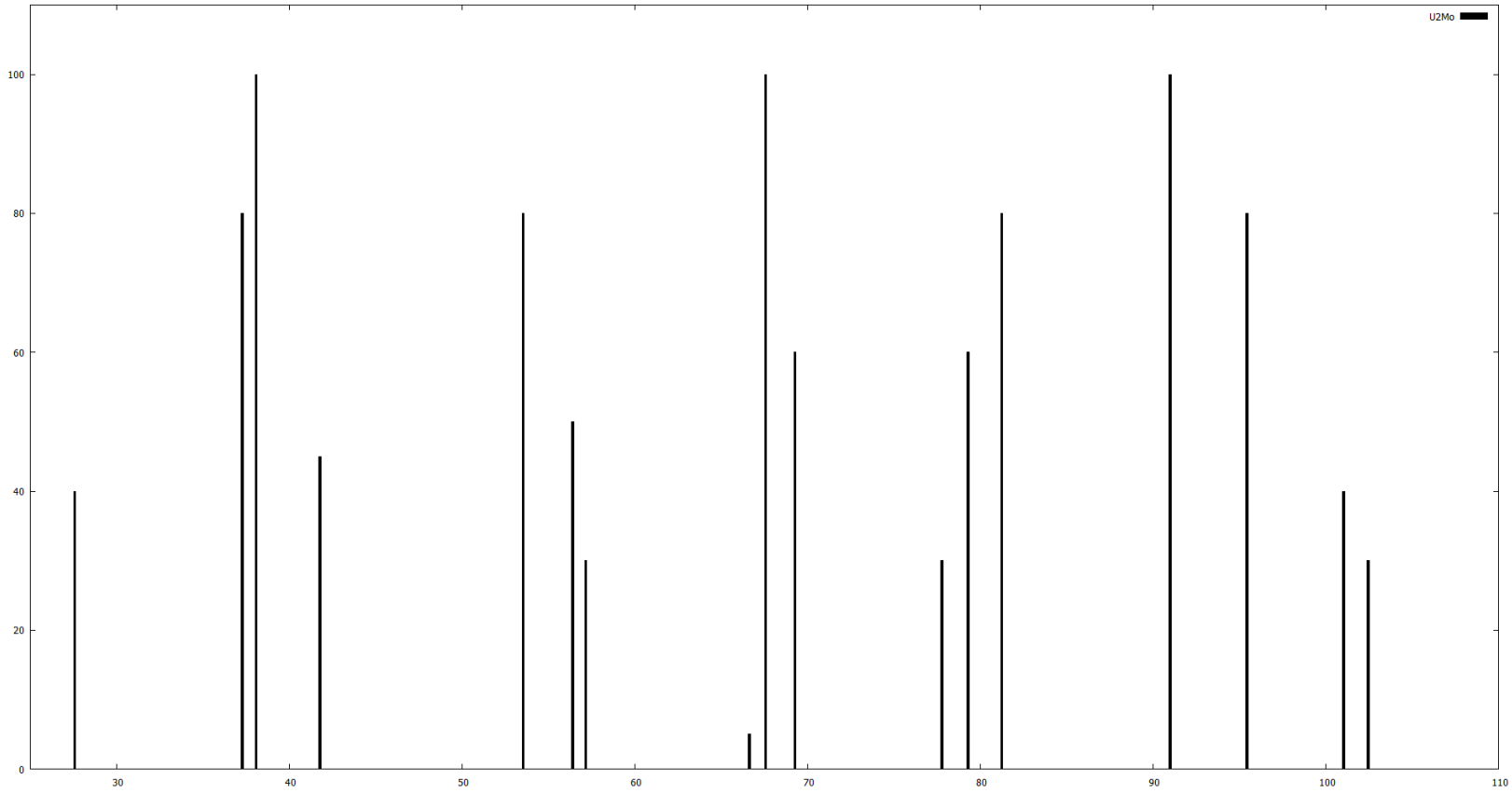

Appendix Figure 3. Reference XRD data for γ'. [35].

Appendix Table 4. Reference XRD data for γ'. [35].

2Θ	Intensity	h	k	l
18.089	10	0	0	2
27.593	40	1	0	1
37.28	80	1	1	0
38.1	100	1	0	3
41.784	45	1	1	2
53.546	80	2	0	0
56.402	50	0	0	6
57.166	30	2	0	2
66.654	5	2	0	4
67.581	100	2	1	3
69.288	60	1	1	6
77.772	30	0	0	8
79.312	60	2	1	5
81.253	80	2	0	6
90.995	100	3	0	3
95.453	80	1	0	9
101.03	40	2	0	8
102.45	30	3	0	5

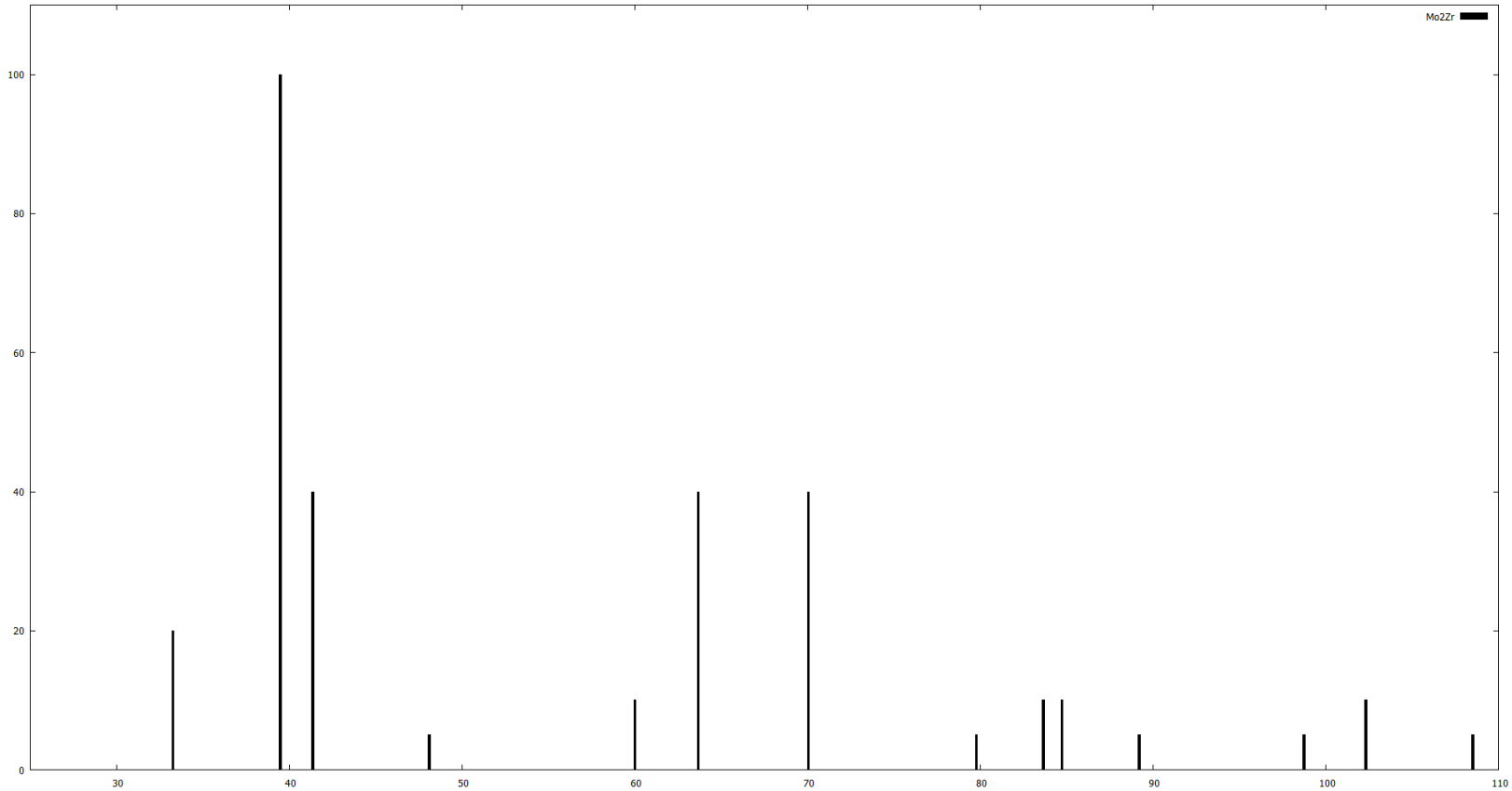

Appendix Figure 5. Reference XRD data for Mo_2Zr phase. [36].

Appendix Table 6. Reference XRD data for Mo_2Zr phase. [36].

2Θ	Intensity	h	k	l
20.258	5	1	1	1
33.279	20	2	2	0
39.491	100	3	1	1
41.383	40	2	2	2
48.103	5	4	0	0
60.024	10	4	2	2
63.685	40	5	1	1
70.056	40	4	4	0
79.787	5	6	2	0
83.658	10	5	3	3
84.739	10	6	2	2
89.203	5	4	4	4
98.734	5	6	4	2
102.31	10	7	3	1
108.52	5	8	0	0
122.87	10	7	5	1
124.34	10	6	6	2

APPENDIX B: ADDITIONAL XRD DATA

The following two plots show the effect of varying zirconium content for a given heat treatment and molybdenum concentration.

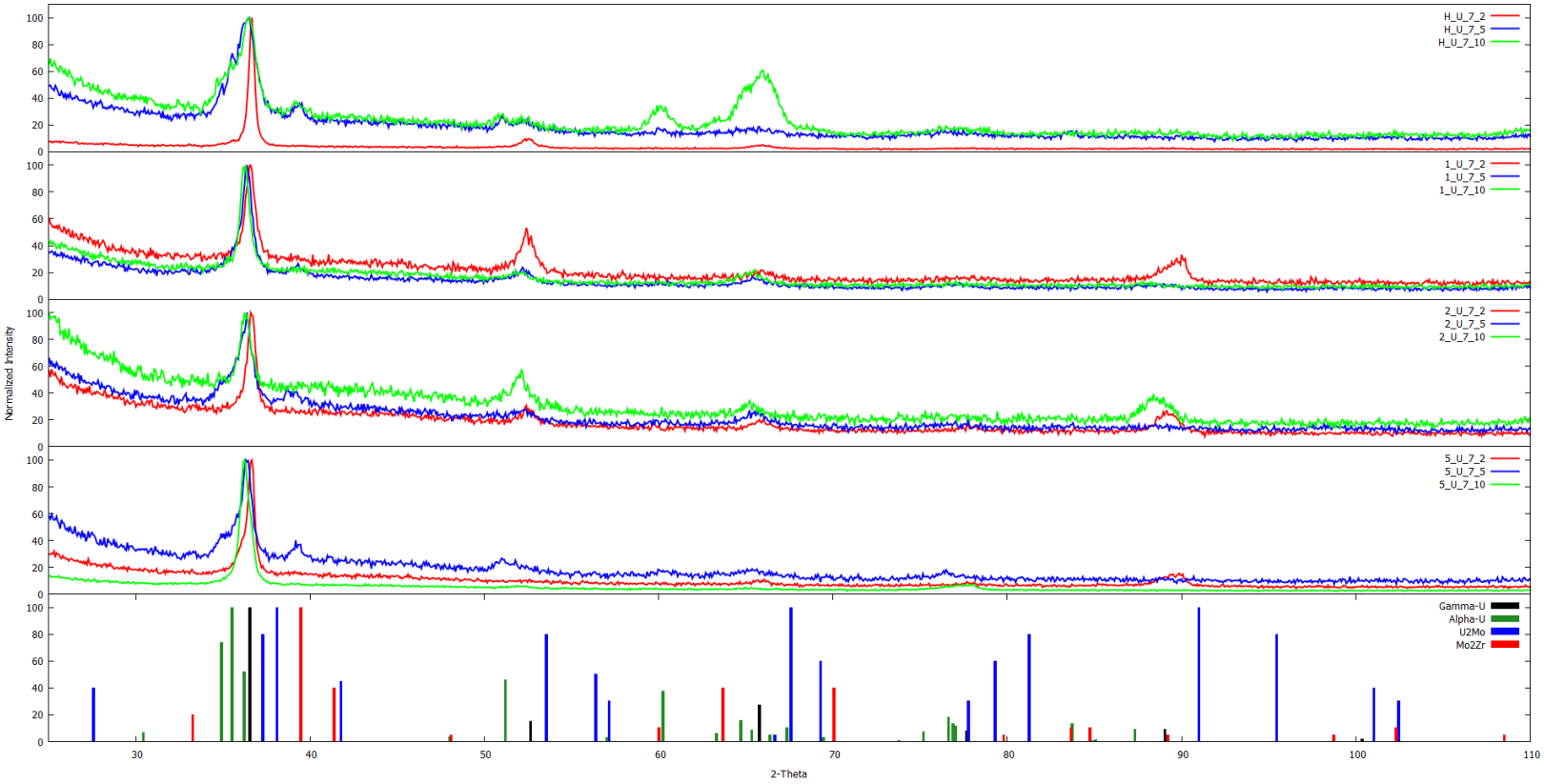

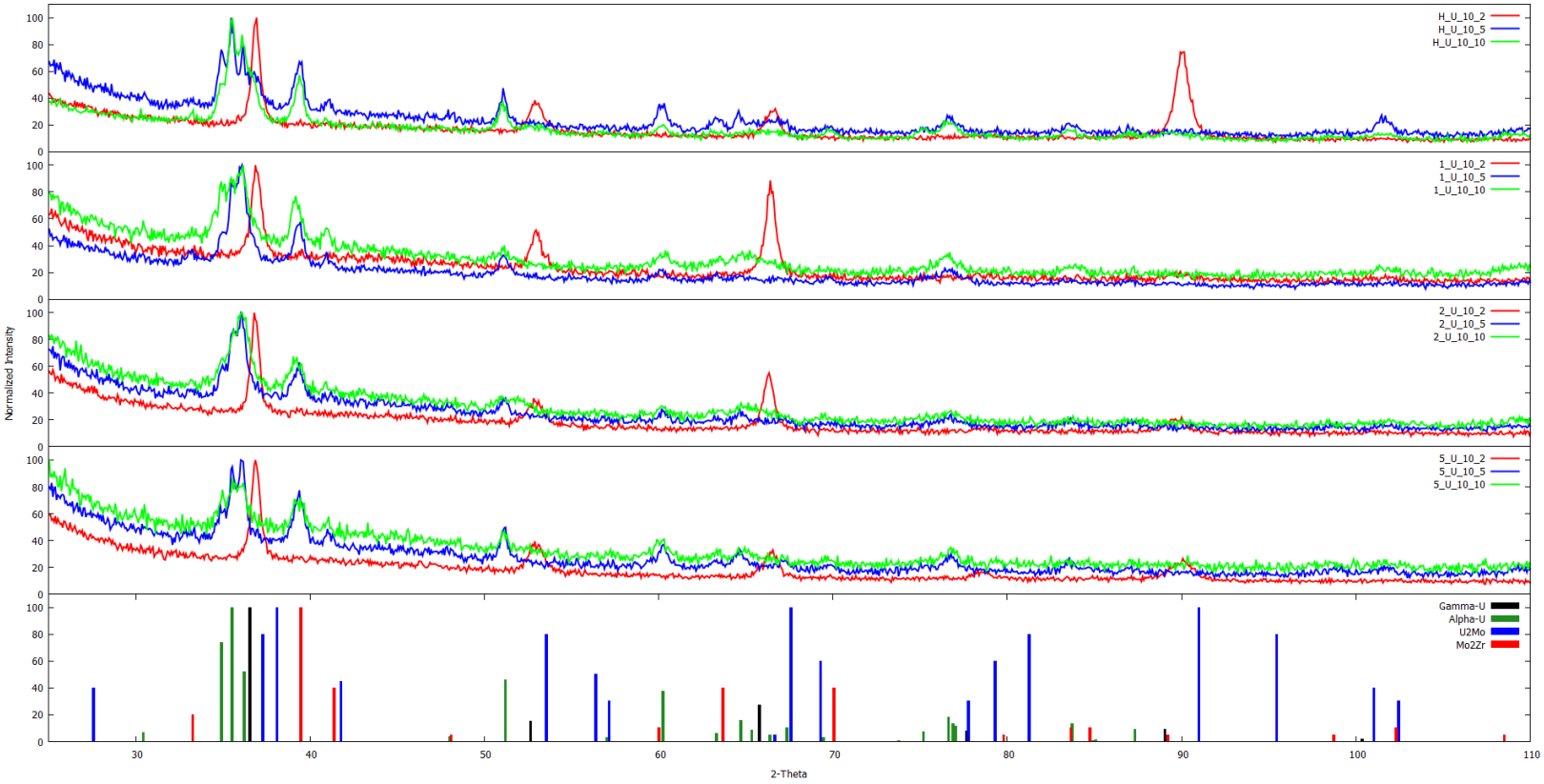
H_U_10_2
H_U_10_5
H_U_10_10
1_U_10_2
1_U_10_5
1_U_10_10
2_U_10_2
2_U_10_5
2_U_10_10
5_U_10_2
5_U_10_5
5_U_10_10
Gamma-U
Alpha-U
U2Mo
Mo2Zr
Normalized Intensity
2-Theta
0
20
40
60
80
100
30
40
50
60
70
80
90
100
110

The following three plots show the effect of varying molybdenum content for a given heat treatment and zirconium content.

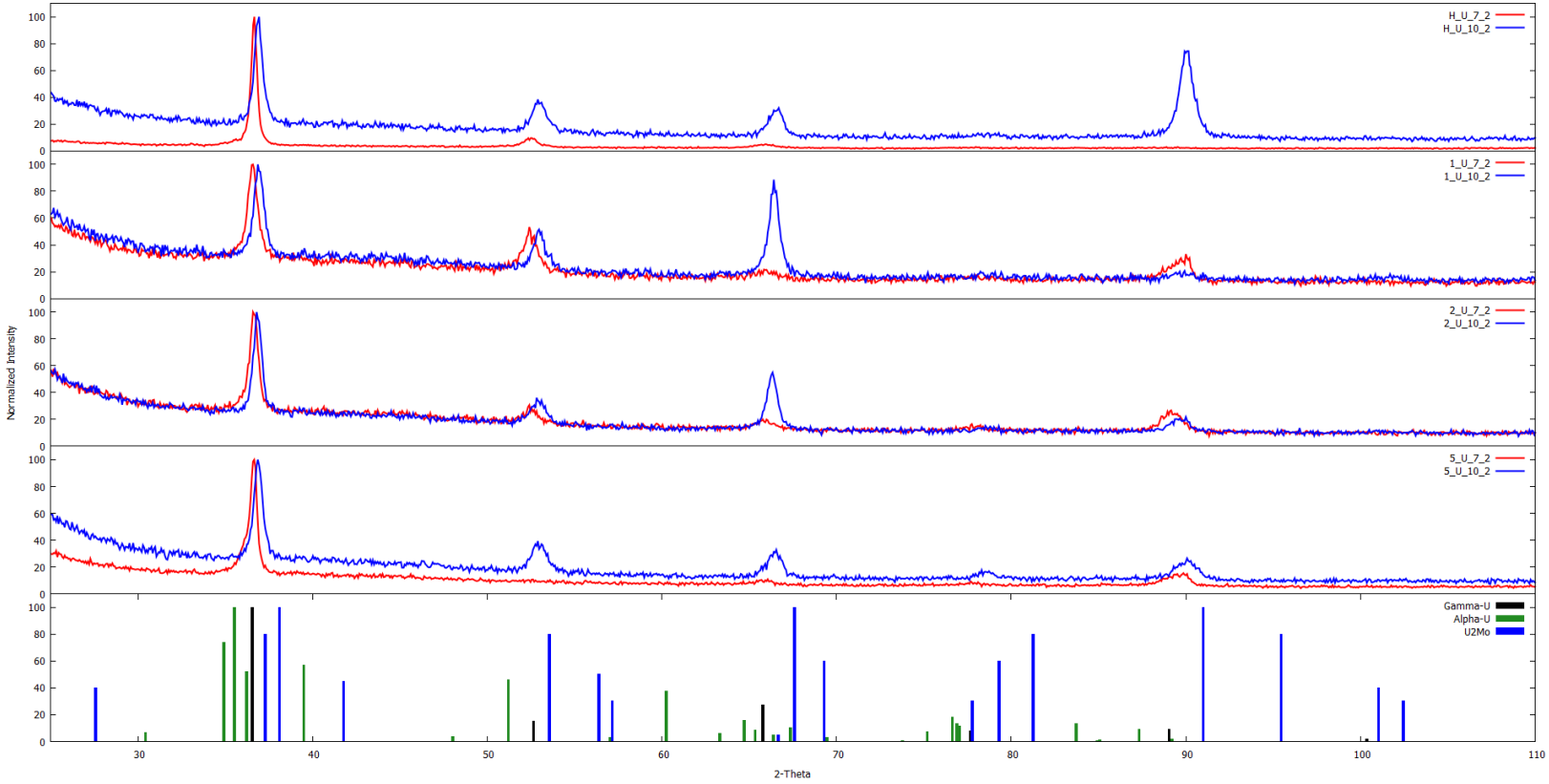

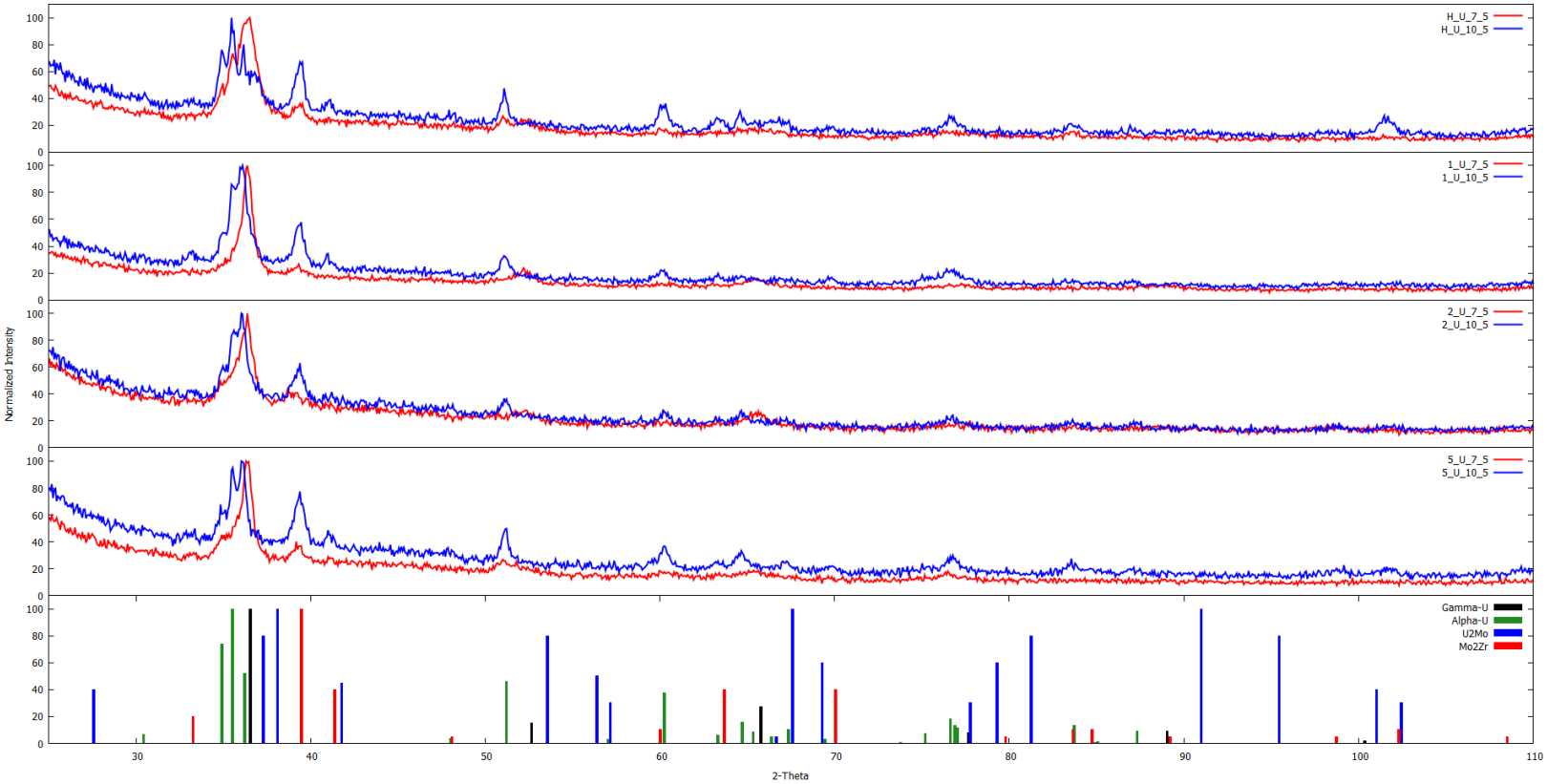
H_U_7_5
H_U_10_5
1_U_7_5
1_U_10_5
2_U_7_5
2_U_10_5
5_U_7_5
5_U_10_5
Gamma-U
Alpha-U
U2Mo
Mo2Zr
Normalized Intensity
2-Theta

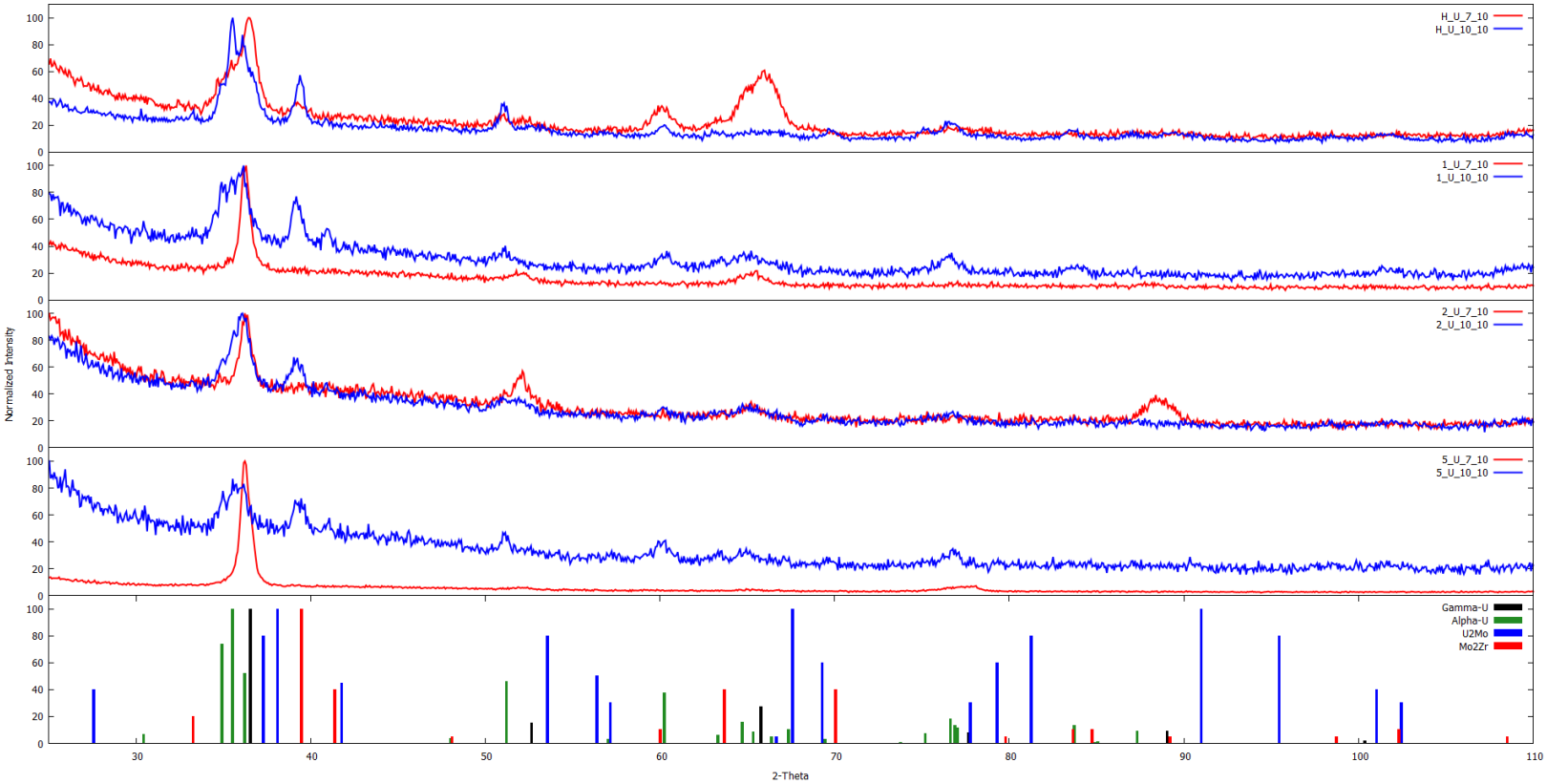
H_U_7_10
H_U_10_10
1_U_7_10
1_U_10_10
2_U_7_10
2_U_10_10
5_U_7_10
5_U_10_10
Gamma-U
Alpha-U
U2Mo
Mo2Zr
Normalized Intensity
2-Theta

APPENDIX C: DIFFERENTIAL SCANNING CALORIMETRY PLOTS

All DSC plots presented here contain six DSC heating curves. Throughout all plots, the same color corresponds with the same heating cycle: Blue-1, Green-2, Dark Blue-3, Purple-4, Pink-5, Light Blue-6.

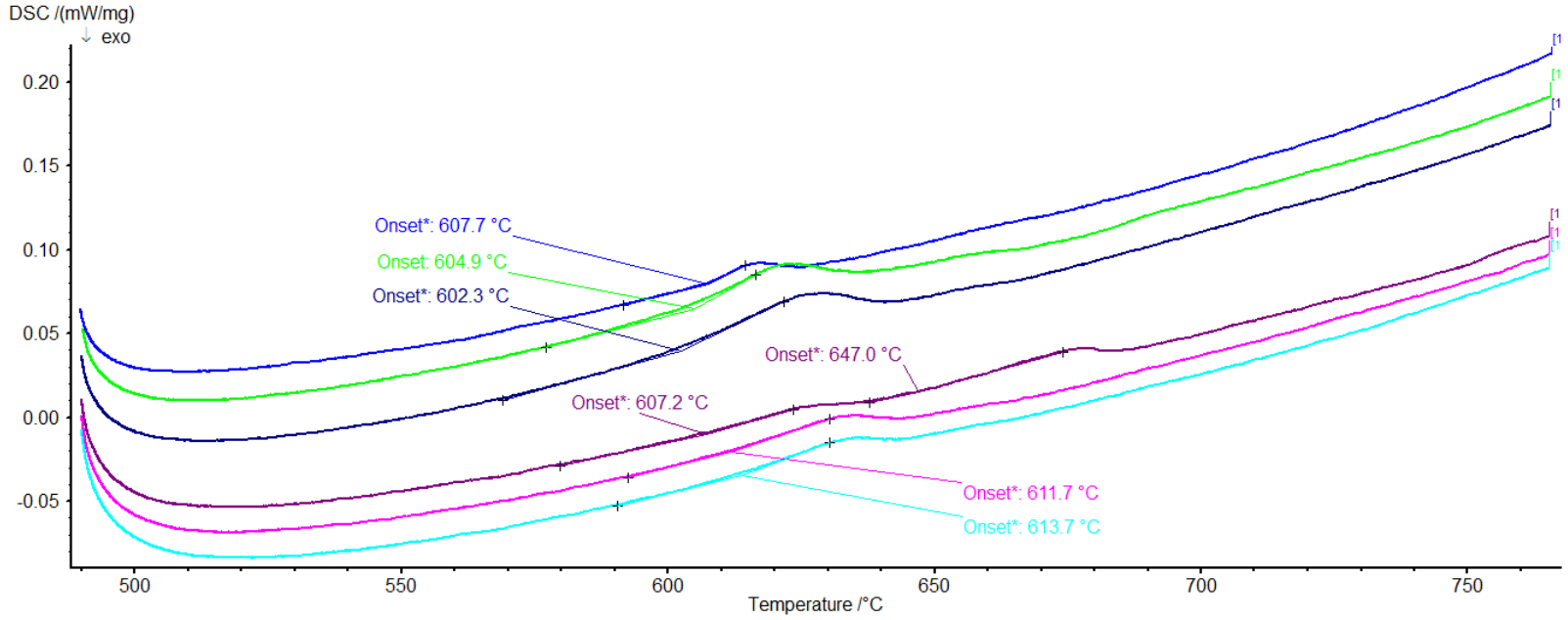

H-U-7Mo-2Zr

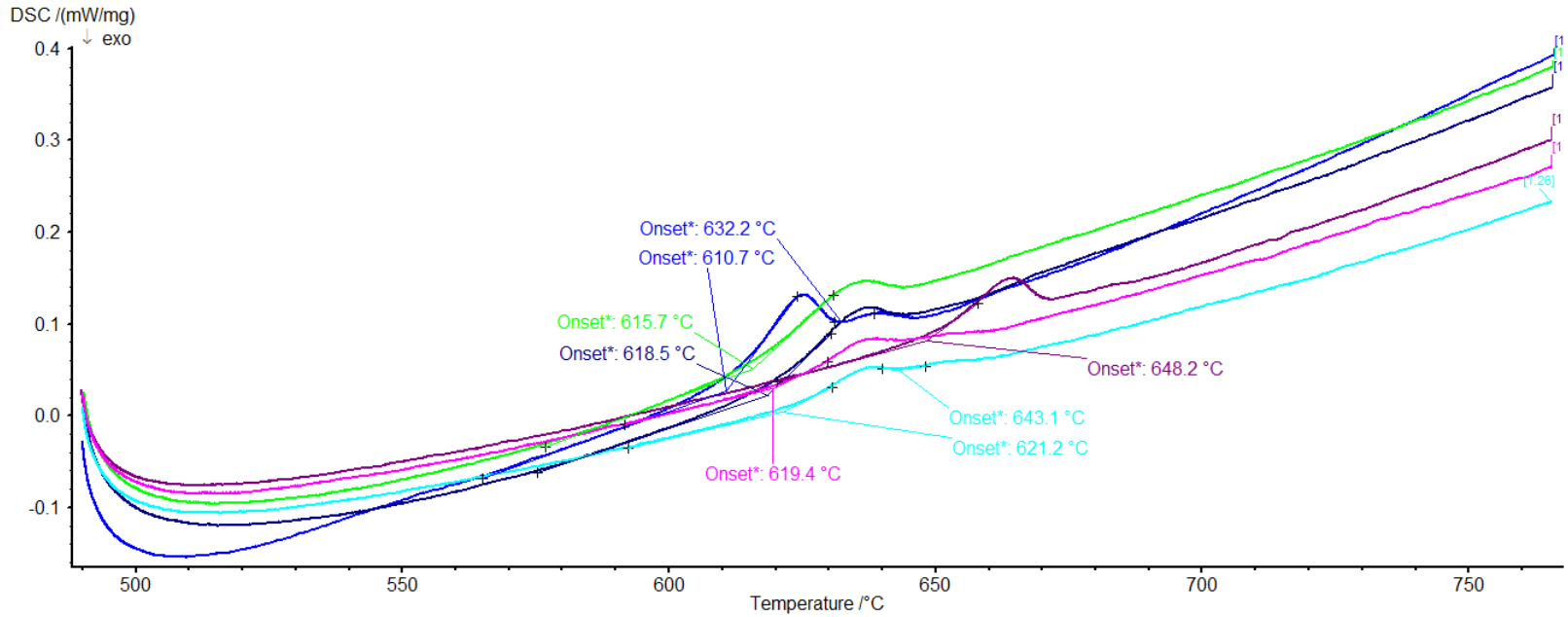
DSC /(mW/mg)
exo
0.4
0.3
0.2
0.1
0.0
-0.1
500
550
600
650
700
750
Temperature /°C
Onset*: 632.2 °C
Onset*: 610.7 °C
Onset*: 615.7 °C
Onset*: 618.5 °C
Onset*: 648.2 °C
Onset*: 643.1 °C
Onset*: 621.2 °C
Onset*: 619.4 °C

H-U-7Mo-5Zr

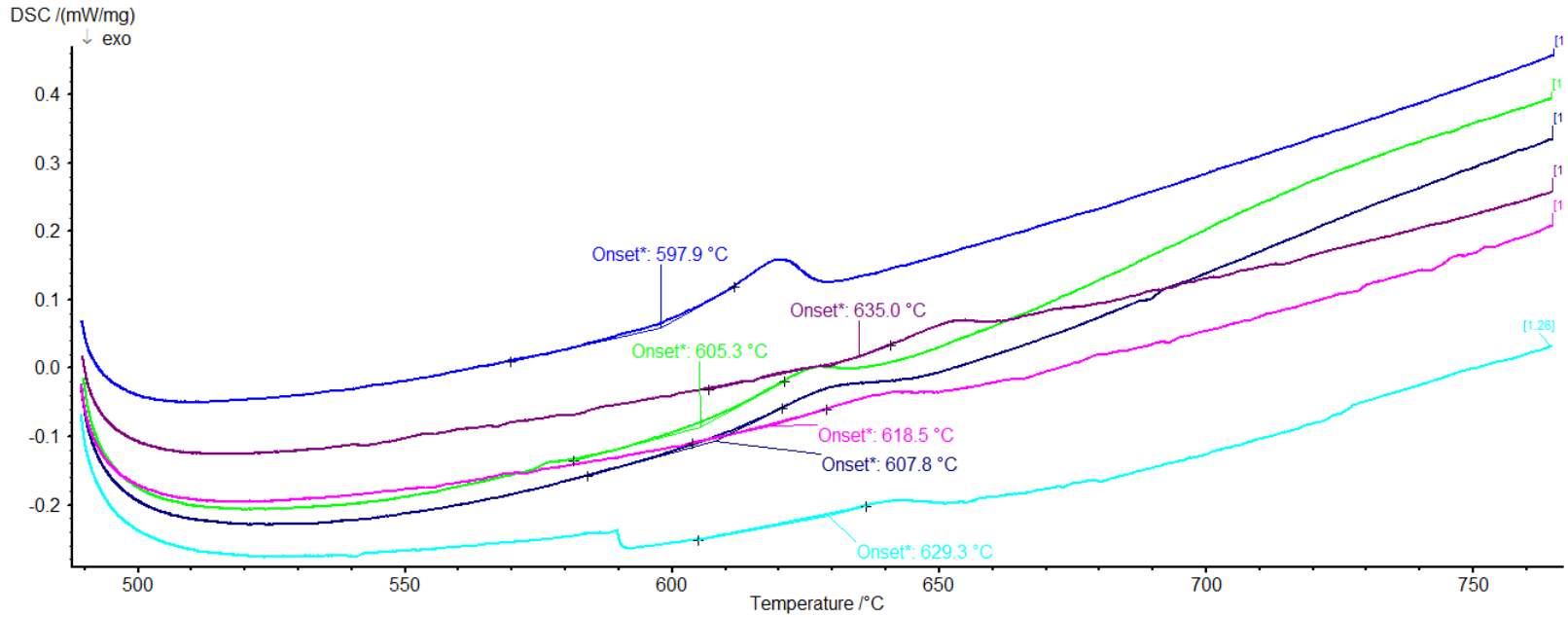
DSC /(mW/mg)
exo
0.4
0.3
0.2
0.1
0.0
-0.1
-0.2
Onset*: 597.9 °C
Onset*: 635.0 °C
Onset*: 605.3 °C
Onset*: 618.5 °C
Onset*: 607.8 °C
Onset*: 629.3 °C
[1.26]
500
550
600
650
700
750
Temperature /°C

H-U-7Mo-10Zr

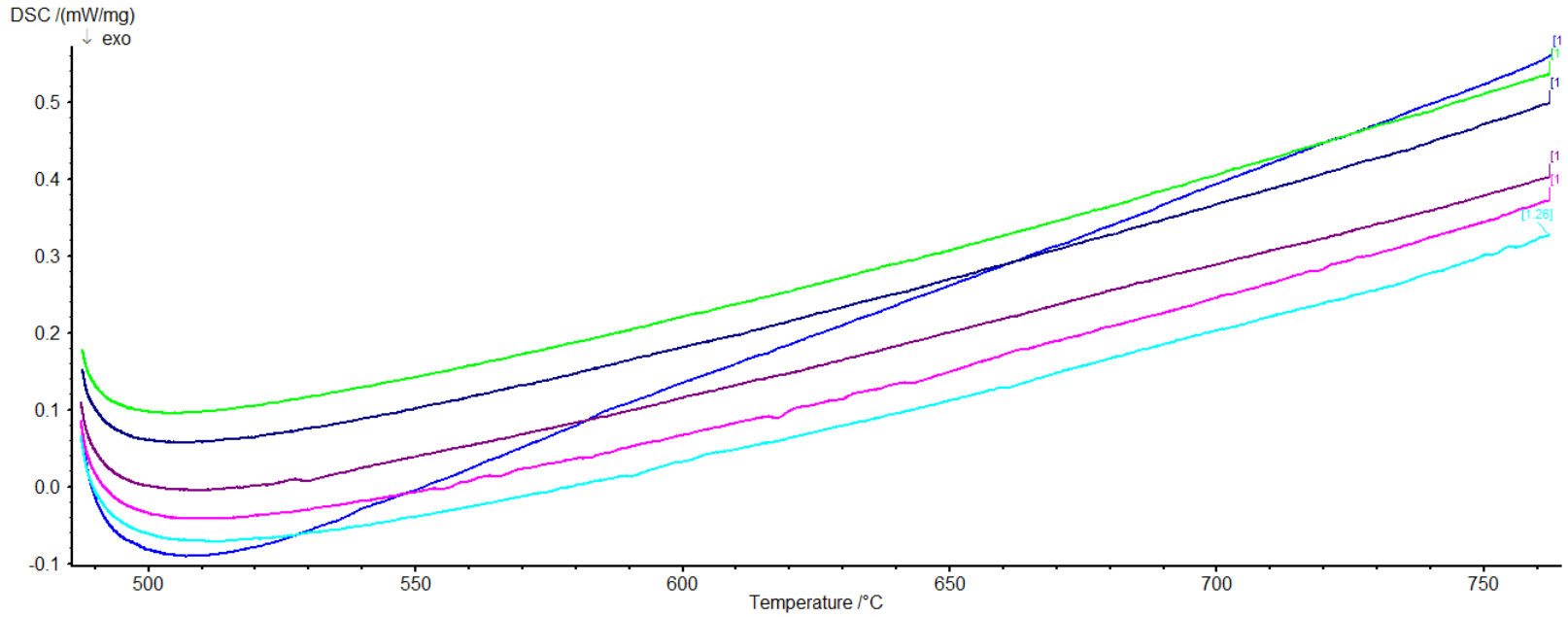
DSC /(mW/mg)
exo
0.5
0.4
0.3
0.2
0.1
0.0
-0.1
500
550
600
650
700
750
Temperature /°C

H-U-10Mo-2Zr

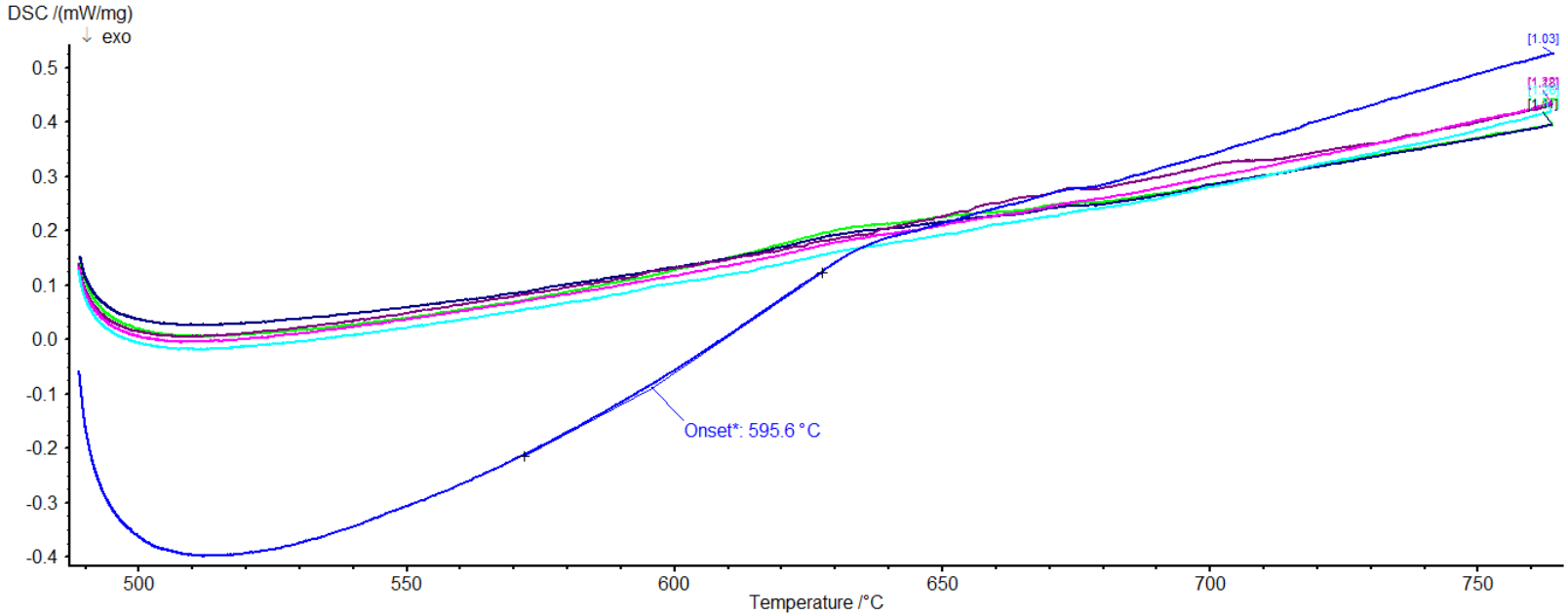
DSC /(mW/mg)
exo
0.5
0.4
0.3
0.2
0.1
0.0
-0.1
-0.2
-0.3
-0.4
500
550
600
650
700
750
Temperature /°C
[1.03]
Onset*: 595.6 °C

H-U-10Mo-5Zr

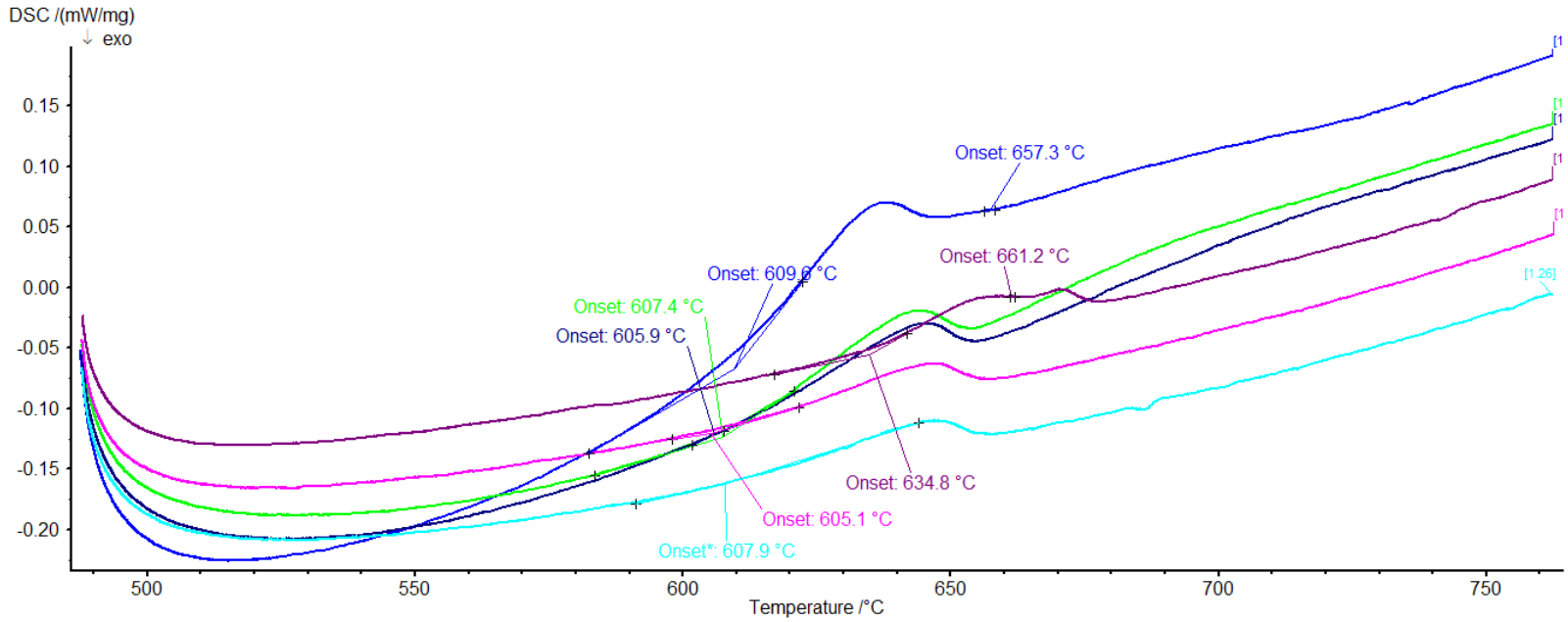
DSC /(mW/mg)
exo
0.15
0.10
0.05
0.00
-0.05
-0.10
-0.15
-0.20
500
550
600
650
700
750
Temperature /°C
Onset: 657.3 °C
Onset: 609.6 °C
Onset: 607.4 °C
Onset: 605.9 °C
Onset: 661.2 °C
Onset: 634.8 °C
Onset: 605.1 °C
Onset*: 607.9 °C
[1.26]

H-U-10Mo-10Zr

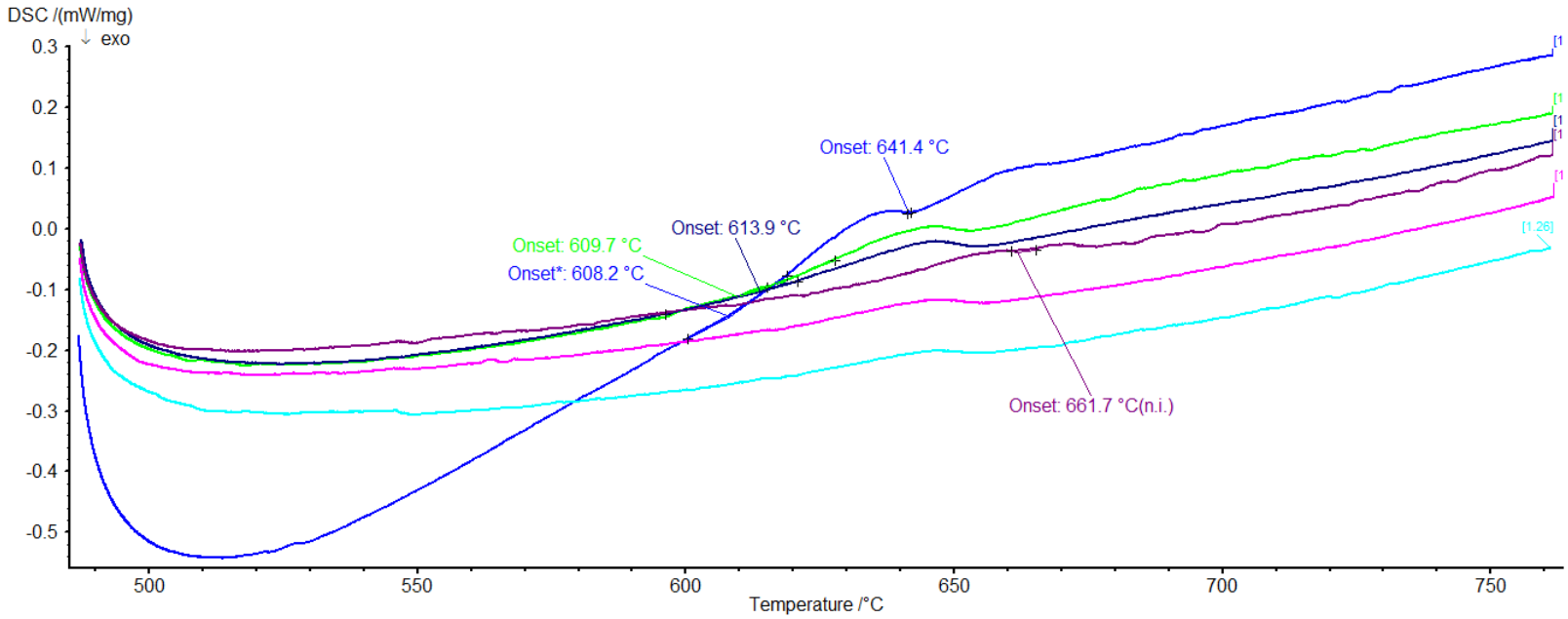
DSC /(mW/mg)
exo
0.3
0.2
0.1
0.0
-0.1
-0.2
-0.3
-0.4
-0.5
500
550
600
650
700
750
Temperature /°C
Onset: 641.4 °C
Onset: 613.9 °C
Onset: 609.7 °C
Onset*: 608.2 °C
Onset: 661.7 °C(n.i.)
[1.26]

1-U-10Mo-10Zr

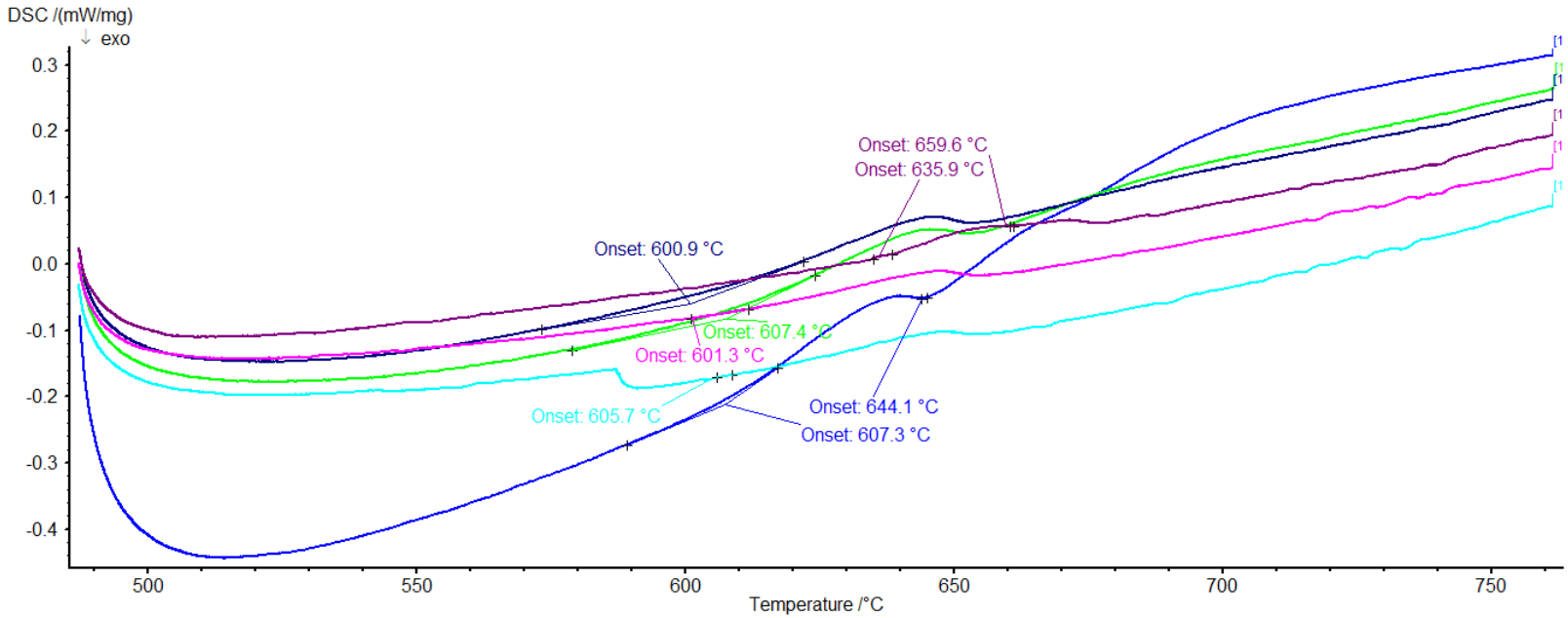
DSC /(mW/mg)
↓ exo
0.3
0.2
0.1
0.0
-0.1
-0.2
-0.3
-0.4
500
550
600
650
700
750
Temperature /°C
Onset: 659.6 °C
Onset: 635.9 °C
Onset: 600.9 °C
Onset: 607.4 °C
Onset: 601.3 °C
Onset: 605.7 °C
Onset: 644.1 °C
Onset: 607.3 °C

2-U-10Mo-10Zr

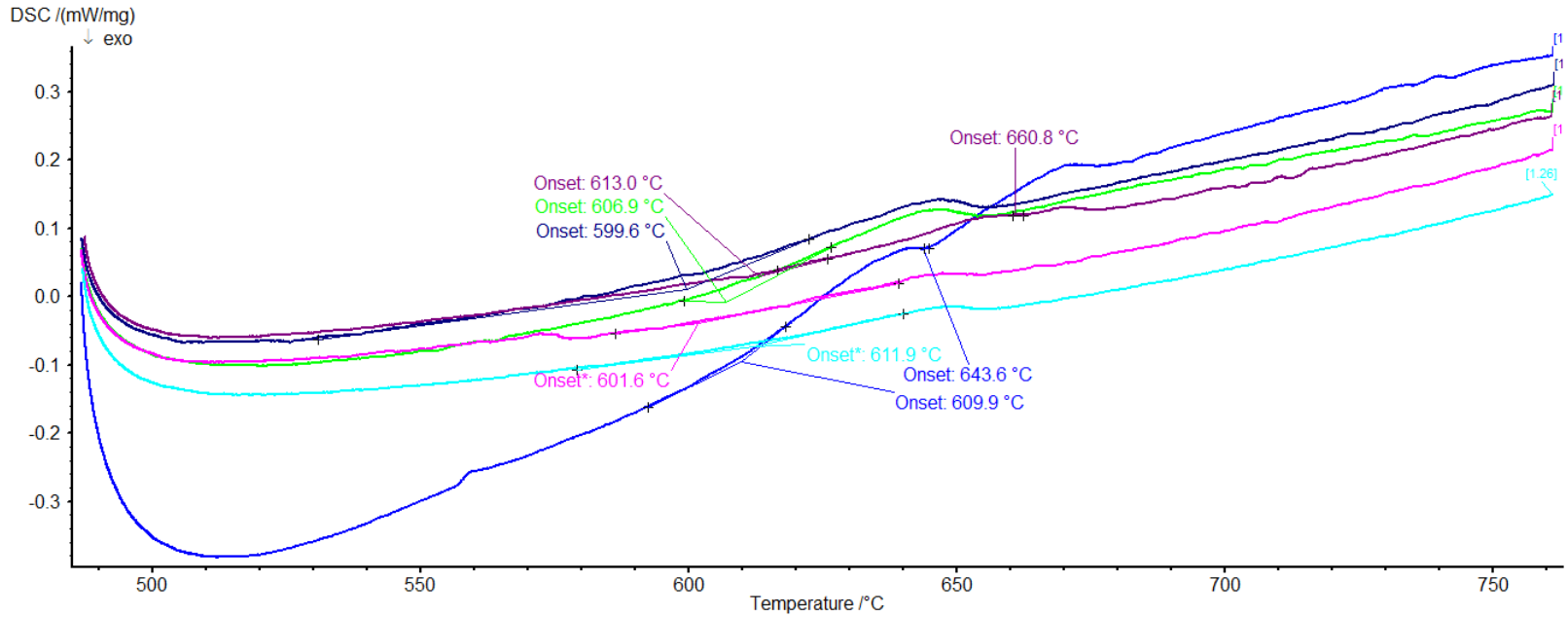
DSC /(mW/mg)
exo
0.3
0.2
0.1
0.0
-0.1
-0.2
-0.3
500
550
600
650
700
750
Temperature /°C
Onset: 660.8 °C
Onset: 613.0 °C
Onset: 606.9 °C
Onset: 599.6 °C
Onset*: 611.9 °C
Onset: 643.6 °C
Onset: 609.9 °C
Onset*: 601.6 °C
[1.26]

5-U-10Mo-10Zr